Spring 5-6-2022

Structure From Motion Methodology Captures Seasonal Influences on Coastal Bluff Erosion and Landslide Hazards in Casco Bay, ME

Nicholas Whiteman
University of Maine, nicholas.whiteman@maine.edu

STRUCTURE FROM MOTION METHODOLOGY CAPTURES SEASONAL INFLUENCES ON COASTAL BLUFF EROSION AND LANDSLIDE HAZARDS IN CASCO BAY, ME.

By

Nicholas Robert Whiteman

B.S. Tufts University, 2012

A THESIS

Submitted in Partial Fulfillment of the

Requirements for the Degree of

Master of Science

(in Earth and Climate Sciences)

The Graduate School

The University of Maine

May 2022

Advisory Committee:

Joseph T. Kelley, Professor of Earth Sciences, Advisor

Daniel F. Belknap, Professor of Earth Sciences

Peter O. Koons, Professor of Earth Sciences

STRUCTURE FROM MOTION METHODOLOGY CAPTURES SEASONAL INFLUENCES ON COASTAL BLUFF EROSION AND LANDSLIDE HAZARDS IN CASCO BAY, ME.

By Nicholas Robert Whiteman

Thesis Advisor: Dr. Joseph Kelley

An Abstract of the Thesis Presented
in Partial Fulfillment of the Requirements for the
Degree of Master of Science
(in Earth and Climate Sciences)
May 2022

Shoreline erosion in response to rising sea level is a global problem. Recognizing the need for observational data on coastal bluff recession in Casco Bay, Maine, we employed *Structure from Motion* (*SfM*) photogrammetric methods in a dynamic intertidal environment. Evaluating the method as a means to measure and monitor dynamic geomorphological changes occurring at a coastal bluff shows that a spatial resolution of centimeters over an area of 10's to 100's of meters can be attained at relatively low cost. The efficient methodology allows for frequent surveys at an operational scale, leading to greater temporal resolution and quantification of bluff erosion activity that supports understanding of the local geohazard. With the greater temporal resolution gained from this evaluation additional inferences are made towards seasonal controls on bluff geomorphology. In the local temperate climate, the dominant erosional actor is characteristically linked to seasonal transitions. Given the urgency of coastal erosion, the lack of local records, and newfound feasibility of repeat surveys, *Structure from Motion* presents the opportunity to address the uncertainty of bluff instability with an approach that accounts for quantified change over time. Observations were evaluated with respect to: 1) the coastal bluff erosion cycle conceptual model; 2) local landslide hazards; and 3) preservation of a shoreline status record.

ACKNOWLEDGEMENTS

I acknowledge that the sea has risen a bit more than I'd like to admit while drafting this thesis. And so I'm indebted to those who have shown the extraordinary patience it took to allow me to bring some resolution to the many things collected in the pages that follow. Ultimate thanks go to my advisor Joe Kelley who, among a page-full of other accolades, quickly made U. Maine the obvious choice and granted me the opportunity to return to this world. It follows that such thanks also go to Ms. Kathleen Leyden of the Coastal Program, in that she awarded the contract, and Stephen Dickson as a partner of the contract, named Building Resiliency Along Maine's Bluff Coast, a NOAA-Project of Special Merit, that opened the door for me to attend.

Thanks as much again to the other members of my committee. Dan Belknap, who has forever improved my writing, my presentations, and my knowledge of the state that I call home. And Peter Koons, who has challenged me to recognize all that I have learned and to find the language that serves what hints come of intuition. The shared comraderies over the dynamics of all things: tea, music, and surf breaks, just to name a few, have tricked me into learning even more.

To Alice Kelley, I am ever grateful, for always helping me to feel courageous and useful and cared for, even when COPE-ing with conference travel. Marty Yates and Kristin Schild, I thank two enduring friends from the front-lines of remote sensing and spatial informatics. Working with you on the developing Geomatics coursework has had a lasting impact and greatly improved the quality of the work presented here. There are many more from the School of Earth and Climate Sciences deserving of mention and thanks, all who made the time -even once- to go to bat for me, build me up, grant a reality check. I'll have to settle for the idea that if you're reading this, you're likely one of them.

Special thanks to those of the Maine Geological Survey who welcomed my shoe-gazing shadow for a week as I prepared to graduate high school in 2008. Thanks again to them the same whom I'd never imagined I'd end up meeting with a decade later: Bob Marvinney, Peter Slovinsky, and especially

Stephen Dickson who has celebrated and encouraged my work every step of the way throughout its course. To think I turned up to the first professional meeting with figures sketched by colored pencil, recreating those graphics on the computer too tall an order at the time. Thank you Steve, for bringing the drawings to my defense, like some checkered-flag.

And lastly, without Ben Partan's introduction to *Structure from Motion* and Seth Campbell's generous trusting of the new drone, none of this would've gotten far off the ground. I owe you each a share of all the Ooo's and Awwe's I've ever caught from an audience.

TABLE OF CONTENTS

LIST OF TABLES

LIST OF FIGURES

LIST OF ABBREVIATIONS

(In Alphabetical Order)

BEC the Bluff Erosion Cycle as described in Kelley and Hay 1986

CPU Central Processing Unit

DSLR Digital Single-Lens-Reflexive (a camera technology)

GCP(s) Ground Control Point(s)

GIS Geographic Information System

GNSS Global Navigation Satellite System

GPR Ground Penetrating Radar

GPS Global Positioning System

GPU Graphical Processing Unit

LR# Little River (and numeral for specific sub-site)

ME Maine

RAM Random Access Memory

RTK Real-Time-Kinematic (a GPS survey method)

SfM *Structure from Motion*

S.I.F.T. Scale Invariant Feature Transform

TLS Terrestrial Laser Scanner (Scanning)

UAV Unmanned Aerial Vehicle (used synonymously here with 'drone.')

CHAPTER 1

INTRODUCTION

Rising sea level raises great concern for the stability of Maine's coastline. For hundreds of years since European colonization there have been detailed property surveys and yet a coherent record of the sea's advancing front seems nonexistent, aside from the many individual efforts to fortify the position of shoreline property. Retreat of the shoreline here is ongoing. The coincidence of chronic wasting of bluffs of glaciogenic sediment coupled with sudden episodes of large-scale landslide failures threatens loss of life and property. The idea of such impermanence has been publicized by government and university scientists (Kelley et al. 1989, Kelley and Dickson 2000; Hampton et al. 2004a, b; Kelley 2004, Hapke et al. 2014; Maine Geological Survey 1998-2006), but public awareness is faint, allowing for hazardous or inconsiderate development. Attempts to stabilize and fix a shoreline in the defense of property are often conducted hastily, with little regard to the adjacent environments, and are typically made only in reaction to a significantly damaging or threatening event such as a storm or a landslide.

While a sequence of landslide events is often viewed as an average rate of retreat over time these events represent discontinuous, rapid failures with a low degree of predictability (as is the case for earthquakes). The continuous *vs.* discontinuous behavior patterns observed in cases of coastal erosion (**Figure 1.1**) (Sunamura 1983) illustrates the need for a refined temporal resolution when addressing the problem. Modeling erosion by century-long averages to predict future shoreline positions does not serve coastal management well. Often assuming uniform retreat in the context of some trend, forecasts of change following 100 years of present conditions will leave decision-makers without recourse when facing development concerns on the order of decades or less.

More recently, statistical and numerical modelling approaches have been explored as a reasonable solution for coastal management (Hapke and Plante 2010, Lentz et. al. 2015, Deng et. al. 2017), but it is important to note that these models commonly draw their strength from a robust and

accurate historical record of past and present shoreline behavior. To be successful, a regional management tool must be empowered by numerous and widespread case studies. Many projects aiming to analyze soft-shoreline erosion with numerical models bemoan the necessity to either oversimplify model parameters or greatly extend the time series to produce an average rate of shoreline retreat (Hapke and Plante. 2010, Lentz et. al. 2015, Deng et. al. 2017), regardless of the often-episodic nature of the erosion events (Sunamura 1983). Such generalized results are of little use to communities with site-specific concerns or with the need to consider the administration of coastal zones in a practical timeframe.

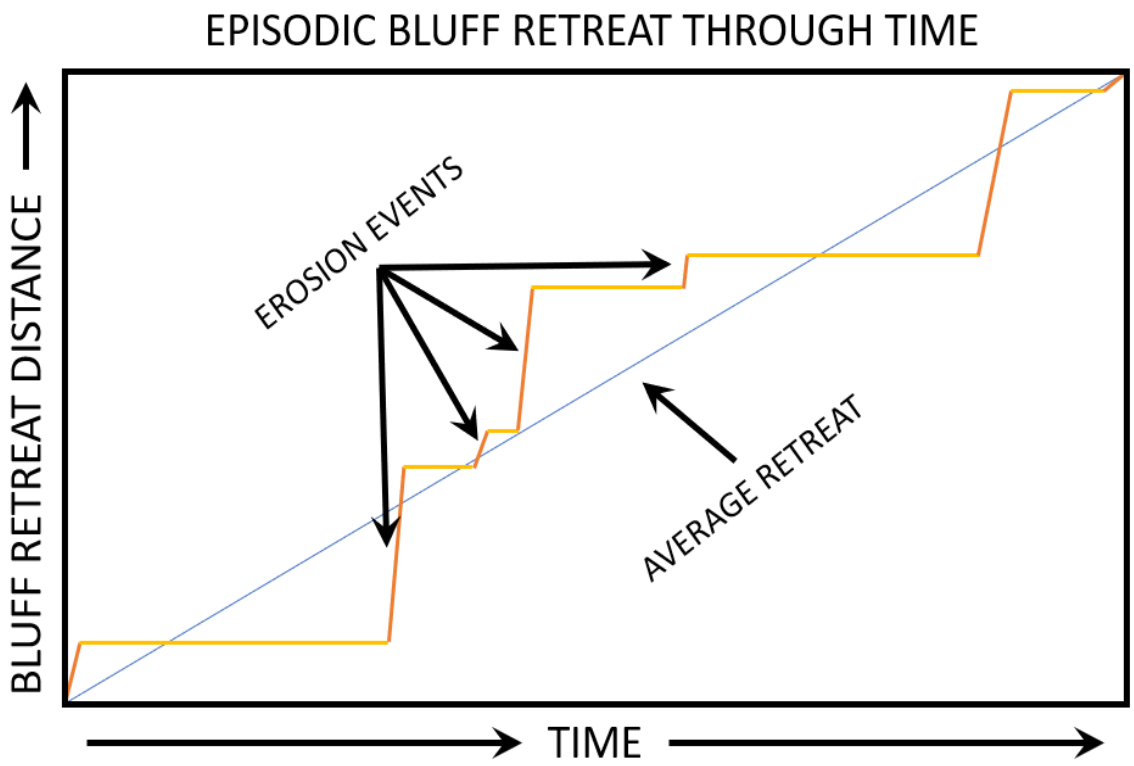

Figure 1.1. Episodic Bluff Retreat Through Time. A conceptual graph of the episodic nature of bluff retreat in contrast to the assumption of an average rate of retreat. From Sunamura (1983) as modified by Keblinsky (2003) and colorized here.

A lack of systematic observations of coastal bluff erosion challenges understanding and stunts the growth of situational awareness. The great scale of Maine's coastline compounds the problem by keeping a comprehensive survey out of practical reach and places the onus of coastal zone management on individual property owners under the jurisdiction of local municipal offices. Some 90% of *Vacationland's* coast is privately owned (Ringold and Clark 1980) and populations continue to grow northwards from the more developed south. Continuing development alters the land use and puts more people and property in harm's way. Most newcomers are not prepared to properly anticipate the vulnerability of a given site to high-water events nor any preexisting landslide hazard the ground beneath conceals.

Lack of preparation brings consequences that reach further than the recent settler's back yard. The negative effects of "hold-the-line" shoreline armoring strategies, often implemented in reaction to a sudden erosion event, make them less than ideal solutions. Hard-armoring focuses erosional forces onto adjacent sites, putting neighboring properties in jeopardy. On the other hand, erosion of bluffs supplies the fine-grained sediments that provide substrate for salt marsh environments and tidal flats (Smith 1990). Hard-armoring a shoreline to preserve property impounds that sediment source and starves its nearby environments.

To address the pressing bluff-retreat hazard, and to support the development of a more comprehensive modeling and management program, I chose to closely monitor eroding sites by testing the application of *Structure from Motion* (*SfM*) (Ullman 1979) as a tool to effectively evaluate the mechanisms and measures of retreat.

Why Employ *Structure from Motion*?

Structure from Motion techniques are expected to offer the efficiency and flexibility required to address the concern of monitoring coastal erosion within a practical timeframe. A long-term record of shoreline retreat measurement is lacking along the 6,200 km of Maine's coast. While there are aerial photographs available on a decadal time frame and a single LiDAR survey for the whole coast, these are insufficient to develop predictive models. The aerial photographs do not support an historical record of shoreline change at the necessary scale (Miller 2018) and without repeat surveys, LiDAR provides a coarse baseline at best. Field mapping of bluffs by the Maine Geological Survey (Maine Geological Survey 1998-2006) dates back more than 20 years in some instances and is out of date. Anecdotal interviews with homeowners suffering bluff erosion are not quantitative and inadequate for modeling and management efforts. There is a current need to establish a baseline of modern measurements on a site-by-site basis and advances in *Structure from Motion* methods offer an efficient means to do so. We have maps indicating the location of dangerous bluffs statewide (Maine Geological Survey 2006), but

developing a long-term system of periodic observation of noteworthy bluffs is required for prediction and forecasting purposes. With the trend of rising sea level in the Gulf of Maine (**Figure 1.2**) and the expectation that this trend will continue, if not accelerate (Watson et al. 2015), the earlier this baseline is established, the better.

The purpose of this work is to demonstrate an efficient method of measuring bluff erosion at an appropriate scale to provide both communities and scientists with critical observations as well as to better inform the development of regional coastal management tools. *Structure from Motion* has been heralded as an emergent and easily deployable survey method (James and Robson 2012; Westoby et al. 2012; Clapuyt et al. 2016). Favored for its ease of use; budget-friendly equipment; and low start-up costs, *SfM* is, ultimately, an updated photogrammetric technique that: 1) shows its strength in facilitating simple, fast surveys in dynamic environments; 2) produces quantifiable measurements; and 3) captures a photographic and easily communicable account of change over time. In practicing its application, I will also present demonstrable detection of shoreline change and seek to note more incremental morphological indicators of slope failure activity that may prove useful in predicting extraordinary failure events.

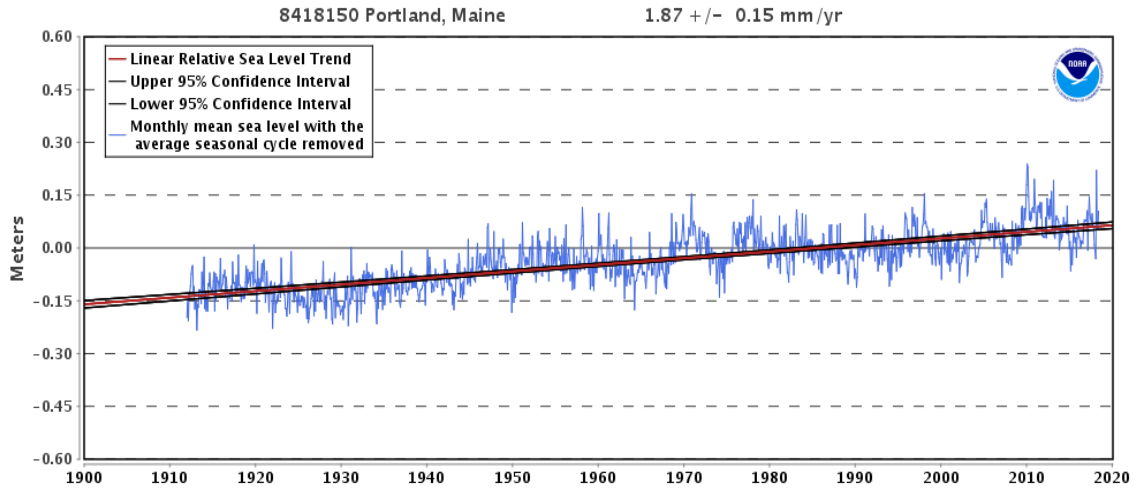

Figure 1.2. A Century of Sea-Level Rise in Portland, Maine.

Local sea level rise is demonstrated by the Linear Relative Sea Level Trend logged at the Portland, ME, tide gauge, Station ID: 8418150. Graph produced with data and tools from the NOAA Center for Operational Oceanographic Products and Services (CO-OPS): <https://tidesandcurrents.noaa.gov/sltrends/sltrends_station.shtml?id=8418150>

CHAPTER 2

GEOLOGICAL SETTING AND PREVIOUS WORKS

Background

Coastal bluff erosion is an ongoing process coincident with rising sea level (Johnson 1919). Bluffs are steep-sided, poorly consolidated sedimentary deposits, not bedrock (Kelley 2014). They differ from "banks" in that they are composed of *in-situ* material (as opposed to shoreline materials, which are frequently reworked) and extend beyond the height of flood-tide. Here in Maine, the unconsolidated material is generally of glacial origin, commonly till, but often glacial-marine sediment (the Presumpscot Formation, Bloom 1963) from the late-Pleistocene marine transgression following the latest glacial maximum. Till has been found to form bluffs up to 10 m high (Thompson 2015). The bouldery nature of the till deposits tends to resist slope failure and the large boulders that accumulate at the toe of the bluff reduce wave attack on the bluff face. The Presumpscot Fm. muds, however, lack the enhanced support and consequential armoring that can be afforded by the presence of larger clasts. The problem of slope failure with such unconsolidated materials is compounded when property owners construct massive structures on coastal bluff sites and alter the local hydrological situation when doing so, in part by cutting forest and shrub vegetation and watering lawns (Kelley and Dickson 2000).

Several large landslide events in recent history drew attention to the geohazard and the overall problem of coastal bluff erosion in Maine (Berry et al. 1996; Kelley et al. 1989). Early bluff erosion studies in Maine, such as those of Amos and Sanford, 1987; Novak 1987; Kelley and Hay, 1986a, b; and Kelley and Dickson, 2000, describe the hazards (Keblinksy 2003) but are all found to be lamenting the lack of public awareness. Most mass movements go unnoticed until property is directly affected and slope failures are reported in panic (**Figure 2.1**). Description of the landslides provided an understanding

of the specific incidences but did little to resolve the timeframe in which these events are likely to reoccur or to clarify what events are expected to lead to a large failure.

***Rockland, 1996** - Landslide on the shore of Rockland Harbor.*

Figure 2.1. The 1996 Landslide in Rockland Harbor brought public attention to Maine's coastal geohazards. Note the relatively small size of the hollow escarpment as compared to the wide and lobate spread of the toe of the debris, indicative of the fluid behavior of the sediment during the retrogressive collapse. From Berry et al. 1996.

Accessed on <http://www.maine.gov/dacf/mgs/hazards/landsldies/case/case.htm>

The first studies focused on measuring erosion of specific sites that were publicly accessible and monitoring the behavior of the erosion products on the adjacent tidal flat (Hay 1988, Smith 1990). To address the problem as coastal development spread, the State began mapping coastal erosion hazards at a 1:24,000 scale in map units of: 1) No Bluff, meaning exposed bedrock or low relief landward of a wetland; 2) Stable, covered in mature vegetation and showing no evidence of past slope failure; 3) Unstable, with patchy vegetation with a few bare spots and dead and creeping trees at the base of the bluff; 4) Highly Unstable, featuring visible signs of slope failure and no vegetation. Additionally, landslide

potential was noted for bluffs with a relief of greater than 6 feet (1.8 meters). While this brought some information into the public eye, it has not stopped unwise coastal development.

A number of issues came to light following the publication of the map series. The classifications as mapped were only a snapshot representation of an ever-changing setting and as such they were essentially outdated soon after they were published. Notably, armored and engineered bluffs were classified as Stable even though they were likely once in a period of instability significant enough to prompt an armoring response in the first place. This may have skewed the perception of a bluff stability scenario later on (Keblinsky 2003).

The State passed the Natural Resource Protection Act (38 MRSA 480-B, 1998) to preclude coastal construction within 75 feet (22.86 meters) of Mean High Water and to disallow construction on unstable bluffs. This is often overlooked, as the bluffs' high relief alongside the sea and their flat tops make them a prize of real estate interests. As popular and valuable property, the bluff's alarming proclivity for failure tends to be left unspoken. Problems arose when landslides occurred on slopes mapped as "Unstable," not "Highly Unstable," (recall the April 1996 Rockland landslide, Berry et al. 1996) and it was recognized that all bluffs are inherently unstable when exceeding 6 feet (1.8 meters) in height and that bluffs passed through a cycle of activity elaborated on earlier in a conceptual model (Kelley and Hay 1986a, b, Kelley et al. 1989) (**Figure 2.2**)**.** Thus, a bluff may have appeared "Stable" when originally mapped but had later changed over time to one that was dangerous. In part this is because the period (the time between successive events) of the bluff erosion cycle (abbreviated: *BEC*) (Kelley and Hay 1986) is shown in this work to be possibly shorter than originally assumed, and that the current assumptions about the *BEC* do not describe the behaviors observed here either. One reason for this may be that the sea is rising (**Figure 1.2**), which brings wave action to the toe of the bluff more often, increasing the likelihood of over-topping toe marshes and more rapidly carrying away the debris of one erosion event to set up the next. These findings underscore the reason we need to more

quantitatively understand the periodicity of erosion and parse out the mechanisms that advance and/or inhibit each phase of the *BEC* model so we can more certainly determine which locations are subject to rapid or large changes.

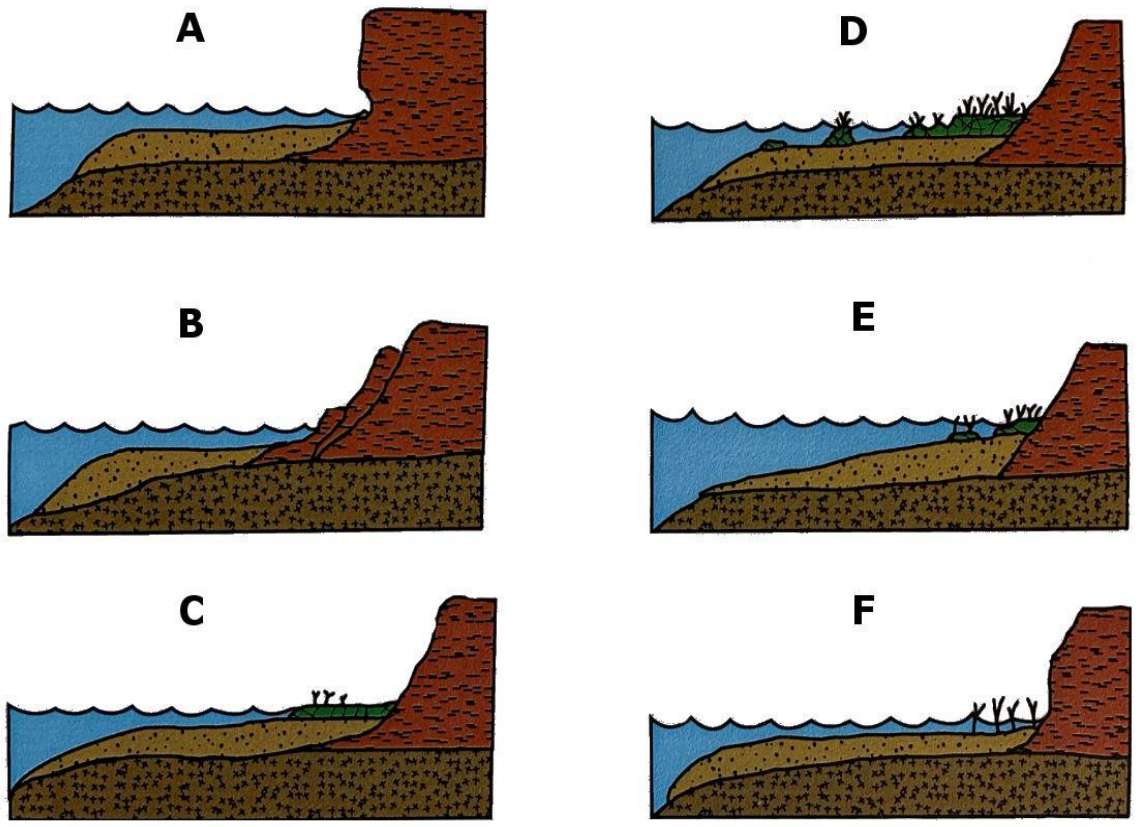

Figure 2.2. The Conceptual Bluff Erosion Cycle Model. From Kelley and Hay (1986a, b) as modified by Keblinsky (2003).

Undercutting of the bluff toe (A) provokes a slope failure (B) which, in turn, delivers sediment into the intertidal zone where the new deposit supports the colonization of halophyte flora. A fringing marsh develops seaward of the bluff (C) and provides some dampening of incoming wave energy, affording temporary protection to the bluff toe behind it. With time the fringing marsh succumbs to chronic erosion (D) and/or rising sea level (E). Eventually the bluff toe is once again directly exposed to incident wave action (F-A), restarting the cycle.

Every time moving water passes over the bluff toe it contributes to erosion. The fine sediments that make up Maine's coastal bluffs are so easily suspended and readily transported. Shoreline armoring is placed as a buttress to resist and reduce the more severe erosive strikes by incoming waves, with the

intention of permanently "fixing" today's position. That is of little usefulness in the long term. Current predictions for rising seas (Church et al. 2013) suggest that the extent of a high-water event that would be at-present considered an over-reach of today's shoreline could be "reached" 100% of the time in a relatively near future. For example, considering **Figure 1.2**: 1) Present day Mean Higher High Water at the Portland, ME, tide gauge is 1.51 meters (4.95 feet). 2) Present day Mean High Water at the Portland, ME, tide gauge is 1.38 meters (4.53 feet). 3) At the current local rate of sea-level rise it will take 71 years to passively cover the distance between the two. Historically, management practices have focused on armoring and stabilization programs but these efforts are clearly seen as reactionary and only in response to particularly damaging events. Now focus is slowly shifting towards more elegant designs as public awareness of "a living [and impermanent] shoreline" grows (Currin et al. 2010, Bilkovic et al. 2016, O'Donnell 2017). Attention has turned towards sophisticated drainage solutions and/or natural vegetative systems not only for their more attractive aesthetic but also for fostering local habitat support and remediation.

The composition of the bluffs and the nature of their original deposition, in a setting unlike that of their present situation, makes them predisposed to both chronic weathering and dramatic failure at the shoreline. In contrast to local bedrock cliffs and ledges, the soft sediment bluffs are exceptionally vulnerable. Here and now, local sea-level rise brings water up against formerly dry hillsides. As the water level is elevated so is the vertical range of wave action, from a short distance below mean sea level to a short distance above, and translated further up against the bluff profile with sea-level rise. The ongoing elevation of an erosive cutting-plane defined by the climbing waterline (Johnson 1919) ensures that the bluffs are kept in a perpetual state of erosive impermanence. Nearshore reworking of sediments delivered from failures up-slope redistributes this sediment resource from a terrestrial deposit to the intertidal zone, and beyond. Due to compositional and depositional differences in origin, coastal bluffs, unlike beaches, are not readily restored after they erode. Once the high-relief landform collapses and its constituent materials are carried away the bluff becomes, in essence, extinct. Sediment removed from the

bluff is never returned to the bluff. This activity, as a function of time, cannot be monitored without a quantification of change.

Climate Patterns of Coastal Maine

Maine's coastal climate has humid, north-temperate conditions with low average annual temperatures. Prevailing summer winds from the southwest are relatively light, in contrast to those of the winter: generally, from the northwest with occasional storms producing winds from the northeast as a product of passing offshore low-pressure systems (Hill et al. 2004). Northeast winter storms drive down-welling and direct sediment transport offshore (Hill et al. 2004). In Maine, winter holds the greatest potential for large, destructive waves.

As surface wave energy is dependent on the intensity, durations, and fetch of the winds, the orientation and aspect of a bluff site is important. A strong tendency was demonstrated for bluffs classified as Unstable and Highly Unstable to face to the south and east (Keblinksy 2003), an offshore-facing aspect vulnerable to higher wave energies. In Maine, storms, protracted rain, and rapid snow melt are episodic triggers of coastal retreat, likely due to the added water-weight and increased pore pressures (Berry et al. 1996).

It is important to note another feature born from the climate patterns described above. Sea ice is known to collect and briefly take a sustained hold in sheltered inlets during the coldest time of year (**Figure 2.3**). The presence of sea ice is expected to have mixed effects: on one hand, ice will block wind-driven waves from reaching the bluffs; in contrast, however, tidal flux and larger swells might mobilize the ice accumulations and abrade the shoreline at their landward edges.

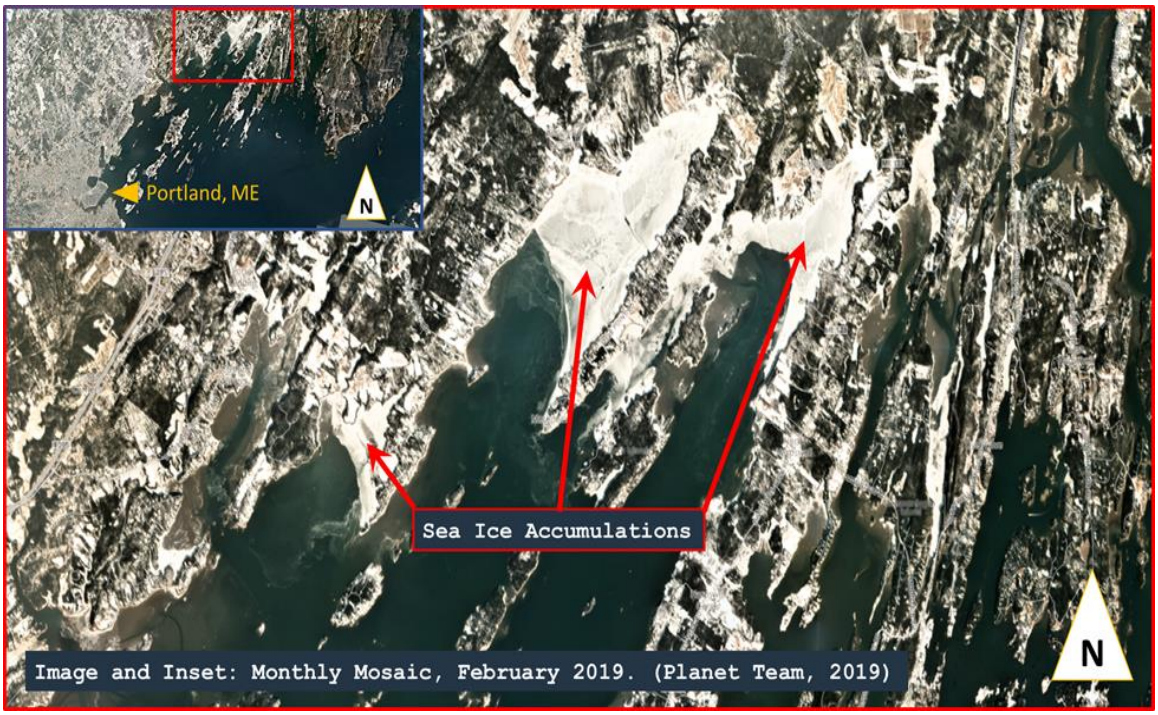

Figure 2.3. Sea ice in Casco Bay, Maine, February 2019.

Much of the ice is accumulated in the northern termini of the major wind-fetch corridors defined by the regional islands and peninsulas, suggesting that it is gathered from the bay and brought into shore by wind and waves. This is consistent with both the seasonally characteristic wind and wave directions and the aspect of unstable bluffs discussed in the text.

Satellite imagery data provided by Planet Labs of California. Annotated here.

Casco Bay, Maine

Southern Maine has a mixed-energy shoreline with wave energy strongly governed by the fetch limitations and parallel alignment of the peninsular bedrock outcrops (Keblinsky 2003). Casco Bay, bounded by Cape Elizabeth to the southwest and by Small Point to the northeast is often referred to as a drowned coast (Johnson 1925), featuring many islands and indented, compartmentalized coves (**Figure 2.4**). The elongate nature of the sheltering islands and peninsulas creates long fetches coincidentally parallel to dominant wind directions (SW, NE), focusing wave erosion and governing sediment transport (Keblinsky 2003) on unconsolidated sediment outcrops. The exposed bedrock exerts control by shaping coastal compartments and refracting waves. This affects the likelihood that wave energy will be able to

build in a given setting and act on a bluff. It is no coincidence that the shorelines of the most seaward islands in Casco Bay are bare rock and that most bluffs exist in sheltered coastal indentations; the mud flats are found here too. It is important to note that the bedrock coast of Maine, for the most part, is not actively eroding (Kelley 2004) and is considered unyielding within the timeframes of this study.

One colloquial theory holds that the bay's name is derived from the Abenaki name *Aucocisco*. *Aucocisco* is translated not only as 'place of herons' but also, fittingly, translated as 'muddy,' (Caldwell 1982). In contrast to the bedrock, the soft sediments that make up Maine's coastal bluffs are far more vulnerable to erosion. These sediments were deposited during the late marine transgression accompanying deglaciation by the Laurentide Ice Sheet (Thompson 2015). Till blankets the landscape except where buried by marine mud, which covers much of the coast of Maine, running inland up river valleys and draped over bedrock outcrops (**Figure 2.5**). Along the coast, this is a stretch of nearly one thousand six hundred kilometers of soft shoreline. The dichotomy of rock and soft mud in the landscape make the evaluation and prediction of hazards more complex. The instability of the bluffs and the many degrees of unknown thresholds for failure poses great risk to private, commercial, and industrial development along Casco Bay. Again, with such sharp contrast in resilience to the adjacent bedrock, the soft cliffs are expected to be the most responsive to increasing sea levels, but precisely how they will respond is uncertain.

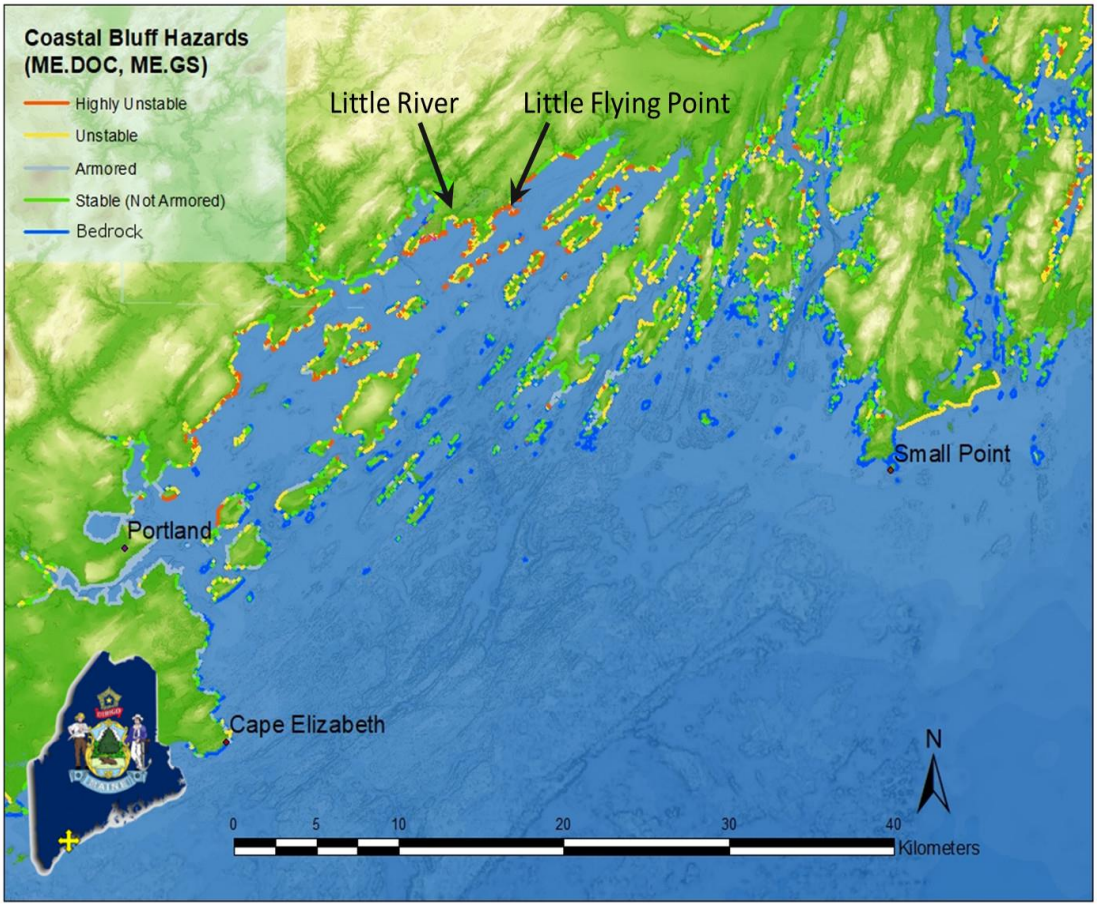

Figure 2.4. Bluff Hazards in Casco Bay, Maine. A map of Casco Bay marked by the Coastal Bluffs and Landslide Hazards classifications ([Map Series] Maine Geological Survey, 1998-2006), described more thoroughly in the text.

Casco Bay is bounded by Cape Elizabeth to the southwest and by Small Point to the northeast. The study detailed in this thesis takes place primarily at Little River and Little Flying Point (marked top-center), near Freeport, ME. Portland is marked because it is Maine's most populous city. Note the many elongate islands and peninsulas that govern the landward reach of Casco Bay. Note also the blue-colored bedrock shorelines are generally on the most seaward loci; red and yellow unstable shorelines are in the inner, sheltered regions.

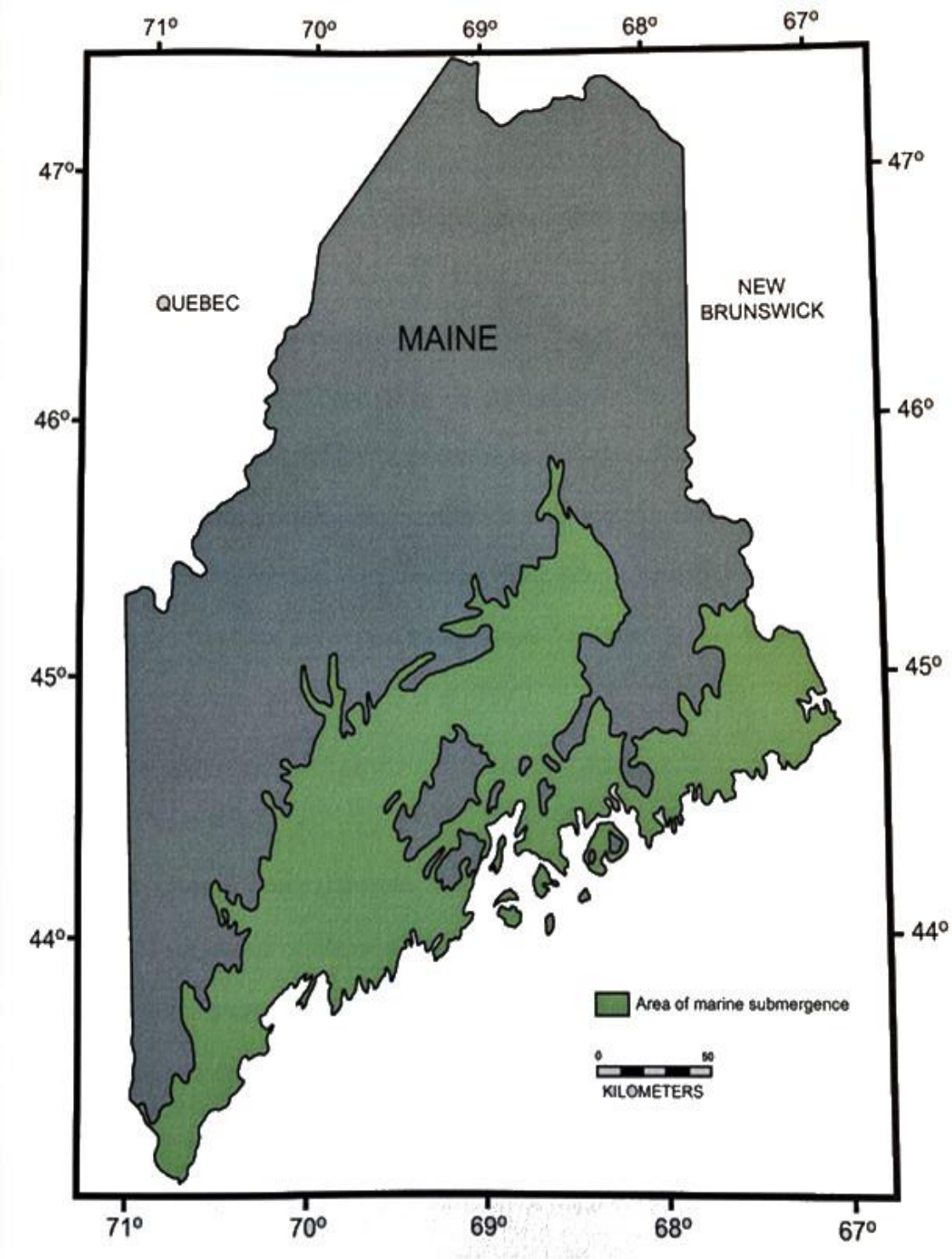

Figure 2.5. The Extent of Marine Transgression in Maine. Shown by the area of marine submergence during the sea level high stand ca. 12.8 kya. From Belknap et al. (1989), modified after Thompson and Borns (1985) and modified by Keblinsky (2003).

The Presumpscot Formation

The Presumpscot Formation (Bloom 1963; Thompson 2015; Belknap and Kelley 2015) is a stratified deposit of glaciomarine sediment deposited as a consequence of isostatic crustal depression between 15,000 BP and 11,000 BP (Borns et al. 2004). At this time, marine transgression brought sea level to its relative high-stand, against the terminus of the retreating Laurentide Ice Sheet. The presence of buried DeGeer moraines, arctic clams, and occasional dropstones are indicative of the marine-terminated glacier environment that persisted along the coast of Maine during an interplay of local sea level and the isostatic rebound of the land itself (Thompson and Borns 1985) (**Figure 2.6**).

Glacial milling of the region's metasedimentary bedrock produced the great volumes of rock-flour (Kelley 1989) that make up the Presumpscot Fm., delivering and distributing it subaqueously in the low-energy waters that were probably insulated from atmospheric disturbance by sea ice. Following glaciation, isostatic rebound led to a fall in relative sea level 60 m below its modern position (Belknap et al. 1987, Kelley et al. 2013). This left the Presumpscot Fm. quasi-stable but unsupported; the Presumpscot Fm. is a blanket of unconsolidated and geotechnically sensitive sediment. When subject to bluff erosion, it is subject to slump failure. Sea level has risen since its lowstand, and continues to rise, cutting back the glacial mud as a ravinement unconformity throughout the area (Belknap et al. 1989, Barnhart et al. 1997, Kelley et al. 2004).

When working to understand the evolution of Maine's coastal bluffs it is important to consider the relative weakness of the Presumpscot Fm. rock-flour clays, their inherent sensitivity to displacement by water and their low shear strength (reported in one measurement, for example to range from 24 kn/m^2 to 155 kn/m^2 at the oxidized surface and 10.3 kn/m^2 to 72.2 kn/m^2 below.) (Amos and Sandford 1987). Amos and Sandford include the caveat that the effect of fissures that occur in the surface stratum is likely not reflected in their measurements and that the strength contributing to stability is likely to be less than the values reported. There is also notably little to adhere these sediments to the bedrock ledge

or to naturally cement them in place. The micaceous, fine sediments, with an extremely low permeability, already hosting a high water-content, yield readily as a consequence of their low shear strength. Andrews, 1987, reports that the water content of the Presumpscot Formation near the Portland area is around 42%, increasing slightly with depth, and that the "stiff crust" at the surface has a lesser content of around 20-25%. The boundary between these two conditions may play a role in surficial slope failures described later on.

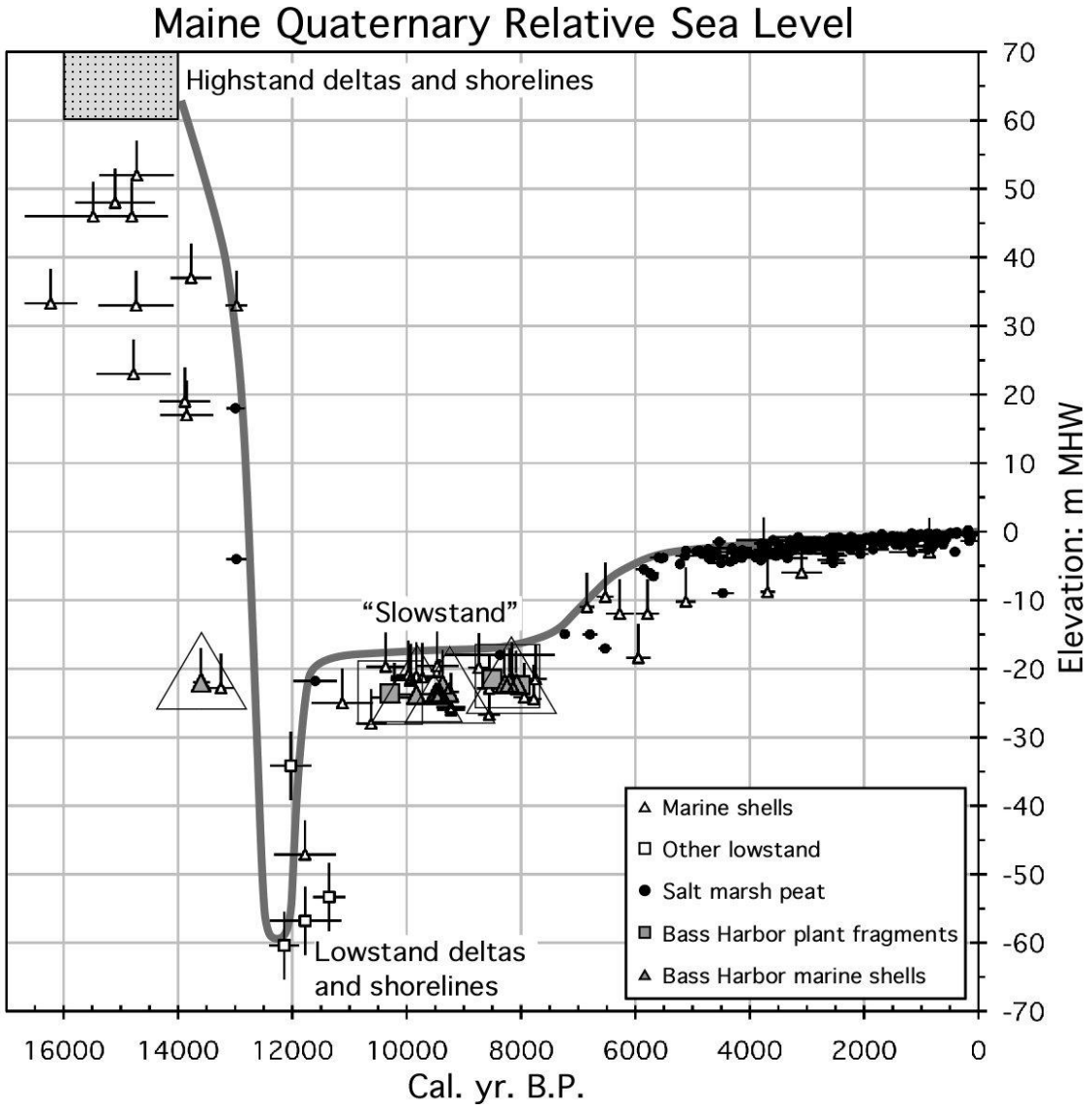

Figure 2.6. The Relative Sea-Level Changes in Coastal Maine. Quaternary period subsequent to the Wisconsinan deglaciation. From Kelley et al. (2013).

Much of the sediment is well preserved: found as un-weathered, fine grained silts and clays with sand and some larger clasts, reflecting the composition of deconstructed, pulverized Maine granites and metamorphic rocks from inland (Thompson 2015, Kelley et al. 1989). The mass and widespread distribution of the Presumpscot Fm. demonstrates the erosive capabilities of a glacier's passing. Depositional volumes vary across the extent of the formation due to the lively nature of tidal glacier margins during retreat. As such, the soft shoreline's distribution is not uniform and consequently its

sensitivity to erosion will vary by site and by chance, presenting another challenge for modeling and forecasting efforts. The contrasting strength of adjacent bedrock, however, is significant enough to consider it invulnerable in this context, and it may serve as useful boundaries for model development. Yet the depth to bedrock is not everywhere the same (Berry et al. 1996).

While silts and clays tend to interlock it is important to note there is little to no chemical source, such as lime or iron, present here to bind the formation's sediments (Andrews 1987). Therefore, the material strength of a bluff is primarily governed by pore-pressure and saturation of groundwater in addition to height and steepness of exposures. The introduction of excess water, thus, may provoke dramatic failure. The substantial size and significantly high relief of the deposits, characterized by low coherence overall as well as an observed history of instability, warrant focus on imminent landslide hazards and chronic coastal bluff erosion in the long-term.

Landslides in the Presumpscot Formation

In order to better evaluate the geohazardous conditions of the Presumpscot Fm. it is necessary to examine the nature of the soft deposit and its expected response to rising seas and changing shorelines. Its weakness is inherent and being so prone to failure has, unsurprisingly, lead to many landslides throughout Maine's recorded history. The Maine Geological Survey curates case studies of eleven notable landslides from 1868 to 2010 for the public on their website: <*https://www.maine.gov/dacf/mgs/hazards/landslides/case/case.htm*>.

Not all landslides in the Presumpscot Fm. are coastal. While management of riverbank erosion hazards is beyond the discussion in this work, riverbank failures are a common occurrence and can be readily associated with persistent undercutting by the rivers that define them. The smaller slides damaged roads and trails or led to the condemnation of adjacent property. The largest was a 20-accre mass movement that impounded the Presumpscot River (the formation's namesake) resulting in a major flood.

Unfortunately, coastal bluff erosion has not been as easily paired with such a clear cause and effect as that of a coursing river. However, occasionally some triggers can be determined. In Brunswick Maine, 1997, a contractor piled a load of rocks on a very steep, nearly un-vegetated bluff and it led to catastrophic bluff collapse. Earlier, in Gorham, Maine in 1983, a landslide eliminated a property that a later engineering study demonstrated resulted from the load of a gravel road laid on it (Gerber 1983, Novak et al. 1984).

While the examples are dramatic, recall **Figure 2.1**, the roughly decadal period of time that would pass between each event undermined the ability for such cases to resonate with the public. When the bluff stability maps were first produced they did not directly present the threat of large landslides because such events were deemed too infrequent to be evaluated quantitatively along the length of the Maine coast (Kelley and Dickson 2000). Instead, a legend and accompanying exemplary photographs of the varying hazard types were provided with the stability classifications so that the public could recognize concerning erosion activity on their own. However, for fear that the stability mapping would be fundamentally incomplete without acknowledging its greatest hazard, the map series was clarified. Basic guidance on landslides was presented as a consequence of scale; a new map feature for Landslide was designated along all stretches of the coast with bluffs over 6 meters (19.6 feet) in height (Kelley and Dickson 2000).

Land Use and Development

Of historical note, the Presumpscot Fm. provided the foundation for a large brickmaking industry in southern Maine during the late 1800s. Nearly one hundred brick plants produced nearly 100 million bricks per year from the glaciogenic mud (Caldwell 1998). The brickmaking industry has since faded, but human development remains worrisome as the sea-side bluffs of Casco Bay are coveted as outstanding real-estate (Belknap and Kelley 2015a, b).

Surface loading by a structure can lead to failure in the Presumpscot Fm. (Novak et al. 1984, Sandford and Amos 1987, Foley 2009) while the removal of rooting vegetation, sometimes just for the sake of a better view, also jeopardizes the stability of a slope and requires careful consideration (Kelley and Dickson 2000, Giadrossich et al. 2019). New introductions of water and weight to the bluff, such as a septic system or lawn irrigation, can also provoke erosion by driving up the groundwater pressure gradient. Groundwater saturation and the consequential increase in pore pressure within the bluff, primes the mass for movement by drastically reducing the shear strength within the slope. The Rockland landslide of 1996 (**Figure 2.1**) provides a useful demonstration: the mobility of the saturated sediments during a failure event is seen clearly in the lobate form of sediments spread out ~400 feet (~122 meters) seaward from the source at the toe of the slump/slide. Where the landslide occurred, the clay thickness was reported to be 35-45 feet (10-14 meters) (Berry et al. 1996).

Trends in Sea Level Rise

Although local, relative, sea-level has changed dramatically since deglaciation, the Maine coast has endured a gradual incursion of rising waters across the past several thousand years (Gehrels et al. 1996). Recent observations, however, indicate that the local rise in the sea is accelerating beyond the trends of the past few millennia (Gehrels et al. 2004) (**Figure 2.6**). It is expected that these rising seas will further aggravate the sensitivity of Maine's coastal bluffs and potentiate the erosion cycle. Recording the rate of coastal response will be a critical component of understanding and conceptualizing a future mitigation strategy. A century of rising sea level has been recorded in Portland, ME (**Figure 1.2**). It must be accepted that sea-level fluctuates over great spans of time and when preparations are made for long-term sea-level rise now there are often benefits (though not always to those who will experience losses). Formerly remote regions of Maine's coast are experiencing growing numbers of vacation and permanent home constructions. The combination results in an increased public hazard and more pressure on

management. Shoreline adaptation strategies developed *now* in consideration of the changing nearshore system will begin to protect against any short-term surges as soon as they are implemented.

Shoreline Retreat

Shoreline retreat is a natural response to rising waters (Johnson 1919). While the physical marine processes acting on the shore could be considered common across all intertidal environments, including fluctuating seasonal influences, the variety of geological make-up and history makes for different geomorphological expression from site to site. Waves exceeding mean sea level will act above the present shoreline and force its retreat over time as a consequence of repetitive erosive events. Waves occasionally exceeding the high-water line deliver higher-than-average energies to the present shoreline and with that they result in exacerbated erosion. These episodic interactions enhance bluff erosion by removing extra sediment from the bluff toe and affecting deposition to the intertidal zone, where more consistent erosive processing and reworking occurs. In general, bluff erosion is likely to continue where it has already occurred and in areas that share similar compositions which have been recently exposed to similar environmental stressors.

Slope-failure episodes occur irregularly over time, but new sediment delivered to the intertidal zone is persistently processed by regular tidal flooding and draining. Chronic mass wasting and terrestrial processes continuously supply some amount (not yet quantified) of sediment from the bluff face to the intertidal zone. Sediments brought beneath the high-water mark is more vulnerable to removal from the area (Hay 1988, Smith 1990). As described by the bluff erosion cycle model (Kelley and Hay 1986a, b), constant erosion below the high-water line leaves the bluff face unsupported and slumping in compensation, resulting in a conveyance of material downslope. The newly introduced sediment from such slope failures supports mudflat and salt marsh environments while affording a periodic and natural defense for the source bluff behind it. A slump of significant size will resist wave energy and redirect incoming water, preventing erosive energy from reaching the landward body of sediment directly behind

the slump (Kelley and Hay 1986a, b). However, it will focus energy to either side of the mass, as a seawall might, making adjacent landforms more susceptible to attack.

Uncertain Timing of the Bluff Erosion Cycle (*BEC*)

The timing of individual phases of the Bluff Erosion Cycle (BEC) remains uncertain. Observations show that bluff loss continues at an unsteady rate even in areas where large landslides are not observed. Bluff loss continues unpredictably and nonuniformly. Close examination reveals that smaller events occur in a consequential fashion similar to the large events, and in the end, the result may be long-term retreat rates equal to areas suffering catastrophic landslides. Quantifying this activity will depend on a regular observational pattern from which erosional behaviors may be timed.

The Little River (**Figure 2.4**) bluff exhibits slopes in many disordered phases of the bluff erosion cycle simultaneously (**Figure 2.7**). Whether or not a given bluff moves smoothly through each stage of the *BEC* or whether its progression may stall at times remains unclear. Due to the relatively low frequency of large, episodic, landslide failure events it is also unclear as to whether or not such occurrences propagate laterally along a shoreline more readily than directly landward (retrogressively) instead. As the *BEC* presents the concept in only two dimensions, more questions arise for the interaction between adjacent slopes in different stages of failure along a given bluff face. What could be the appropriate context in which a full cycle of the *BEC* occurs? At what scale? At the creeping toe of a slump deposit, already in failure and detached from its parent bluff, the cycle can be seen playing out in imitation of its entirety without the bluff top retreating at all. Surely this processing of post-failure materials by minor *BEC* revolutions leaves the parent bluff over-steepened and prepared for more significant failure. But without a more significant failure can any major revolution of the *BEC* be said to have occurred? Is there a critical threshold of mass necessary for a failure deposit to persist long enough in the intertidal zone (*i.e.*, colonization by halophytes) to be considered tributary or limiting to the *BEC* progression?

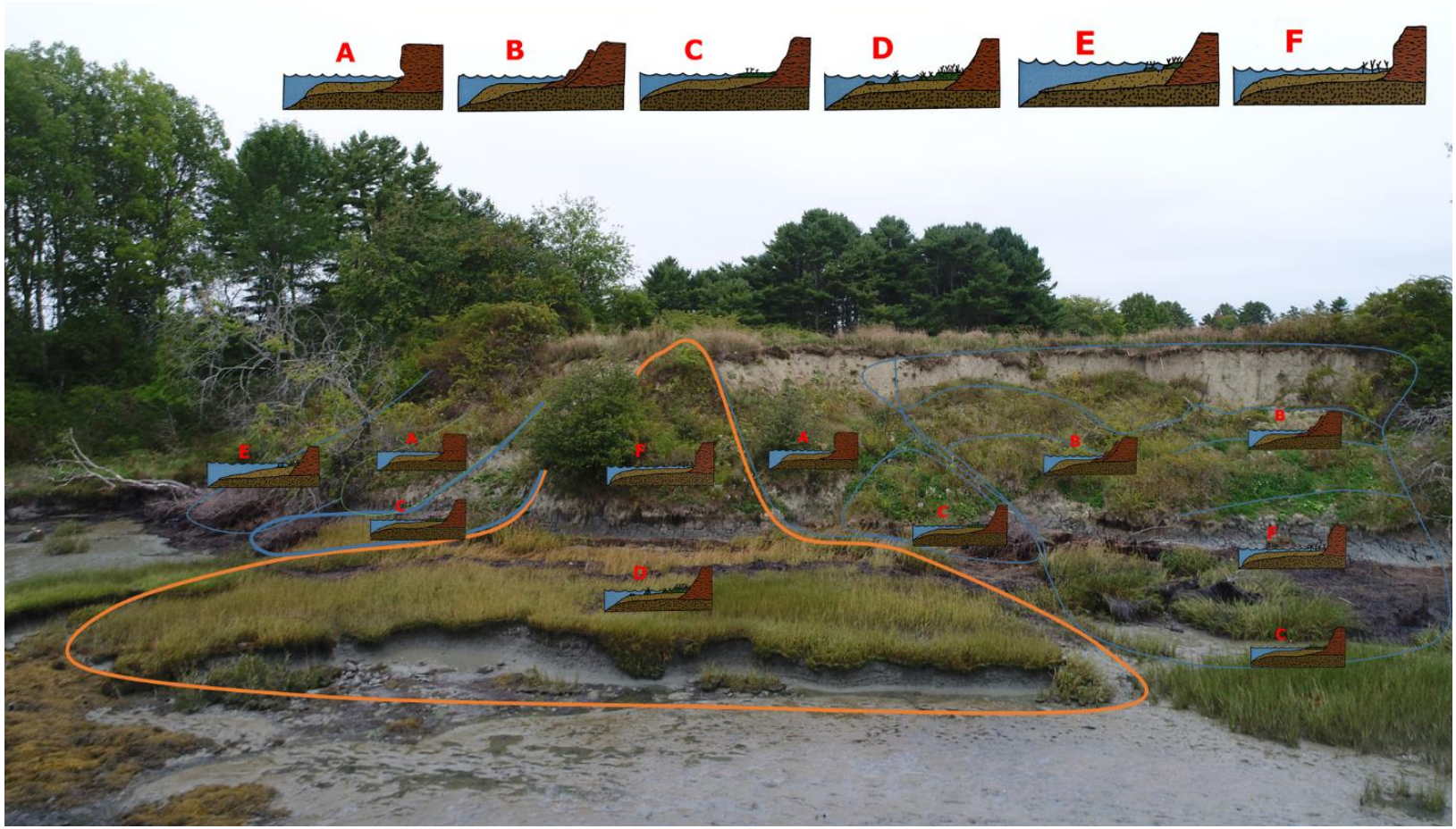

Figure 2.7. One Bluff Exhibits Many Phases of the Bluff Erosion Cycle. Little River, Freeport, Maine, as seen on September 19, 2017. One bluff can be seen exhibiting slopes in many disordered phases of the Bluff Erosion Cycle at once.

Mechanics of a Landslide

Keblinsky (2003) determined that most dominant slide types exhibited by Maine's coastal bluffs were earth/soil flows and more minor slumps. Changes in slope geometry, from top to bottom as well as laterally, changes the distribution of stress and therefore the conditions required for a sensitive mass of bluff material to fail. One slide may disrupt neighboring masses and soon trigger adjacent failures. Sandford and Amos (1987) found this to be true of the Gorham Landslide (1983), describing the large retrogressive slide as having started with the failure of one block that was significantly smaller than the rest of the material that followed it (Sandford and Amos 1987, p.14).

When wet, the Presumpscot Fm. has great plasticity, especially in contrast to the brittle, oxidized, and fractured yellow-brown sediments often found at the top of the unit (Sandford and Amos 1987, Andrews 1987). It is worth noting that the twice daily incursion of water against the coastal bluffs by the tides keeps base-sediments hydrated while the material further upslope is left to dry as often as atmospheric conditions allow (**Figure 2.8**). Internally, the low permeability (on the order of $5*10^{-8}$ to $1*10^{-7}$ cm /s, Andrews 1987) of glaciomarine silts and clays reduces the permittivity of groundwater. The broad and flat top surfaces of the bluffs collect great amounts of rain and meltwater which is not readily evacuated once it is absorbed, allowing pore pressures to rise by saturation. Natural stratification suggests that permeability is different in the horizontal and vertical directions, which may lead to perched lenses of water and regions of uneven pore pressures. Perhaps the corruption of the surface materials, by weathering, oxidation, soil formation, bioturbation, etc. helps to create a distinct and more easily separable rind-layer of sediment from the insulated internal sediments of the bluff body. Recall, that Andrews (1987) noted a "stiff crust" at the surface of the Presumpscot Fm. that had ~20% less water content than the gray clays beneath it. At the land/sea interface wave action can easily erode the compromised material, removing the support of the exposed bluff face. Shallow-depth sloughing downslope of the weathered and partially vegetated surface was a notably common occurrence.

Wave action in and of itself is not specifically correlated with landslides. And yet, undercutting and toe erosion reduce the amount of material over which the stress of the overbearing slope material is distributed and increases the bluffs sensitivity to normal stresses. This is described as a loss of the buttressing-effect. Further concentrating stress, whether by continued undercutting, weakening of the base, or by increased surface loading, provokes failure. Structural development and land-use modification is a prime suspect for slope-failure by surface loading. But excessive loading is not a strictly human factor, as heavy rainfall, large trees or snowpack can contribute extra mass to the bluff. Added weight to the bluff and an internal lubrication of the micaceous sediments by groundwater allows for greater plastic deformation at depth. When a sufficient pore pressure is exceeded a shear-slip plane may develop, decoupling large portions of surface material from the parent bluff-body and resulting in a collapse.

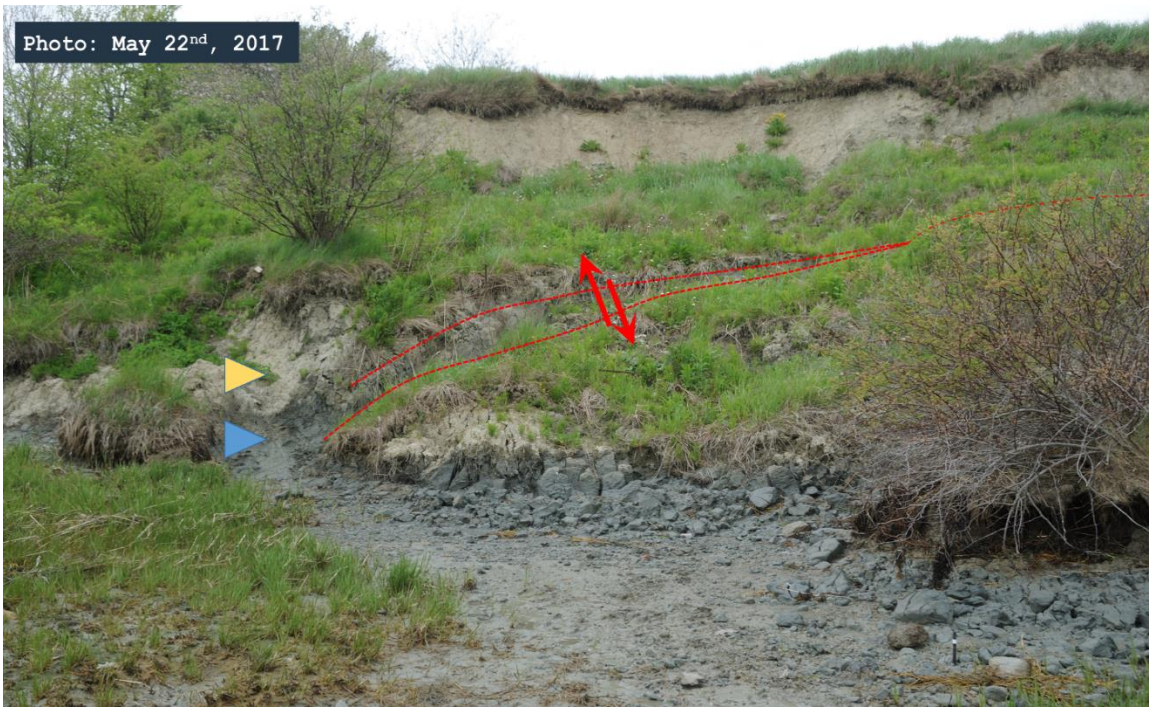

Figure 2.8. The Contrast Between Weathered Surface Materials and Maine's "Blue Clay." Little River, Freeport, Maine.

The contrast between the weathered surface materials (yellow arrow) and the namesake "blue clay," of the wetted and freshly exposed (blue arrow) Presumpscot Fm. sediments is featured throughout the photograph. A recent slump of vegetated surface material that has detached (red lines) from the slope can also be seen as having pushed forward the soft sediments in its path.

Continued straining along the developing slip planes under stress within a bluff slope potentiates the significance of the particular slip plane and likelihood of full and sudden detachment. Faults along these internal surfaces conduct groundwater more efficiently (due to the alignment of sediment grains with straining motion), which further softens the material. In well-developed cases groundwater that flows more efficiently through these features can entrain sediments and excavate their flow-paths. Pipes and groundwater springs can develop as paths of least resistance, aiding in the decoupling of and further weakening of the slope. This undermines support and leads to further slippage, exacerbating sensitivity and propagating the internal planes of failure. Repeat observations of the study sites showed that some of the most profuse slope-face springs marked the edges of portions of the slope material that failed later on.

Further complicating the interpretation of the geohazard, there is poor understanding of the site-specific internal compositions of the bluffs beyond the context of their depositional history and glacial-milling as an original sediment source. There is no practical way to comprehensively determine the internal make-up of individual bluffs with the necessary resolution that would show local heterogeneities in the sediments that may govern site-specific failure conditions. Previous work with ground-penetrating radar in the area was unable to detect subsurface desiccation or tension cracking, and the salt-laden fine sediments of the formation are poorly suited to exploration by ground penetrating radar (*GPR*) methods (Jacobacci 2014). Adding to the challenges of modelling these landforms is the difficulty in determining the depth to bedrock between the bounding bedrock peninsulas. It is notable that Berry et al. (1996) cite terrestrial seismic evidence that the two Rockland slides occurred over the thickest sections of local glacial marine material.

Agents of Erosion

Nearshore Wave Action

Much of the ecologically important erosion that is threatening property is commonly attributed to nearshore waves. Incident waves, those that move onshore to strike the coast, deliver their energy when reaching the opposing shoreline and dislodge sediment out of its original position. While a portion of this energy is lost to breaking waves in the shallow waters before making landfall, momentum carries water and sediments as wash that continue to act until all of the incoming energy is dissipated and suspended material is allowed to rest (Komar 1983).

Wave action is not the sole cause of bluff erosion. The multitude of factors that govern the stability of a coastal bluff such as its: 1) composition, 2) water content, 3) depositional history, 4) degree of development, and 5) the bluff's size, are important variables. Many seek to manage wave action when addressing the erosion of their property, associating the obvious and "ugly" scars of wave erosion with loss and working to halt its cause. But it is necessary to understand that nearshore wave energy, both as

an erosional actor and a popular target of management, is tangential to the inherently mobile unconsolidated sediments that oppose (or fail to resist) its impacts. It will also be important to acknowledge that managing wave energy alone is unlikely to remedy a problem-situation outright. Present strategies of shoreline management were deemed inadequate as damage and loss continues unmitigated (Kelley and Dickson 2000).

In the case of the tidal flats, residing within the bedrock bounds of the coastal compartments where the bluffs occur, there are a number of controlling factors that limit the influence of incident waves. The shoreline profile of a tidal flat is gentle and highly dissipative of incoming wave energy. The position of the tide will govern whether or not water is even present in appropriate volumes to carry such waves landward over the flat to reach the bluff. Both the depth of water and the fetch within a given embayment necessary for the generation of waves are transient properties time-dependent on the local tidal cycle. While seawater is absent from the bluff toe during a significant portion of the tidal cycle it relieves the bluff of wave attack but enhances the groundwater drainage gradient for some time. Sediment distribution over a tidal flat is therefore controlled by the oscillation of the tides and their associated ebb and flood currents (Reineck and Singh 1973).

Arguably, within the intertidal zone, the very presence of such fine sediments as those sourced from the Presumpscot Fm. suggests a lack of significantly erosive wave energy in these areas. The mudflat would be completely removed by a higher-energy wave regime, as exists on the outermost, exposed coastline (**Figure 2.4**). The semi-diurnal tide in the Gulf of Maine brings water in excess of mean sea level twice daily and it is normal for water to spend a part of each day above Mean Higher High Water especially when elevated by atmospheric or surging effects. Observations show that the water level reaches and acts upon the toe of the bluffs for a period of time before the peak of high tide is reached and subsequently for a period of time afterwards. This is supported by the presence of *Spartina alterniflora* at the bluff toe but a notable lack of *Spartina patens* that cannot withstand the same prolonged

inundation by seawater (Davis and Fitzgerald 2003). High tide leaves a clear mark of its previous reach in other ways too: by hydrating the sediments and by depositing wrackline detritus right up against the bluff (**Figure 2.9 a, b**).

Figure 2.9 a. The Reach of High Tide. The mark of the high tide (yellow dashed line) as a clear and level cut dividing two differing environments. Note both the wet and dry portions of an old landslide deposit (blue shading) as well as the seaweed dangling from the branches of the overhanging tree (unmarked).

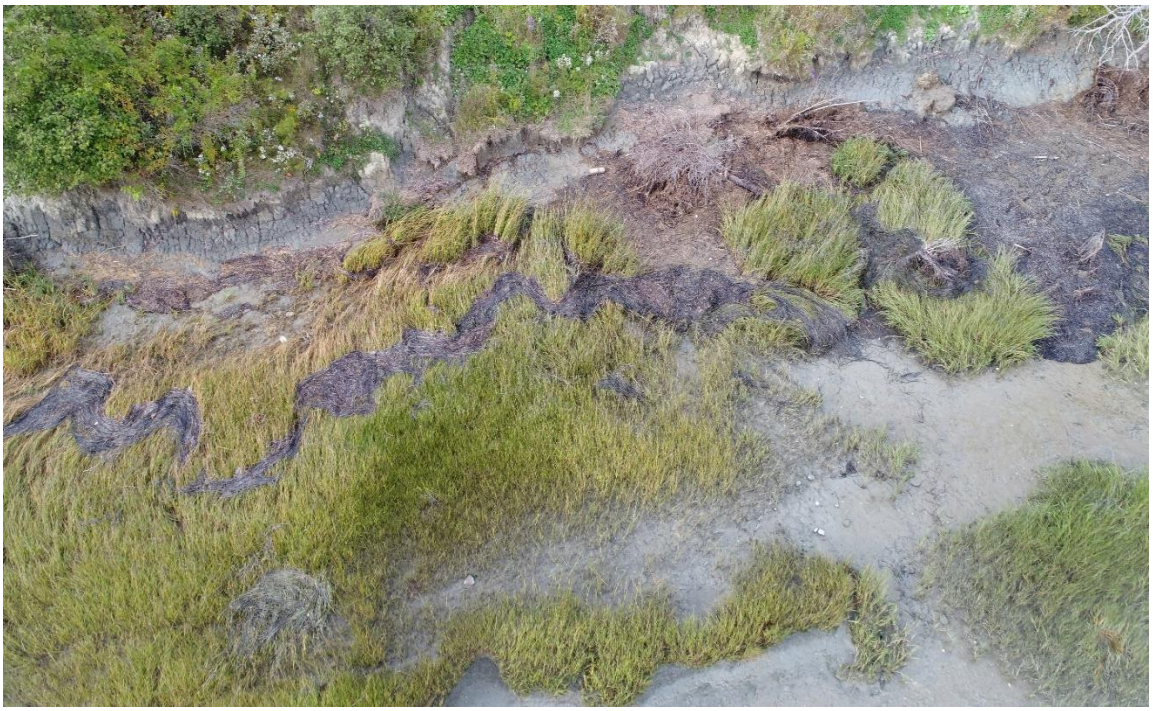

Figure 2.9 b. While some detritus is caught by the filter of marsh grasses, the water's landward reach is clear in this UAV image. Note the bluff-toe erosion directly behind the grasses. The span of this image is approximately 30 meters from left to right.

During high water events a significant depth of water is present to allow waves to act on the bluff directly. A consistent tidal current may develop, and the available fetch is fully realized to the extent that the coastal compartment allows. It is during this time that sediments at the bluff toe are most susceptible to further processing and transport by nearshore wave action and currents, as seen by sediment plumes sourced from the bluff toe (**Figure 2.10**). The current water level; intertidal profile; and coastal compartment geometry, with respect to wind patterns, all play a role in whether or not waves will act on the bluff in a given moment. A better understanding of the residence time of water acting against the bluff toe, with site specificity, will support modeling efforts and coastal resiliency planning.

The constant washing by the tidal cycle sustains an ongoing coastal erosion process and is a fundamental control on the movement of material from land to sea (**Figure 2.10).** In this way processes occurring in the intertidal zone still influence erosion well above the high-water line. Steady removal of sediment from the bluff toe over time will over-steepen the base and allow for more significant collapse as a compensation response; drawing sediments downward to the shoreline. The effect of chronic nearshore erosive processes is thought of as preparatory for slope failure (Lawler 1997, Neitzel 2014), leaving the bluff more sensitive to collapse by undermining its base.

Wave energy and sediment transport at the bluff toe is also influenced by intertidal ecology. The near-constant presence of salt water inhibits the growth of slope-stabilizing vegetation and allows only halophytes such as *Spartina alterniflora* to take hold. Significantly large slumps from the bluffs, providing a sediment platform seaward of the shoreline, are often colonized by marsh grasses within the first growing season. While it is unclear how long bluff toe sediments are stored in fledgling marshes, continued erosion of the bluff may provide sufficient material for sustained vertical marsh growth down-drift and accommodated (if not surpassed) by rising seas (Kelley et al. 1988).

The development of small fringing marshes along the base of bluffs affords some protection by attenuating wave energy and stilling water. A wave breaking over vegetation is locally more turbulent but

simultaneously the energy carried in the turbulent water is more rapidly and evenly dissipated, resulting in less sustained lift or erosion of sediments, which quickly resettle in the immediate area. However, the observation of bluff toe erosion directly behind fringing marshes (**Figure 2-9 b, Figure 2-11**) raises some concern as to the lasting efficacy of fringing marshes on wave attenuation when considered in the context of an increasing rate of sea-level rise. Will fledgling colonies of fringing marshes be capable of sufficient accumulation and upwards growth to keep pace with accelerating local sea-level trends (Wood et al. 1989)?

Figure 2.10. UAV Image of a Sediment Plume. Little Flying Point, Freeport, Maine, as seen on October 28, 2017. *Altitude ~70 meters*

UAV image of a sediment plume advecting from an eroding bluff (scarp visible in the center of the photo). The bright objects in the top-right corner of the image are sea-going kayaks at a commercial recreation and training center provide a rough sense of scale.

Figure 2.11. Erosion of the Bluff Toe Directly Behind a Fringing Marsh. Little River, Freeport, Maine, as seen on September 19, 2017.

An example of erosion and over-steepening of the bluff toe directly behind the seaward fringing marsh. The seaward prominence of this portion of the bluff, and the ragged edge of the marsh grass colony, suggests that the marsh has at least to some extent protected the bluff behind it in keeping with the expectations of the bluff erosion cycle. However, the toe erosion continues. It may be due in part to sea level rise out-pacing growth of the marsh and more frequently overtopping it. Frequent slope failures on either side of the marked (orange line) region also suggest that while protecting one portion of the bluff, the marsh has been redirecting erosive energy to either side.

Local Sea Level Rise

"Sea level continues to rise and is ultimately responsible for the ongoing retreat of the coast." (Kelley and Dickson 2000, p. 48). Without a rising sea-level the envelope of potential nearshore erosion would remain stationary, allowing a more stable slope to develop and halt the retreat of the bluff. While small waves, even just the presence of flowing water, can winnow sediment and undermine the bluff toe, a rising sea level elevates the platform on which waves act, sustaining the erosion. Accelerating sea-level rise will increase the bluff erosion. Still, a large-scale erosional event generally takes less time to occur than the time in between events (Kelley and Dickson 2000). More concerning is the occasional

coincidence of astronomically high waters with that of strong storms, episodically exaggerating the water's reach and intensifying the erosive potential of nearshore wave action.

When high water encounters the toe of the bluff it cuts into the soft sediments and provokes slumping. Waves working on the slump-deposits resuspend materials readily and wash away the freed material over time. The continual digestion of sediments delivered downslope from the bluff by high tides and high-water events is an unyielding process as long as local sea level continues to rise above its present reach. With rising sea level more high-water events are expected, and a greater water depth to host incident waves by prolonged inundation implies a greater erosive potential and carrying capacity for vulnerable sediments.

Terrestrial Processes and Groundwater

Terrestrial processes are potentially as significant to bluffs as the influences of marine processes are. The eye-catching surface expression of nearshore erosion often leads to a conclusion that favors the influence of nearshore waves as the sole culprit while distracting from internal geological troubles. Yet the majority of a bluff face is considered hydrologically disconnected from the present-day intertidal zone (Neitzel 2014). The high-relief bluffs provide an optimal point from which groundwater can exit the soil profile and erosion results as seepage and lateral flow is sufficient enough to entrain particles (Wilson et al. 2006). Broad, flat bluff tops capture a large area of water and snow melt and fractures in the bluff surface open conduits for water to flow. Piping phenomenon and spring sapping effects are seen (**Figure 2.12**) most significantly in the spring season.

Rising groundwater pressures due to rain, snowmelt, excessive watering of lawns; agriculture and waste-water discharge; and rerouting by rooftops, roads, etc. can all raise the water table even in typically dry times. Removal of vegetation also heightens the local water table by inhibiting the uptake provided by roots and removing the dissipative nature of a canopy. Excessive groundwater within the bluff

simultaneously adds mass and lubricates the unconsolidated sediments, priming the material for movement by reducing its shear strength near the areas of saturation.

Slumping, faulting, and scarping tear away the bluff face, exposing the glaciomarine clays to surface run-off and groundwater release. Subsequent channelization results in more efficient erosion every time water passes over the surface. Water may cut behind mid-slope slump blocks (**Figure 2.13**) or work at a break in slope (say, from near-vertical to near-horizontal, where material has detached, translated, and rotated downslope) and exaggerate vulnerabilities at the interface between the more cohesive surface features and the soft hydrated clays underneath. Bluffs this unstable erode too rapidly to support fully-developed vegetation coverage that could possibly stall erosion.

There is also an observable trade-off with the expectation of stability that a partially vegetated surface tends to provide. The extra cohesion afforded by rooting only extends as far as the roots do, and sediments bundled in this manner hold no attachment to the unconsolidated material they overlay. The interface between root-bound sediments and the untouched sediments beneath may make for an ideal slip-plane. The extremely low permeability and cohesion of the underlying Presumpscot Fm. makes it susceptible to slipping when wet, and the portions of these sediments bound by root networks are frequently seen to creep or detach completely (**Figure 2.14**), tumbling down to the waterline.

Figure 2.12 a. Piping Phenomenon and Spring Sapping. Photos taken February 27th, 2017. Fast-flowing springs near the base of the bluff are marked by the red arrows. Scale bars in the left image are 1.5 meters in length. Note the clear contrast in coloration between the oxidized surface sediments and the unaltered formation freshly exhumed by winter erosion. Some recently liberated drop stones can also be seen at the base of the scale bars.

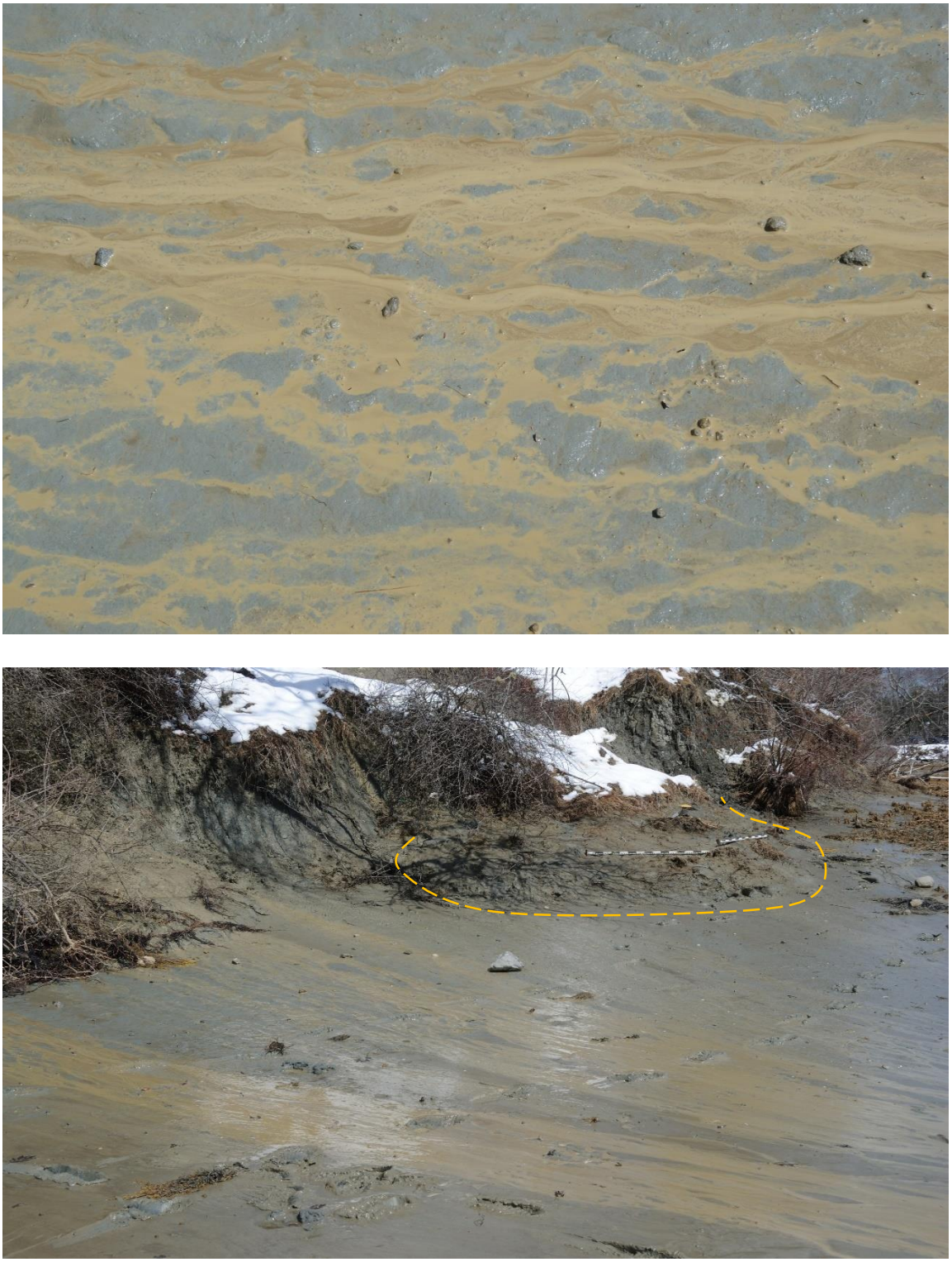

Figure 2.12 b and c. Photos taken April 2nd, 2017. Spring sapping and winnowing provide a colorful display of fine sediments as they are removed from the thawing bluff by seaward drainage. Note the recent splay (yellow line, second photo, scale bars = 1.5 m).

Figure 2.13 a-c. Mid-slope Slump Blocks and Tension Cracks. Breaks in slope behind slumped fault blocks (a, b), as well as associated tension cracks (c), present clear conduits for surface water to get into slip-planes and increase sensitivity to further slope failure.

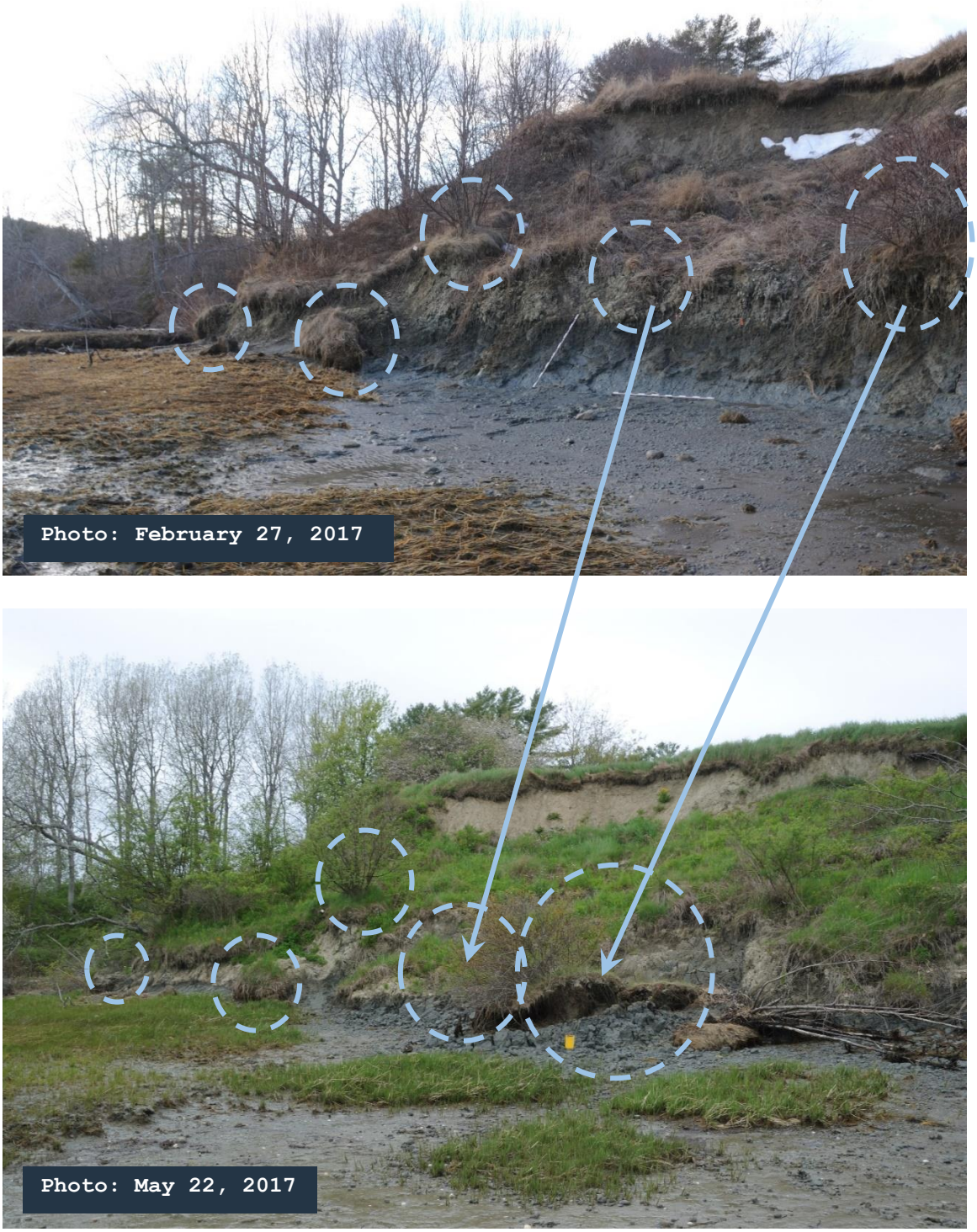

Figure 2-14 a. Vegetation Packages Sediments, Enhancing Removal. Little River, Freeport, Maine. Vegetation plays a more complicated local role on the bluff face than simply adding stability to the overall bluff. Here it is seen aiding in the removal of sediments by packaging them within their roots.

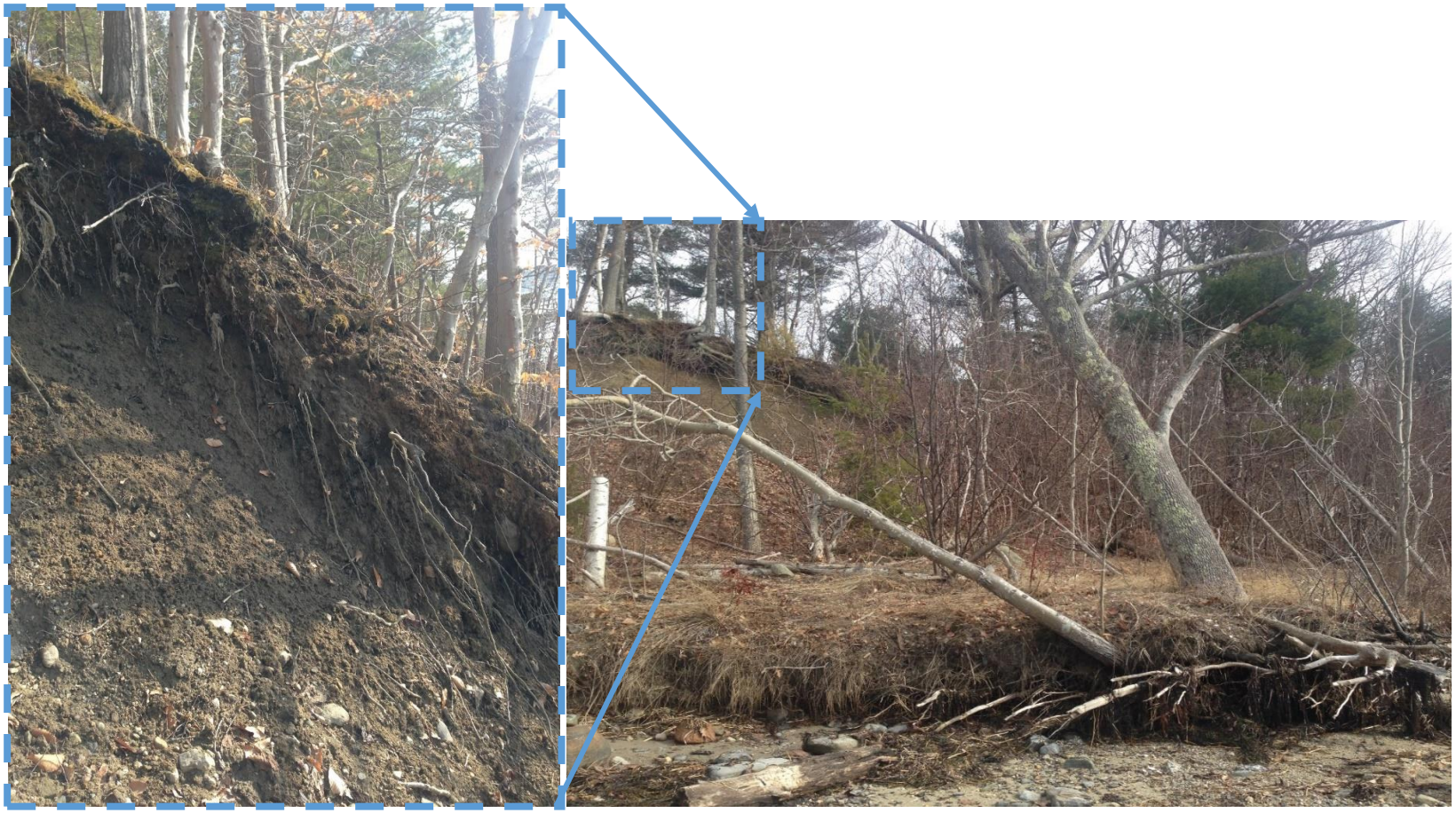

Figure 2-14 b. Underneath a bind of roots there is still just soft, unconsolidated sediment with little-to-no ability to hold surface materials fast to the slope face. Note the uniform thickness of the still-rooted run-out (right image) compared to the soil it detached from (left image). The newly deposited raft of sediment and roots now rests in the intertidal zone. It may afford protection to the till-bluff from waves, but it has also removed a significant amount of material from the slope and exposed a large surface area to weathering. Photos taken in the Fall of 2016, at Cousins Island, Yarmouth, Maine.

Seasonally Specific Agents of Erosion

Freeze-Thaw Cycling

The temperate nature of Maine's climate subjects the coastal bluffs to inconsistent conditions throughout the year. Frequent freeze-thaw cycles and wetting-drying fluctuations contribute significantly to weathering. On monitoring bluffs in the St. Lawrence Maritime Estuary, Quebec, Bernatchez and Dubois (2008) concluded that cryogenic weathering processes were responsible for 65% of the bluff erosion despite the common assumption that winter's influence was negligible. They also found that desiccation effects in summer influenced an average of 20% of the bluff erosion but on one particularly dry summer desiccation affected as much as 48%. Ultimately they concluded that waves and tidal currents mainly act as agents of clearing and "evacuation," of sediments that were primarily eroded by seasonal weathering processes (Bernatchez and Dubois 2008).

During periods of cooler temperatures, the freezing of groundwater binds bluff sediments and holds them fast (Carter and Guy 1988), but the thawing cycles are particularly disruptive to sensitive, unstable landforms (Kok and McCool 1989) such as Maine's coastal bluffs. Kok and McCool (1989) describe an inverse relationship between the shear strength of the material and the periods of freeze-thaw that it is subjected to, attributed at least partially to a consequence of the reduced interlocking of granular particles forced by each cycle of freeze and thaw (Dietrich and Gallinatti 1991). Neitzel's (2014) study of riverbank erosion, inferred that the likelihood of erosion increases as freeze-thaw cycles decrease a soil's bulk density. Freeze and thaw activity also causes spalling off the bluff face, evidenced by the accumulation of frozen talus as the base of the slopes (**Figure 2.15**).

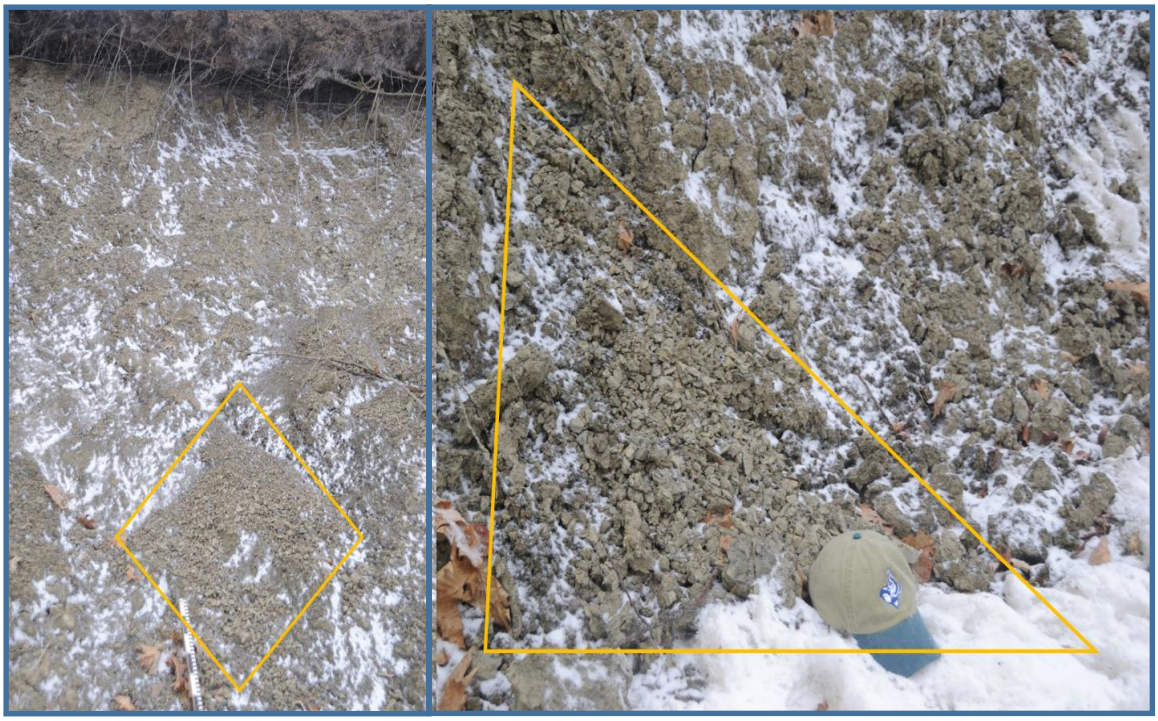

Figure 2.15. Accumulations of Frost-liberated Talus. Photos taken March 24th, 2017, Little Flying Point, Freeport, Maine.

Frost-liberated talus accumulating at the base of the bluffs. This is yet another seasonally governed mechanism by which material is removed from the bluff face and conveyed downslope. The two images exhibit different occurrences of the phenomenon, frozen clasts can be seen in greater detail in the right image. Note the ballcap for scale.

Spring Sapping

Hydrated as they thaw, the fine sediments of the Presumpscot Fm. become softened and expanded. At this time, they are at their most mobile, and vulnerable to flowing water. Spring sapping is widespread across the exposed face of the bluff (**Figure 2.12**); small mass movements are seen as fluidized flows; and fast-flowing water is seen piping from within the bluff. Internal mass loss may not be as voluminous as the amount of sediments sloughed from the surface, but could be expected to be consequential for the state of stability of the bluff later on.

Desiccation

After the bluffs have lost most of their spring water content, and temperatures begin to increase steadily from spring into summer, the material that has slumped, flowed, and splayed forward during the wettest, most plastic period of the year begins to dry in the sun. The aspect of bluff orientation and exposure, governing the extent of insolation periods, plays a role in how quickly the sediments may dry but the overall trend is towards desiccation. The expanded clays begin to contract and crack, and the exposed surfaces of the bluff become more brittle than ductile. The cracks and fractures in the dried clays leave the bluff toe vulnerable to hydraulic forcing during high tides or rainfall events. Observations of this effect and its consequences, are saved for later discussion.

Sea Ice

Perhaps less of a concern following a warmer future, but evidence suggests that sea ice in the area is one of the most influential actors on the bluff toe and nearshore environment. Movement of sea ice by wind and tide wears down surfaces it comes in contact with. Sea ice is notorious for its ability to abrade concrete structures and resisting the abrasion is a common technical challenge for artic operations (Hanada et al. 1996, Shamsutdinova et al. 2018). Recalling **Figure 2.3**, sea ice has been found to accumulate against bluffs in Casco Bay. A sufficiently thick covering of ice will attenuate incoming surface waves but the short window in which it accumulates here in Casco Bay limits the lifetime of a shorefast existence. Its buoyancy makes it destructive when carried by the rise and fall of the local tides. Sediments frozen on while the ice is at rest can be plucked when the ice is made to float, and mobile broken up masses of ice can be forcefully pushed and dragged by water up against the toe of the bluffs. This makes for an effective removal of toe materials already fractured and fragmented from the parent bluff by the warm and dry habit of the summer before. The shoreline profile of the bluff toe is found to be at its steepest following the seasonal visitation by sea ice.

Insufficient Historical Record Precludes Popular Approaches to Risk Assessment

As described earlier and detailed in the works of Deng et. al. (2017), Lentz et. al. (2015), and Hapke and Plante (2010), popular risk assessment and numerical modeling methods, mostly statistical, draw their strength from a robust and accurate historical record of past and present behavior. Such a record is missing from the coast of Maine. Without it there is little to no baseline for informing predictions beyond the LiDAR survey conducted in 2006 (from Elliot, ME, to Harpswell, ME) and 2010 (from Phippsburg, ME, to Calais, ME) (Maine Office of GIS 2016). Some alternative sources for historical data are discussed below.

Satellite Imagery

Analysis of satellite imagery as a means of risk-assessment at the shoreline has been ruled out at this time. Pixel resolution is the limiting factor. The Operational Land Imager (OLI) sensor aboard the Landsat 8 satellite provides publicly available imagery at 30 meters' resolution (visible spectrum) and 15 meters' resolution (*panchromatic*) (<https://landsat.gsfc.nasa.gov>). This resolution is suitable for observing the increase in land use and coastal development in the region but the present scale and rate at which bluff erosion is known to occur in Casco Bay is lost within the bounds of a single pixel from the Landsat 8 imagery. Higher resolution (down to the federal limit of 50cm/pixel for civilian use (https://www.aaas.org/resources/high-resolution-satellite-imagery-ordering-and-analysis-handbook)) imagery data is available from commercial satellite ventures but comes at a prohibitively high price and coverage in temperate mid-latitude regions is often incomplete or obscured by weather conditions; making it a simultaneously expensive and undesirable source of baseline information.

Air-Photo Reconnaissance

Some historical air-photo sources exist, but the experiences of Miller (2018) show that they lead to inconclusive and unreliable measurements as well, owing in part to the difficulty of selecting the top

edge of the bluff amid overhanging vegetation. This does not get easier with *SfM* methods, as the top edge of the bluff is usually vegetated (no one dares to mow it). However, the resolution and 3D environmental detail afforded by *SfM* products will allow a monitor to more accurately track changes once a baseline survey is established.

Terrestrial Laser Scanning (*TLS*)

Neitzel (2014) utilized *TLS* to obtain sub-centimeter resolution bluff erosion data at seasonal transition points. *TLS* would provide the high-resolution insight required for monitoring bluff retreat activity along the coast of Maine, but a major reason for the lack in widespread usage is the barrier created by the price of the hardware. For this reason, it is unreasonable to expect adoption of *TLS* for a statewide monitoring program. In contrast, *SfM* utilizes digital photography to capture the area of interest and software to model it in a 3-D environment at a resolution that is competitive with that of *TLS* survey data (Westoby et al. 2012, James and Robson 2012). Use of *SfM* dramatically decreases entry costs and increases accessibility in contrast to *TLS*. *SfM* survey methods were identified as the superior tool for recording coastal erosion over time due to the accessibility and adaptability it provides.

CHAPTER 3

AN INTRODUCTION TO *STRUCTURE FROM MOTION*

Structure from Motion (Ullman 1979) is a digital revival of traditional stereoscopic photogrammetry (**Figure 3.1**). The principles behind the digital description of 3D space are nothing new, but the computational demand has, until recently, remained too prohibitive to make it common-practice. New advances in computing power and machine-learning programs have facilitated the transfer of survey tasks from hardware to software. Unlike modern laser scanning systems, which require an expensive complex of equipment, *SfM* utilizes little more than a collection of digital photographs to model an area of interest. Whereas photographs captured on film needed to be evaluated manually, digital images are recorded in a controlled, rasterized format that can be processed extensively by software. Feature and edge detection algorithms (to be discussed later) can identify details within not only one image but details that are common to many of the images in a set. The spatial relationships of features within a given scene is then worked out by evaluation of the apparent changes in their position (*i.e.*, the parallax effect) across the variety of perspectives afforded within the collection of images supplied by the user.

Figure 3.1. An Earlier Approach to 3D Photogrammetry. Image Titled: *USGS Cartographer at Work*. No name provided, U.S. Geological Survey. Public Domain. <https://www.usgs.gov/media/images/usgs-cartographer-work-6>

The Parallax Effect

The parallax effect describes the apparent shift in displacement of objects due to a shift in an observer's position. The early applications of parallax found use in the field of astronomy, for example Friedrich W. Bessel, who in 1838 showed comparisons of the trigonometric relationships of star 61 *Cygni* to neighboring stars at two different times of year (therefore at different positions along Earth's orbit) in order to more certainly describe the apparent range of 61 *Cygni*'s motion (Bessel 1838).

When an observer moves, objects closer to their position appear to shift their position much more than objects that are further away do. The observer's movement, crucial for a *SfM* survey, is commonly pointed to as the "*motion"* in the phrase: "*Structure from Motion."* This serves as a handy mnemonic device to encourage a user to effectively capture the parallax effect in their survey. *SfM* exploits the principles of the parallax effect to describe the geometric relationships of features within a scene for use in 3D model construction. This improves upon traditional stereoscopic photo pairs by utilizing collections of $n>4$ images that provide a greater wealth of perspectives. Computer-vision techniques (*e.g.*, Ullman 1979, Lowe 1999, Triggs et al. 2000, and Furukawa and Ponce 2010) are used to track and to reason-out the parallax displacement of select features within that collection of photos, algorithmically interpreting the scene and faithfully reconstructing the environment as it was captured.

The Interpretation of Structure from Motion – Ullman (1979)

How can three-dimensional structure be inferred from two-dimensional images when no three-dimensional information is conveyed by the individual images themselves? Fundamentally ambiguous, there is no "unique structure and motion consistent with a given 2-D transformation (Ullman 1979)." Ullman describes a *rigidity* test from his *rigidity assumption:* "Any set of elements undergoing a 2-D transformation [*i.e.*, features in a scene projected through a lens and recorded as a photographic image] that has a unique interpretation as a rigid body moving in space, should be interpreted as such a body in motion." To note: it is actually this interpretation of a feature as a body-in-motion, not the motion of the user, that lends itself to the name of the method.

If the test is positive, then a unique structure may be imposed on a set of elements. By observing its apparent 'motion' between images the set of elements is discovered to be in motion as a whole, implying its coherence as a feature within the scene. If the scene is composed of "several objects participating in different motions," as with any real-world scenario, then their structures must all be sufficiently describable by elements that pass the test. The perception of 'motion' between images can be

attained by the use of parallax cues and their corresponding "angular-velocities" that can be imagined from one image to the next, consistent for each rigid body and sensible in relation to the overall scene. Ullman (1979) establishes from the structure from motion theorem that 3-D structure can be "recovered from as few as four points in three views…" and goes on to state a need for identifiable elements, commenting that the theorem depends completely on the assumption that it is known which points in each of the views are the projections of the same source point in space. The complete proof can be reviewed in the appendix of Ullman (1979). From here it becomes clear just how necessary is it to have reliable feature recognition algorithms for *SfM* methods to succeed.

Feature Recognition: S.I.F.T. – Lowe (1999)

The *Scale Invariant Feature Transform* (*S.I.F.T.*) presented in Lowe's (1999) "Object Recognition from Local Scale-Invariant Features," provides a foundational computer-vision algorithm for *SfM* methods. The *S.I.F.T.* was developed to provide an object-recognition system for use outside of strictly controlled environments, showing strength even when illumination, 3-D pose, and visibility varies from image to image. *S.I.F.T.* is ideal for natural settings. It finds this strength by examining images on more than a single resolution and determining "Key" locations that remain stable, or "scale-invariant," even as the image is translated, scaled, or rotated, as well as remaining identifiable despite some introduction of noise or distortions. This ensures resiliency of object recognition against the effect of a change in illumination direction on a 3-D surface, which could result in large changes to the magnitude of an image gradient.

S.I.F.T. accomplishes this primarily by building image-pyramids, a tiered resampling of image resolutions so that each level of the pyramid has a coarser resolution than the one above it (**Figure 3.2**). This allows for a staged-filtering approach. Pixels are evaluated against their nearest-neighbors on one tier in a search for local minima (min) and maxima (max) of the color and texture gradients. If found, the position of each min/max is projected to the next level of the pyramid and the test is run again,

eliminating most pixels within a few comparisons. This effectively *sifts*-out identifiable and persistent minima and maxima in the color gradients, defining numerous regions of the image where color and texture fall within boundaries distinct from the surrounding space. This allows them to be characterized as discrete features with a signature collection of directional color gradients.

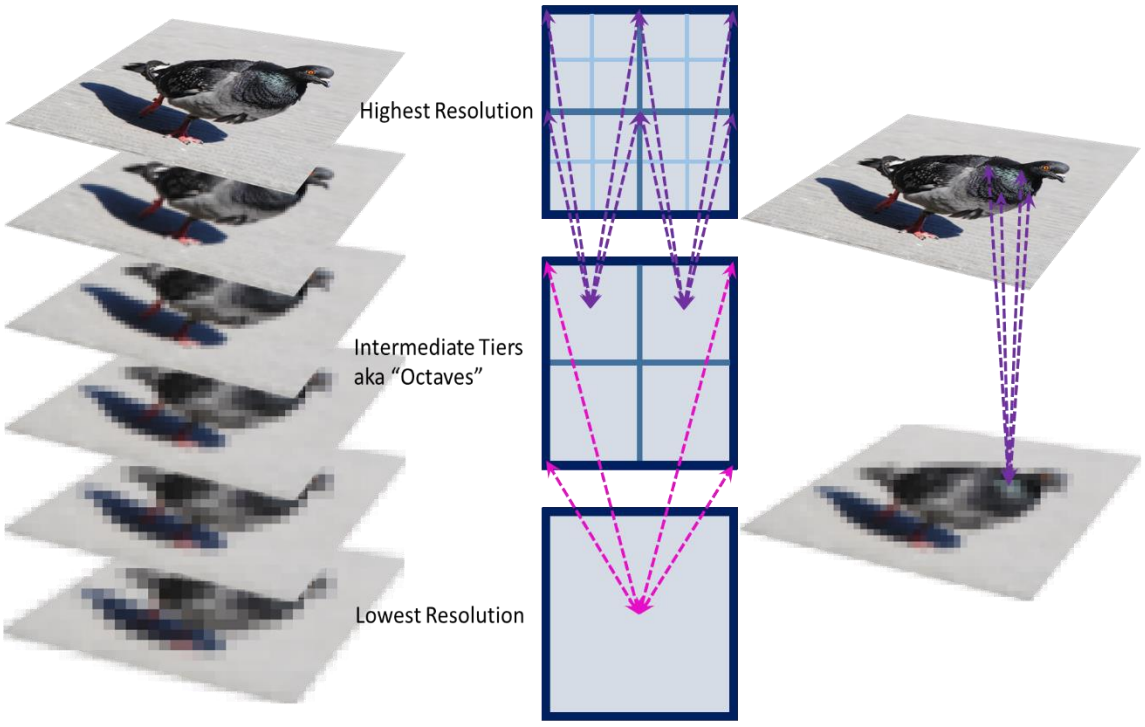

Figure 3.2. An Example of an Image Pyramid.

A given image is resampled such that each tier of the pyramid is of a coarser resolution than the one above it. Different resolutions allow for the efficient detection of distinct regions of color and texture within the image due to the elimination of fine scale noise and coarse scale homogeneity. Note how different features of the pigeon's plumage that may be complicated by texture detail at high resolution can be reduced to still-distinguishable regions of color at lower resolutions. Illustration and photo my own.

Following characterization, *S.I.F.T.* Keys sampled at larger scales are weighted against those generated at smaller scales (relating different levels of the image-pyramid), effectively filtering for the mostly likely neighboring Key features. This improves object and feature recognition by favoring the

least noisy scale (Lowe 1999). The Key features are then indexed, and *S.I.F.T.* returns a transformation of the image as a collection of local feature vectors, each of which is found to be invariant to translation, scaling, and rotation, and partially invariant to illumination changes.

It is worth noting that D. G. Lowe stated in his 1999 conclusion that:

> "An important area for further research is to build models from multiple views that represent the 3D structure of objects. This would have the further advantage that [K]eys from multiple viewing conditions could be combined into a single model, thereby increasing the probability of finding matches in new views. The models could be true 3D representations based on structure-from-motion solutions, or could represent the space of appearance in terms of automated clustering and interpolation . . ."

Camera Calibration Modelling

More sophisticated *Structure from Motion* programs can work with camera meta-data to speed up processing times and to enhance accuracy of the model generation. If metadata isn't supplied by the user, an approximation is made based on a "general" model of a camera: in that a lens at a given length from a sensor focuses an image on that sensor to some degree of fidelity. Camera metadata is now commonly recorded and associated with each digital image as it is captured, providing information such as the aperture, focal length, camera model. With the focal length of a camera lens and the dimensions of the actual sensor properly constrained, the direct relationship between observer distance and the scale of a scene within a digital image can be estimated. (**Figure 3.3**).

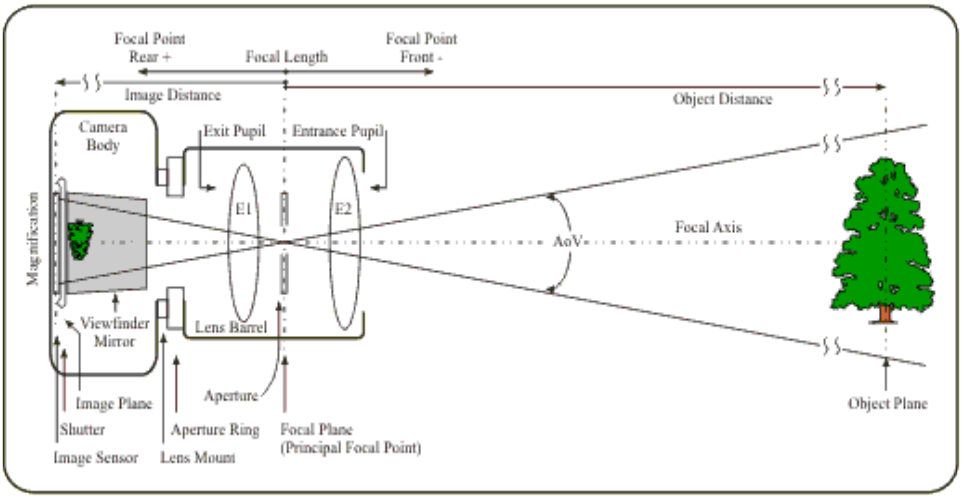

Figure 3.3. A Generalized Model of Camera and Lens Geometry. The height of the tree can be determined by scaling the sensor's dimension by the ratio of the focal length and the distance to the object of interest (the tree).

Image from <htpp://rags-int-inc.com>

***Bundle Adjustment*, an Optimization Problem**

Mapping the potential spatial arrangements between *n*-photographs, the *Bundle Adjustment* process produces estimated 3-D coordinates for every Key feature provided by *S.I.F.T.* Starting with the pair of images with the largest detectable number of Key feature matches, it iteratively develops this estimate, repeating and refining the derivation with each introduction of a subsequent image (Claypuyt et al. 2016). As stated above: with the focal length of a camera lens and the dimensions of the actual sensor properly constrained, the direct relationship between observer distance and the scale of a scene within a digital image can be estimated. By iteratively comparing images in a large enough set, and evaluating the relative spatial relationships of features within those images that are suggested by parallax changes, the features can be arbitrarily related to one another both in size and scale. Including scaling or positional information for a set of features can enhance the estimation and move the model from an arbitrary scale to a representative one. Not only does this process provide 3-D coordinates for features detected within the images, it also returns estimates for the position and orientation of the camera relative to each image.

Unlike traditional ranging systems (*e.g.*, Radar and LiDAR) where knowing the precise position of the sensor is critical to properly ranging and measuring a distance to-and-from that sensor, *SfM* methods ultimately work independently of sensor position, retroactively determining that information from the estimated orientation of features within each image. This takes some operational pressure off of the user, as returning to precisely the same observational point twice is no longer necessary.

Tie-Points: The Sparse Cloud

From the combined efforts of the *S.I.F.T.*, the camera modelling, and the *Bundle Adjustment* algorithms comes a product known as the *Sparse Cloud*. The *Sparse Cloud* is a constellation of points (x, y, z, R, G, B), from here on referred to as "Tie Points," in an arbitrary coordinate space that maintains their geometric relationship. The extra-dimensions in each set of coordinates is provided because the Key point selection process (described above) bolsters its choices by color gradients. Therefore, RGB values for use with an additive color model are a natural inclusion as additional "coordinate" information shared with each *xyz* positional estimate. A novel benefit of this is that point-clouds generated by *SfM* come out with a remarkable aspect of photo-realism without any additional post-processing or virtual lighting effects.

At this point in the process this point-cloud dataset is not referenced to any geodetic coordinate system and does not have a proper "sense of scale," beyond its relationship to a unitless arbitrary coordinate system that is developed during the production of the model. At this stage measurable distances within the model can now be identified by the user to define and correct the model scale. This can be accomplished in a variety of ways, all depending on the setting of the survey. For example, a desktop scan of a hand-sample can be scaled by the inclusion of a meter-stick once a user defines, digitally, the meter as a set of points at opposite ends of the stick as seen within the scene. At an outcrop or larger environmental scale, the use of user-defined Ground Control features and/or GPS positions may be used to scale and project the model into a real-world coordinate and reference system.

The Dense Cloud Product: *Multiview Stereopsis*, Furukawa and Ponce (2010)

Using *patch-based* methods of surface representation, Furukawa and Ponce (2010) put forward a procedure for expanding upon the sparse cloud of tie-points to effectively and more thoroughly generate a full-surface model while filtering for visibility conflicts and false matches that might occur across different images in the set. More broadly known as *Multiview Stereopsis* (Furukawa and Ponce 2010) their proposed procedure is described as simply: "*match, expand, and filter."* First, matches are found in multiple images sharing sparse cloud tie-point features and the matches are then associated with regions within each image. The *expansion* then spreads from the tie-points to neighboring pixels, interpolating a denser constellation of colored points based on information from associated images with respect to their orientation. Lastly, visibility and regularization *filters* are applied to constrain and eliminate incorrect matches or expanded points that can be ruled out as false by other images in the set. The authors go on to warn of a few shortcomings, based on the dependency of the patch-procedure on image textures. Problems can arise where image information is unreliable, such as where shadows or motion-blurs may hide or obscure image textures. Where input is sparse, model accuracy falls off, and like radar shadow: where there is insufficient information, holes are left in the model.

The *Dense Cloud*, as the name suggests, is a point-cloud dataset like that of the sparse cloud, (x, y, z, R, G, B), but, thanks to the *Multiview Stereopsis* procedure, it typically features an order of magnitude more points "fleshing-out" the constellation. With sufficient computing resources and prolonged processing, the *Dense Cloud* can return in a stunningly hi-fidelity fashion. The survey product could now be considered a 3-D photograph, capturing the scene as it was (**Figure 3.4**). The methods designed by Furukawa and Ponce further facilitate the generation of additional data products, such as a triangulated mesh (a.k.a. "wireframe,") surface model or a rasterized digital surface model for import into other software systems.

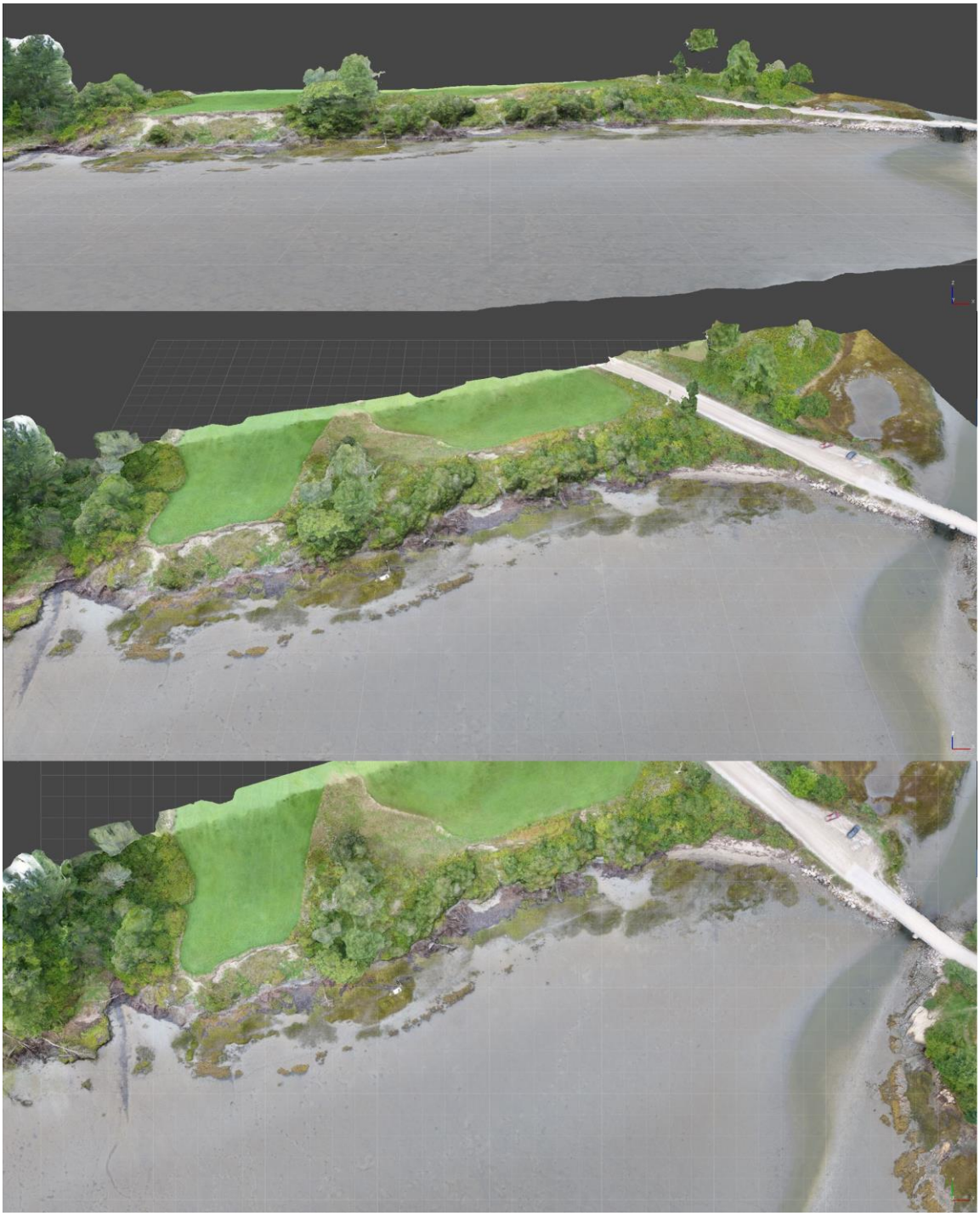

Figure 3.4. A Photo-Realistic Digital Surface Model of an Unstable Bluff. Three views of a photo-realistic digital surface model ("3-D Photograph") of an Unstable bluff produced with *Structure from Motion*. Viewed in 3 perspectives. Representative of Little River, Freeport Maine, on September 20th, 2017. Resolution approx. 5.9 cm / pixel

Reproducibility – Clapuyt, Vanacker, and Oost (2016)

SfM applications in geomorphology studies boast measurement precision on the order of centimeters (*e.g.*, James and Robson 2012, Westoby et al., 2012). But precision within an arbitrary coordinate system isn't sufficient on its own. To properly measure the change in landforms over time it is critical that the *SfM* surface model be projected reliably to a real-world coordinate system with a high degree of accuracy again and again.

Noting poor documentation in the literature, Clapuyt et al. (2016) designed a controlled series of field-tests for a typical *SfM* survey method in order to more appropriately analyze what they described as the 1) *internal* precision: the error that is associated with the *SfM* algorithm and the 2) *external* precision: quantifying the error associated either the location of Ground Control Points (GCPs) limited by the accuracy of the GPS receivers used in survey, and/or errors associated with the quantity and spatial distribution of said GCPs used to compute the georeferencing (Clapuyt et al. 2016). Their findings confirm a very high *internal* precision of the *SfM* algorithm (*i.e.*, the scene reconstruction process has low impact on the data) and, as it may be expected, a strong dependence of accuracy on Ground Control features within a scene and the means by which Ground Control is conducted by a surveyor. Georeferencing error is found to be less in the x and y dimensions as it is in the z, echoing a common concern that GNSS (the *Global Navigation Satellite System*)-derived altitude values are intrinsically lower precision (Clapuyt et al. 2016). Additionally, they find that image resolution is not a limiting factor in reproducibility of results, which supports the widespread adoption of *SfM* as a methodology with a low equipment cost, but their work makes it clear that proper Ground Control is what makes it meaningful. In a coastal setting persistent landmarks can be few and far between, a challenge to be discussed later on.

CHAPTER 4

METHODS

Structure from Motion exploits the principles of parallax to reconstruct a scene in three dimensions. Given a sufficient variety of perspectives and overlap within photographs, landform topography can be modeled with high-fidelity while information about the position of the observer is not only unnecessary but is actually inferred retroactively during the *SfM* process. *SfM* is chosen for this work as practical solution for measuring changes in coastal bluffs because it requires no specialized equipment, minimal training, and grants more freedom to survey at will. Thus, the barrier to entry is low. Its adaptability to scenes of different scale (*e.g.*, James and Robson 2012, Westoby et al. 2012), especially when image acquisition is facilitated by an Unmanned Aerial Vehicle (UAV) or drone, allows for the evaluation of cases within local context and its relatively simple execution should lend itself to achieving repeat surveys within a practical scope of time, delivering informative and useful surface-model products and enhancing coastal erosion prediction efforts.

A Brief Overview of Changes Made to the Survey Approach Throughout This Project

Trial *Structure from Motion* surveys were carried out over the course of two years with the goal of improving the model products of each survey following the last. If successful, the refined digital surface model produced would go on to serve as a baseline for repeat measurements and a standing record of the coastal bluff's state at the time of survey. Best practices learned and issues resolved are presented with this submission. Because of the initially arbitrary relationship of model-scale to the scene it's created from, it was necessary to experiment with *SfM in situ* to establish what approach is appropriate for a given survey. Early field visits were conducted on-foot and yielded *SfM* products with a great level of detail but were lacking in both geospatial and environmental contexts due to the near-sighted nature of capturing images by hand at the foot of high-relief morphology. Building familiarity with the technique

led to improved photographic practices and stronger understanding of what could be used for ground-control landmarks, which are naturally scarce and impermanent in an environment so dynamic as that of an eroding coastal bluff. Introduction of differential GPS devices to the site, captured as part of the scene within the *SfM* survey, provided stronger constraints on model scale and supported georeferencing of the digital surface product. The eventual acquisition of a consumer-grade UAV (DJI brand Phantom-4) revolutionized the conduct of the survey, enabling me to capture a photographic dataset that was rich in detail, perspective, and geographic context in roughly an hour's time, limited primarily by battery-life and weather. The resulting improvements to the digital surface models from the UAV photosets speak for themselves before discussion later on.

Choice and Description of Survey Sites

Sites were chosen for ease of public access and reputation for instability noted in earlier works. Primary focus was placed on the Little River bluff (**Figure 2.4, Figure 4.1 a-b.**). While its size demanded more survey time it also offered a bluff setting in which various phases of the bluff erosion cycle concept (Kelley and Hay 1986a, b) could be observed side-by-side all within a single classification unit of the Coastal Bluff Hazards Map (Maine Geological Survey 2006). When time and resources allowed, surveys were also conducted on the southern face of the Little Flying Point bluff (**Figure 2.4, Figure 4.1 a**). On a few occasions visits were paid to other nearby locales (named in relevant figures) with a reputation for slope failures but due to reasons of private property access or poor *SfM* monitoring potential they were not regularly studied for this project. The Little River site was mapped as an "Unstable" bluff according to the Coastal Bluff Hazards Map and the Little Flying Point site was mapped as a "Highly Unstable" bluff (Maine Geological Survey 2006).

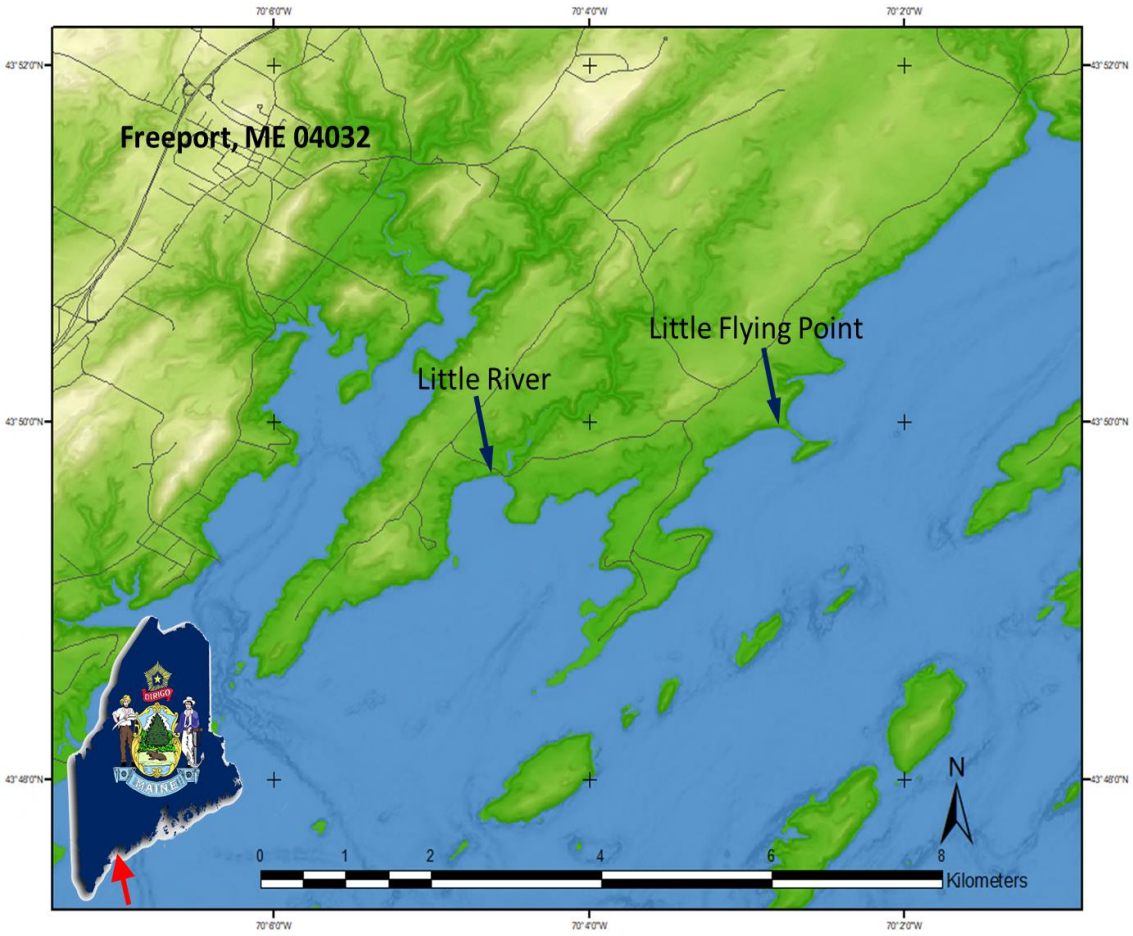

Figure 4.1 a. Primary Study Sites. Little River and Little Flying Point in relation to Freeport, Maine. The bluffs at Little River and Little Flying Point were the primary study sites for this project.

Figure 4.1 b. An aerial image of the Little River bluff site from September 20th, 2017.

Sub-sites (select erosional hotspots) were labeled for the Little River area during the on-foot surveys but eventually abandoned as, for one: some were merged by slope-failures, and secondly: the survey practices expanded beyond focus on hot-spots towards whole-bluff context with the acquisition of the UAV. They are included here in service to reference and description of some of the observed phenomena described later in the text.

The image is oriented north-upwards and covers approximately 400 meters from left to right. The two cars (red and black) parked next to the bridge provide a small sense of scale.

Image Acquisition

The Timing of Site Visits

Site visits occurred when tide, weather, travel, and equipment availability coincided. At the start of the trials we operated on the assumption that landslide behavior and the general period of the bluff erosion cycle concept approximated a roughly decadal pattern (Kelley and Dickson 2004). Evidence from this study suggests, in hindsight, that a much finer-resolution and regular survey schedule would be necessary to answer questions of cycle timing and seasonality posed by our observations. **Table 4.1** details the chronology of primary site visits conducted during this trial application of *SfM* methods.

Table 4.1 The Timing of Site Visits.

Date	Site(s) visited	Time Since Last Visit	Comment
Jun 01, 2016	Little River	-	First Visit of LR
Jun 17, 2016	Little River	16 days	
Jul 01, 2016	Little Flying Point	14 days	First Visit of LFP
Sep 22, 2016	L. River, L. Flying Point	83 days	
Nov 05, 2016	L. River	44 days	Tide rising, survey incomplete
Dec 07, 2016	L. River, L. Flying Point	32 days	Rebar GCPs introduced
Feb 27, 2017	L. River	82 days	
Mar 16, 2017	L. River, L. Flying Point	17 days	Buried in snow, no survey.
Mar 24, 2017	L. Flying Point	8 days	Tide rising, survey incomplete
Apr 02, 2017	L. River, L. Flying Point	9 days	Many rebar GCPs untraceable
May 22, 2017	L. River	50 days	
Jul 20, 2017	L. River, L. Flying Point	59 days	
Sep 19, 2017	L. River	61 days	First trial with UAV
Sep 20, 2017	L. River	1 day	UAV survey
Oct 28, 2017	L. Flying Point	100 days	UAV survey
Nov 09, 2017	L. River, L. Flying Point	112, 12 days respectively	UAV survey
Mar 12, 2018	L. River	123 days	UAV survey

Surveys Conducted On Foot

SfM surveys conducted from June 01, 2016 through July 20, 2017 were carried out on foot. Images were captured using a handheld Nikon D3000 DSLR recording in Large (3872 x 2592 pixels) RAW (12-bit) Format, often producing images around 55-60 MB in size. Still images were captured for the models generated in this work. There are some notable concerns for sourcing images from videos recorded during a survey, a common practice that is more appealing for its efficiency than it is reliable for its accuracy (Terpstra et al. 2016). The reasoning behind this is discussed later on in the *Preferred Methodology* section of the Discussion. The camera was set to "Aperture Priority" setting so that the aperture, therefore the depth-of-field, could be held constant and that the shutter speed would be modulated by the camera to produce consistently exposed photographs. Variance in the shutter speed may lead to motion-blur and degradation of image sharpness but many modern camera lenses have built image-stabilization technology. UAVs are equipped with electronically managed gimbals designed to reduce the engine vibration reaching their cameras, so this is less concerning than the expected effects of an inconsistent depth-of-field amongst a set images when working with a computer-vision technology

designed to interpret depth-of-field. Some researchers (Clapuyt et al. 2016) suggest using the opposite: a Shutter Priority setting to reduce motion blur from the behavior of an swift UAV. However, the trade-offs between Aperture- and Shutter-priorities don't appear to have been formally evaluated yet.

The aperture was locked to *f*/8, chosen arbitrarily as a reasonably intermediate *f*/ value, for every survey. To resist manual zooming and alteration of the focal length, painter's tape was used to fix the position of the zoom lens. It is important to note that the focal length was made consistent during each survey, but has had to be varied from survey to survey. Typical focal lengths used ranged from 25mm to 35mm. While it is necessary to keep the focal length fixed for each *SfM* scan, else a new camera parameter model will need to be generated per change in focal length, it was necessary to change focal length from survey to survey while adapting to site-specific settings. Ultimately the focal length used during on-foot surveys was conditional to the state of the shore on a given day, for example: a rising tide or some particularly deep mud occasionally prevents stepping as far back from the bluff face as usual, and so focal length was adjusted before the survey to a value that could be maintained for the duration of the visit.

Erosional hot-spots were chosen as the focus of each on-foot scan for two reasons; "scan" hereby referring to a subset of photographs from a given day's survey that pertain to a specific site or feature, designed to be processed as a stand-alone *SfM* product. At times it may be used interchangeably with "survey," when the visit concerns only the entire bluff. 1) Because *SfM* works on visual information and the prominent features identified within those images it cannot, like LiDAR, "see through," vegetation. Therefore, vegetation stands out in a digital surface product, obscuring any measurement of a true ground surface. 2) Vegetation is often visually noisy, texturally busy, and features repetitive patterns. An individual leaf may represent an ideal "feature" for *SfM* to identify, but the algorithm will struggle to identify the "same" leaf in multiple images. Often, vegetation canopies can introduce surface roughness

in the model product, or vegetated areas can degrade to holes devoid of reliable tie points in the surface model which leave space in the model that must be interpolated across.

On approaching an erosional feature chosen for a scan it was necessary to work to provide as rich a variety of perspectives on that feature as possible. This was accomplished by "orbiting" the feature at a distance of some terrain-permitted radius and circumference (**Figure 4.2**), capturing images along the radial transit and then moving forward to capture more fine detail. Photos were taken at eye-level; handheld at arm's reach above; and from a squatting stance for each position in order to afford at least some parallax in the vertical dimension (helping to defining the top edge of the bluff from the sky and distant features behind it). With sufficient scale and georeferencing cues (**Figure 4.3**) placed within the scene subsequent models could be expected to come out with the same sense of place and scale without needing a surveyor to precisely retrace the steps taken for previous scans.

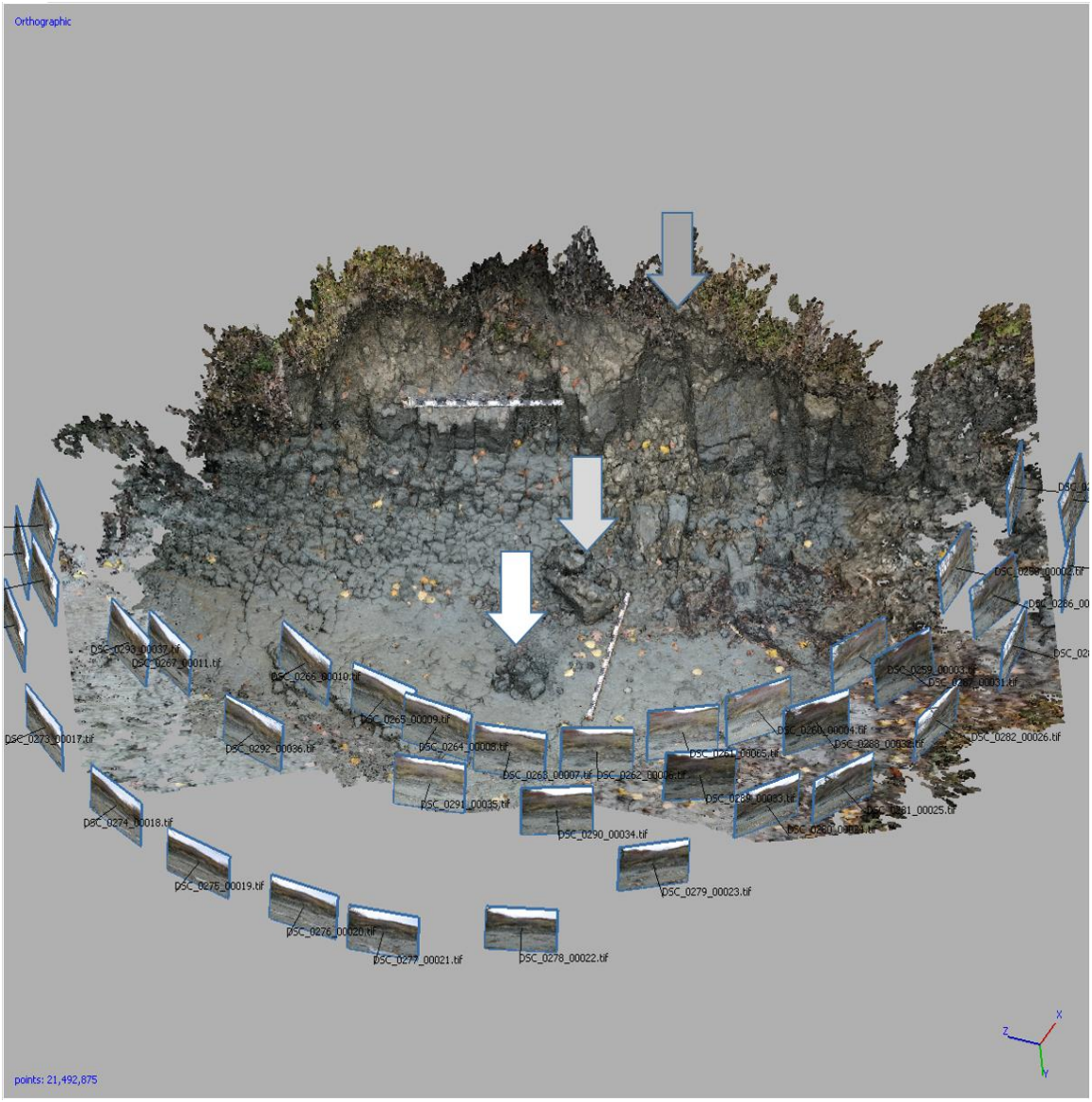

Figure 4.2 a. An On-foot SfM Scan. Located at the LR 5 sub-site at Little River representative of November 5th, 2016.

Presented as an example of the "orbital" nature in which images are collected. The image shows the scene reconstruction as it appears within the *SfM* software (Agisoft's *Photoscan*, now *Metashape*) and features small recreations of the individual source images (each tagged with a consecutive file number and a directional vector) placed in space within the scene. The surface is modeled as a point-cloud of 21,492,875 points sourced from 35 photographs. Focus was on the minute block-fall (grey arrows). The scale bars are 1.5 meters in length. Note that this model is not geo-referenced and is instead constructed in an arbitrary coordinate system: hence the disoriented model axis icon in the bottom right-hand corner.

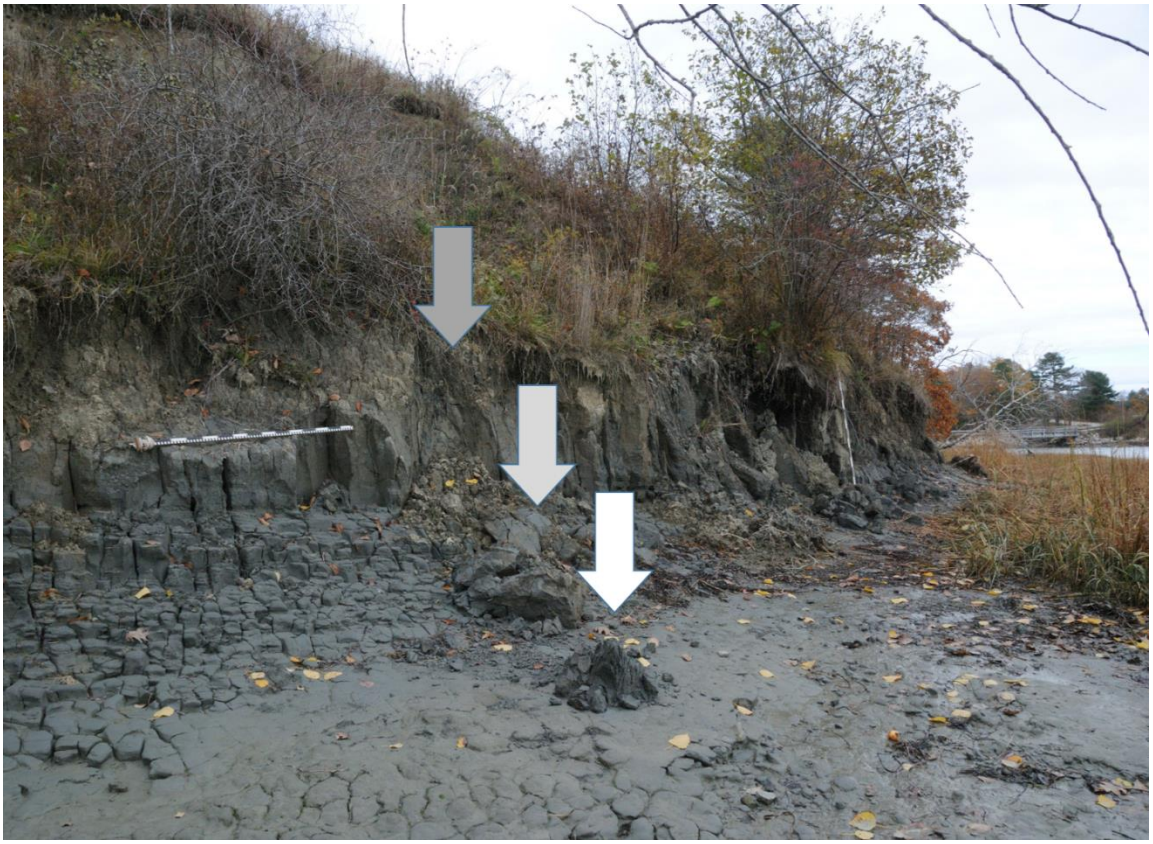

Figure 4.2 b. The LR 5 site as is from one of the source photographs (taken November 5th, 2016). Note on comparison to the scene construction (above, **Figure 4.2 a**) that the perspective is limited and the visually-noisy vegetated slope face escapes recognition in the model generation, resulting in a loss of context and/or potential landmark reference information.

Figure 4.3 a. A Sense of Time, Scale, and Place Within a SfM Scene. Imaged as a *SfM* point-cloud scene reconstruction of the LR4 sub-site representative of November 5th, 2016, captured on-foot. Black-and-white-marked scale bars are 1.5 meters in length. A GPS antenna sits atop the orange tripod. The orange lines demonstrate distance measurements of the model that are made within the *SfM* software.

Figure 4.3 b. The LR4 sub-site as is on November 5th, 2016, from an individual source photograph.

Surveys Assisted by UAV

Surveys conducted from September 19, 2017, through to March 12, 2018 took on a new form as the image acquisition was revolutionized by the UAV. No longer constrained to an on-foot perspective, but now limited only by battery life, a two-flight approach was quickly conceived. The first flight, referred to here as the *context flight*, took to a relatively higher altitude and followed a more regular planimetric pattern common in aerial photogrammetric surveys, capturing the entire desired survey area from the top-down perspective. The greater distance from the ground results in a reduced resolution but the broader coverage insures the inclusion of all Ground-Control-Points (*GCPs*) (to be discussed later) and helps to place the survey site in local context by including nearby roads, structures, bedrock outcrops, etc. where it is possible to enhance georeferencing and modeling efforts.

Immediately following the *context flight*, the UAV is flown again with focus on capturing greater details of specific interest within the environment. It is important that both flights occur sequentially with little to no time transpiring between, as the two are meant to capture the same scene in tandem. The second flight, now referred to as the *complementary flight*, is conducted closer to the scene and does not need to follow a regular pattern, instead improvising orbits around select targets for better perspective and measurement. A *complementary flight* provides additional and higher-resolution photographs of the subjects, which can be aligned and nested into the same *SfM* input, serving to enrich the detail of the end product. The photographs collected during each flight are treated as components of the same survey; should be subject to the same controls on photographic parameters (aperture, sensitivity, etc.); and are input into the same *SfM* project (**Figure 4.4**). The camera settings are maintained between flights and the higher-resolution of the complementary detail images are acquired only by piloting the UAV closer to the survey scene.

UAVs are often used for the bird's-eye-view that they offer. However, it is worth noting that the powerful stabilization technology and ease of control built into modern devices allows for them to also support the development of a *SfM* product with consistent low-altitude horizontal and oblique imagery. As an example from one survey, during the *complementary flight* care was taken to pass the UAV across the face of the bluff maintaining altitude only a meter above the mudflat and pointing the camera horizontally towards the landform. This is particularly important for fore-marsh and slope profiling as there is greater error associated with a singular top-down approach that risks a poor sense of topographic relief if fewer perspectives are represented in the image set.

Figure 4.4. Demonstration of the Two-Flight Approach. The first set of images (top scene, Little River site, images represented by blue squares) are captured in a top-down, planimetric manner to ensure capture of a broader site context and any included Ground Control Points. Beneath (bottom scene, Little River sub-sites 3-4-5, images represented in miniature), images are captured at oblique and horizontal angles along the bluff face during a second flight to complement the detail in the final model product. The two sets are used together as one survey. Note the "holes," (gray where the background shows through) in the surface models amongst and beneath the trees, where noisy vegetal image textures fail to be reproduced.

Ground Control

Originally, rebar segments with painted ends and small plastic orange field-flags were chosen and placed into the bluff face sediments to offer a sense of consistency and ground-control between surveys (**Figure 4.5**). While the Day-Glo color of the field-flags was readily distinguished from nature and easily captured by *SfM* software, the position of the flag relative to the surface was variable, especially in the breeze, and therefore inconsistent, leading to errors in measurement and alignment. Field-flags were quickly over-grown, sun-bleached, or eroded out of place. Unexpectedly (but nevertheless an important result), some of the 4 foot (1.23 meter) rebar sections placed in the bluff-toe were completely exhumed (**Figure 4.6**) in time; some turned-out from the bluff as carried by slope-failures, some buried by shoreline detritus; and remarkably a few at the top of the bluff face remain (as of March 12th, 2018), by sight, relatively unchanged but hazardously out-of-reach.

In addition to the field-flags and rebar some nearby natural features were selected with the expectation that they would remain sufficiently stable over time to align repeat surveys. Referencing to nearby features in coastal erosion studies has been used in other studies such as James and Robson (2012) for example: identifying a telephone pole close to the scene. This expectation was soon invalidated for our test case as trees toppled and a seemingly immovable boulder was overturned (probably by ice action). Features such as nearby roads, buildings, and bedrock outcrops can serve to support alignment efforts but may or may not be available or sufficient on their own depending on the situation. Each site will require careful consideration of what landmarks may be useful and for how long when a preliminary site visit and baseline survey are conducted.

Figure 4.5. Painted Rebar (beneath the red and green triangles) Placed on December 7th, 2016. Note some of the small orange field-flags (orange triangles) that survived since their placement on September 22nd, 2016. The scale bars are 1.5 meters in length. Photo taken at the Little River sub-site LR4 on December 7th, 2016.

Figure 4.6. Rebar Exhumed Over Winter. 4ft. (1.23 m.) rebar ground control point (left, yellow triangle) at the Little River sub-site LR2 exhumed over winter (right). This was an unexpected demonstration of the folly of choosing this approach to landmarks given the dynamic nature of the setting. Image on the left was taken on December 7th, 2016, the date of emplacement. The image on the right was taken the following April 2nd, 2017.

GPS as Ground Control Points (GCPs)

In anticipation of further erosion, and in an effort to avoid site disturbance, I decided that placing more landmark pins as ground control points was no longer an option. Instead, GPS units (TopCon GB-1000, with PG-A1 + GroundPlane antennas were the devices used in this study) to constrain the surveys, given that if the equipment, as with anything captured *in situ,* was within the scene imaged by a scan, they would be faithfully present within the *SfM* model reconstruction (**Figure 4.3**).

Associating GPS coordinates with units or features within the survey defines reliable scale and orientation information in context of the GNSS system, independent of changes to the local environment, reducing dependency on static, or seemingly static, local objects and features. This is common practice in *SfM* survey methodologies (*e.g.*, James and Robson 2012, Westoby et al. 2012, Clapuyt et al. 2016). Surveyors often distribute visibly-unnatural targets about their study areas and record the positions of the markers as precisely as possible, typically with some form of kinematic differential GPS measurement. In this way, the targets can be easily identified within *SfM* models due to their distinct features, for example: a bright and out-of-place color, and then associated with their real-world coordinates to georeferenced the surface product. It is worth noting that there are a number of different measurement solutions, and that while *SfM* is famed for its low cost of entry, raising the bar with a precision RTK-GPS toolkit quickly escalates both the resolution as well as the price tag.

GPS targets located within a *SfM* model have an additional advantage as "virtual" scale-bars, as precise point-to-point distances can be measured across portions of a scene where placing meter-sticks could be impossible or other scaling features would be obscured. With a GPS-enabled approach successful alignment of repeat surveys should no longer be reliant on reuse, or familiarity with, landmarks or the original GPS ground control points from previous surveys as long as enough GPS points are sampled within each subsequent scan to sufficiently describe scale and orientation of the site to be orthorectified in post-processing.

In this project, static-survey (as opposed to kinematic) GPS sampling methods were chosen at first due to initial concerns for limited kinematic-survey accuracy in the shadow of high-relief bluffs and short survey windows limited by incoming tides. Eventually up to six GPS receivers were distributed around a site to track their position during a scan. These were expected to provide the ground-control necessary to orient and scale a model within the *SfM* software. However, as access to high-tech equipment could be a limiting factor and counter to the low-cost ideal of the *SfM* methodology on trial here, it should be noted that it is unlikely to expect that civilian users have access to one GPS receiver per Ground Control target. Kinematic style GPS survey is more commonly employed (*e.g.*, Westoby et al. 2012, James and Robson 2012, Clapuyt et al. 2016) and allows users to place a greater number of handmade Ground Control targets while only needing a minimum of two GPS receivers for a kinematic survey regardless of the number of GCPs. All told, model misalignments by GPS errors can be more readily remedied than correcting *SfM* products that were captured or left entirely without reference information following the loss of a "persistent" natural landmark (**Figure 4.7**).

Following each survey that GPS equipment were used, GPS data was downloaded from the receivers and translated to a working format using the National Geodetic Survey's *OPUS: Online Positioning User Service* (<https://www.ngs.noaa.gov/OPUS/>). Then a table of GCPs was built and the distances between all combinations of GCPs was computed in GIS software.

A case note for this study where GPS antennas were used as GCPs themselves: most GPS systems default to take a user-measured antenna height above the ground as an input in order to report on the ground position beneath the antenna. As *SfM* methods image the top of the antenna casing as part of the scan, obscuring the ground beneath it, it is important to take care to override the default distance-above-ground measurement of an antenna and instead record the point on the visible surface of the antenna casing so that it reports on its own position in space. The user manual should describe the internal distance from the surface of the antenna casing to the focal point of the antenna inside. In the case of the TopCon units used here, this compensation distance is 6mm (Topcon Corporation, 2004).

Otherwise, errors in scaling result as *SfM* tries to reconcile the reported position of the GCP and the parallax effect between the antenna, as it is mounted, and the ground.

Figure 4.7. The Loss of a "Persistent" Natural Landmark. Not expected to move, this boulder seemed to offer a reliable feature for repeatedly aligning subsequent models over time. The red line marks the long-standing original horizontal position, determined by the discoloration and a distinctly sharp break in barnacle habitat. Having moved, this boulder was no longer suitable as a landmark for the purpose of aligning models. Photo taken March 18th, 2018, of the Little River sub-site LR6.

The *Structure from Motion* Process in *Agisoft's Photoscan* (Now Titled: *Metashape*)

Agisoft's *Photoscan* (this project began with version 1.3.4 build 5067 and continued with subsequent updates; under an Educational License) was chosen for its streamlined workflow; degree of control; and common adoption among other researchers looking to avoid technical complications of

coordinating open-source *SfM* batch-process programs. With version 1.5 Agisoft has given the software a new title: *Metashape*, and other changes are described on their website (https://www.agisoft.com). This software suite provides an all-in-one solution for carrying out the development of *SfM* products from image sets to geo-referenced point clouds and surface models.

Image Quality Filtering

After loading images into *Photoscan*, they were rated with the *Estimate Image Quality* tool that produces a numerical measure of confidence for the potential error associated with each image. The rating is based on the lowest-quality region that can be found within the image and is therefore particularly responsive to motion-blur and image sharpness. Images were selected with an intent to find balance in removing lesser-quality images while avoiding the creation of gaps in coverage of the overall scene. Through trial and error, I generally excluded any image with a rating of less than 0.8 (unitless). This reduces the over-all number of photographs needing to be analyzed, improving processing times; relieving memory constraints; and improving the visual quality of the product.

Image Alignment and Preliminary Model (Point Cloud) Generation

With the image quality estimated, poor quality images rejected, and a final image set chosen the software can begin the surface model construction. Most parameters were left to default settings that *Photoscan* determines based on available CPU, GPU, and RAM hardware capability for the computer that is used. Therefore, they will vary from system to system.

During the Alignment step of image processing the Accuracy parameter was held to *Highest*. The Generic Preselection filter was enabled, allowing the software to focus on images that appear closely related first (improving processing time) rather than evaluating any and all images simply by sequential order. The Adaptive Camera Model Fitting feature was enabled, which allowed the software to pause and adjust the modeled camera geometry if it encountered images where focal length or aperture may have

slipped and varied; this prolongs processing time but prevents the software from forcing images into an inappropriate choice of model camera geometry.

At this step *Photoscan* offers an option for "Reference Preselection." It was left disabled during this project. The utility of Reference Preselection is to look at any GPS metadata associated with each image (supplied by default with any GPS-enabled camera device such as a UAV or cellphone, as well as some high-tech DSLRs) and predetermine the positioning of each image before having to back-calculate it as a part of the image analysis conducted under-the-hood of *SfM* programs. This tactic can greatly speed up processing times and in some instances can support better accuracy in the image alignment *if* the scale of the scene is appropriate to the spatial error of the GPS mounted on the camera or UAV. When images are captured close enough together that they fall within the spatial error of the onboard GPS (typically a few meters) numerical errors can arise as the images show a change in position when evaluated by the software while the GPS metadata it also considers may not show the same change. For surveys on the order of 100s to 1000s of meters, Reference Preselection is a useful tool. As the sites in this study were no more than 50-100 meters across, and usually less, the preselection option was not used and georeferencing the models were achieved instead by ground-control methods.

Photoscan also offers the abilities to both mask portions of the images (to be excluded from processing) and to crop/delete any tie points that appear erroneous or distant from the focus of the scene. These are manual, time-consuming processes that are suited for controlled scanning scenarios such as a studio or desktop setting and the practice was not adopted here. Any significantly distant or peripheral points returned in the preliminary processing results are automatically left out when the final model domain was established during the *Dense Cloud* generation and building of the triangulated mesh products.

Imparting Scale and Geo-Reference Information to the Model

With the preliminary point-cloud model of the scene constructed reference information is applied not only to place the model into context, but also to be used by the software to optimize its alignment and positioning estimates. Ground-control targets and landmarks within the scene were identified manually and associated with the GPS coordinate data recorded and post-processed following the survey. Then the distances between each GCP target were calculated and defined within *Photoscan* as scaling features. With the newly input reference information an optimization process was run, which rebuilds the point clouds with new constraints on positional estimates.

Recalculated point clouds, now scaled according to more precise GPS information (and, not forgetting, any spatial error carried by the GPS solutions) can be used by the software to generate more refined products, or exported for analysis by external software designed for managing large point cloud datasets. Scans produced in this study were further formatted into: digital surface models (rasterized format) for evaluation in GIS software. Surface models had the source imagery reapplied to produce high-resolution orthomosaics of the sites, and triangulated mesh models to provide realistic settings for numerical modeling experiments.

CHAPTER 5

RESULTS

Select *SfM* Products from Surveys Conducted On Foot

Screen captures of the *SfM* models are presented from three perspectives to demonstrate dimensionality while limited by reduction to the page. Products are shown in three phases of the model generation process: the Tie Point Cloud, the Dense Point Cloud, and the Triangulated Mesh, all mentioned earlier in the text. While a perspective from zenith is offered here, it is important to recall that for the on-foot surveys no aerial photos were captured and that a nadir perspective is made possible only because features from the scene have been virtually oriented in space. Note that, following this, the models look fuller from the horizontal perspective from which the images were captured and that holes seen from the top-down may be likened to a radar-shadow effect: what is not photographed cannot be included in the model.

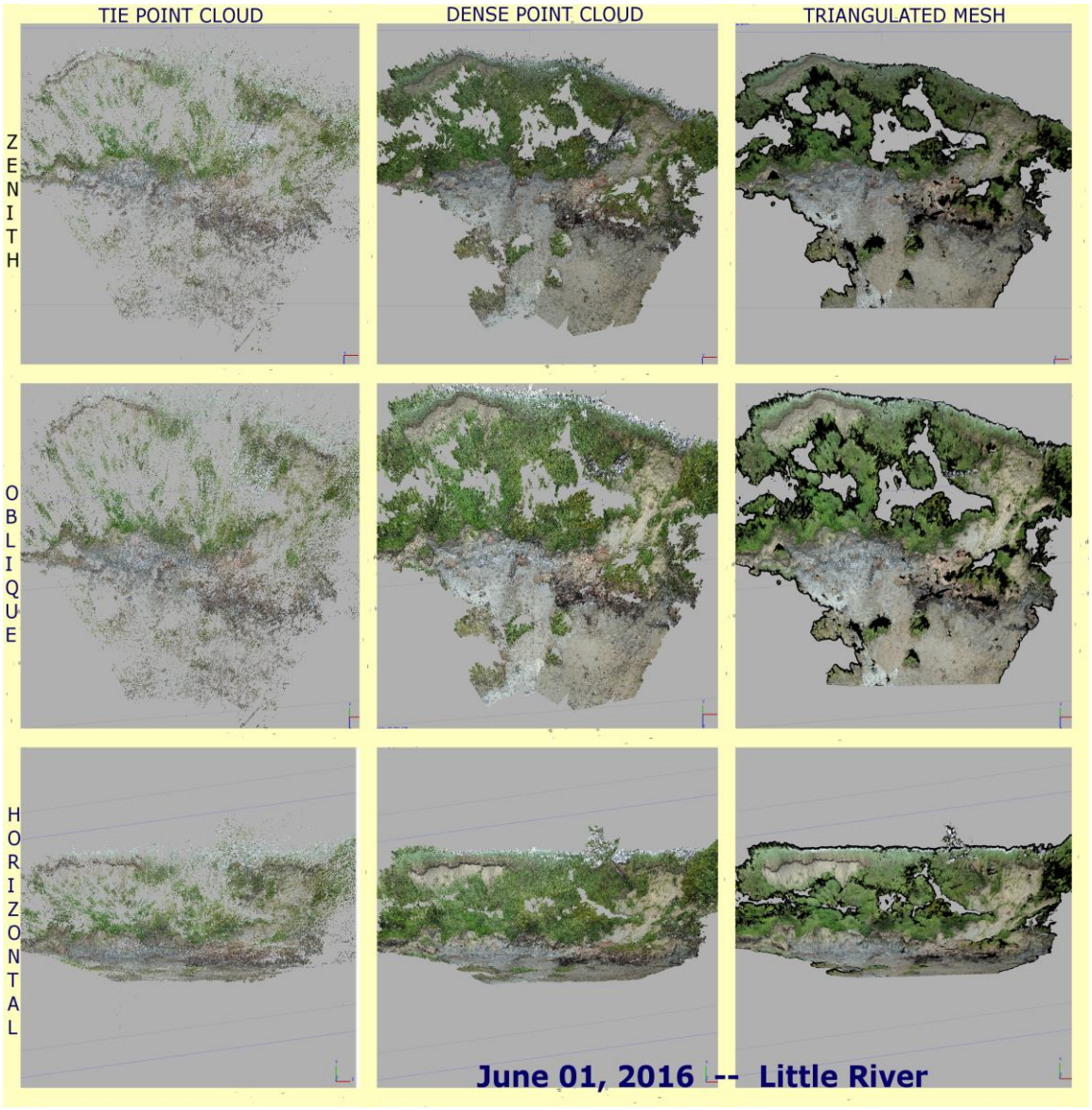

Figure 5.1 a. The First and Second Attempted SfM Site Scans. Little River sub-sites LR 3-4, representing June 1st, 2016.

This was the first attempt at a *SfM* scan of the Little River LR 3 and LR 4 sub-sites, processed together as a single survey.

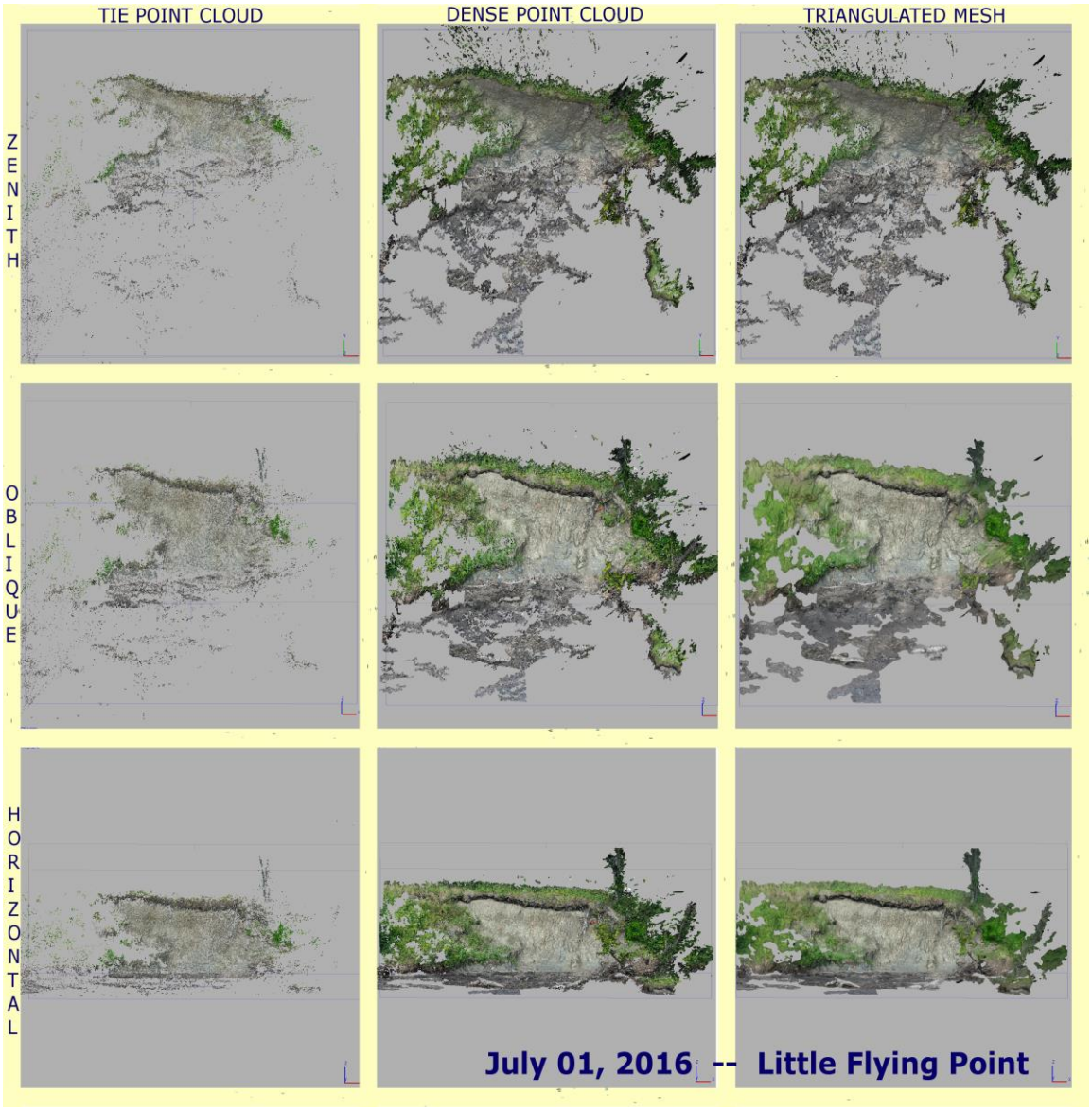

Figure 5.1 b. Little Flying Point, representing July 1st, 2016.

This was the first attempt at a *SfM* scan of the Little Flying Point south face.

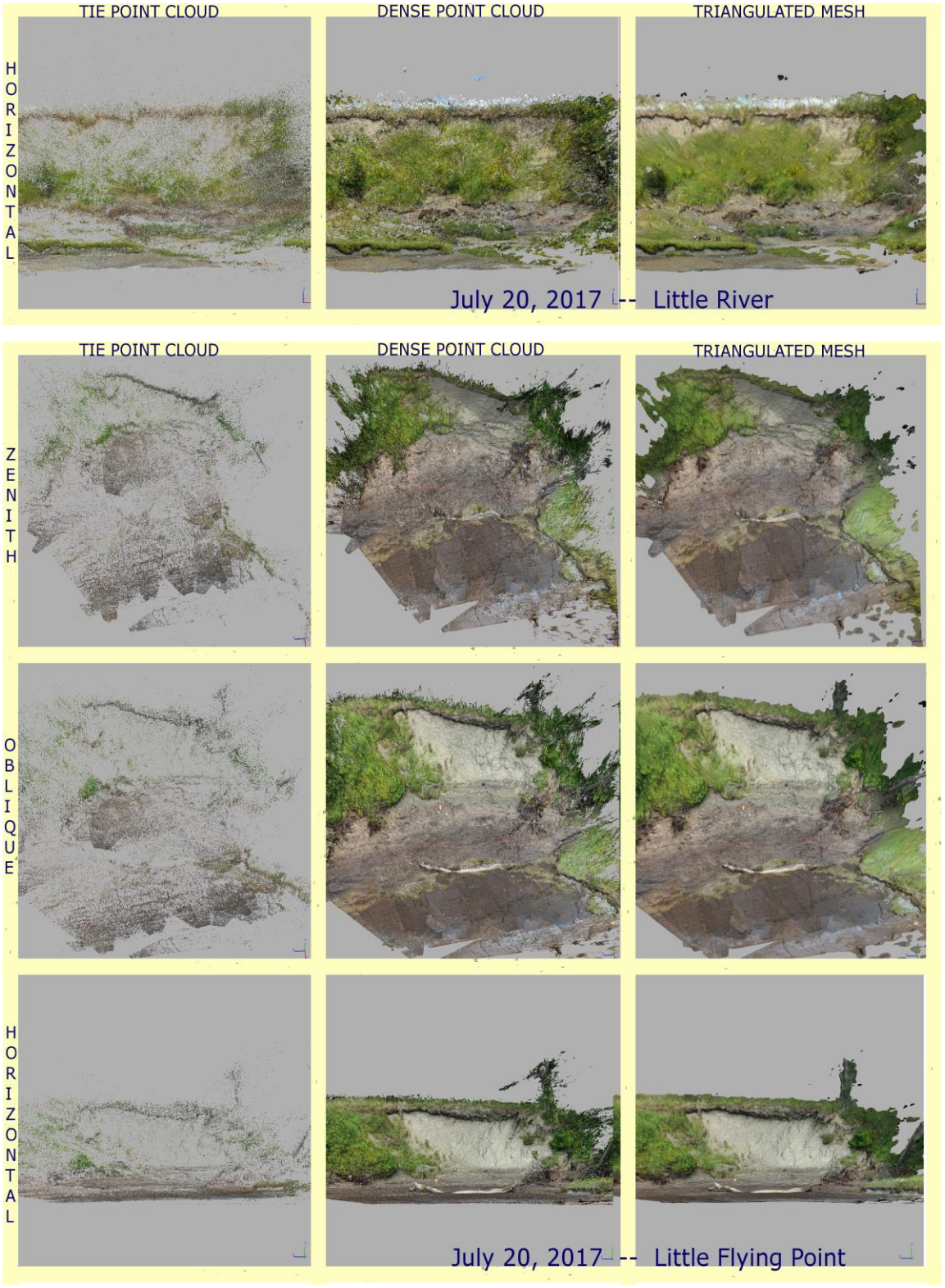

Figure 5.1 c. The second trial of the *SfM* process at both Little River and Little Flying Point, respectively. Included to demonstrate how significant improvements are made after the preliminary visit. A better understanding of the demands of site-scale (*i.e.* necessary coverage area, practical number of

images to record, etc.) can be brought to a follow-up survey after just one work-through of the *SfM* procedures. Witnessing how the software "responds" to a given set of input photographs grants the user a site-specific-working knowledge of how to approach a subsequent survey.

Select *SfM* Products from Surveys Conducted by UAV

The acquisition of a UAV provided obvious advantages for conducting surveys and enhancing model products with a much richer set of perspectives. As above, screen captures of the *SfM* models are presented from three perspectives in order to demonstrate dimensionality while limited by reduction to the page. Products are shown in three phases of the model generation process: the Tie Point Cloud, the Dense Point Cloud, and the Triangulated Mesh, all mentioned earlier in the text. When comparing to the surveys conducted on foot notice the more complete coverage (fewer "holes" in the model from the top-down perspective) and the broader area captured within a given scene, improving model edges and granting greater environmental context for the erosion site in question.

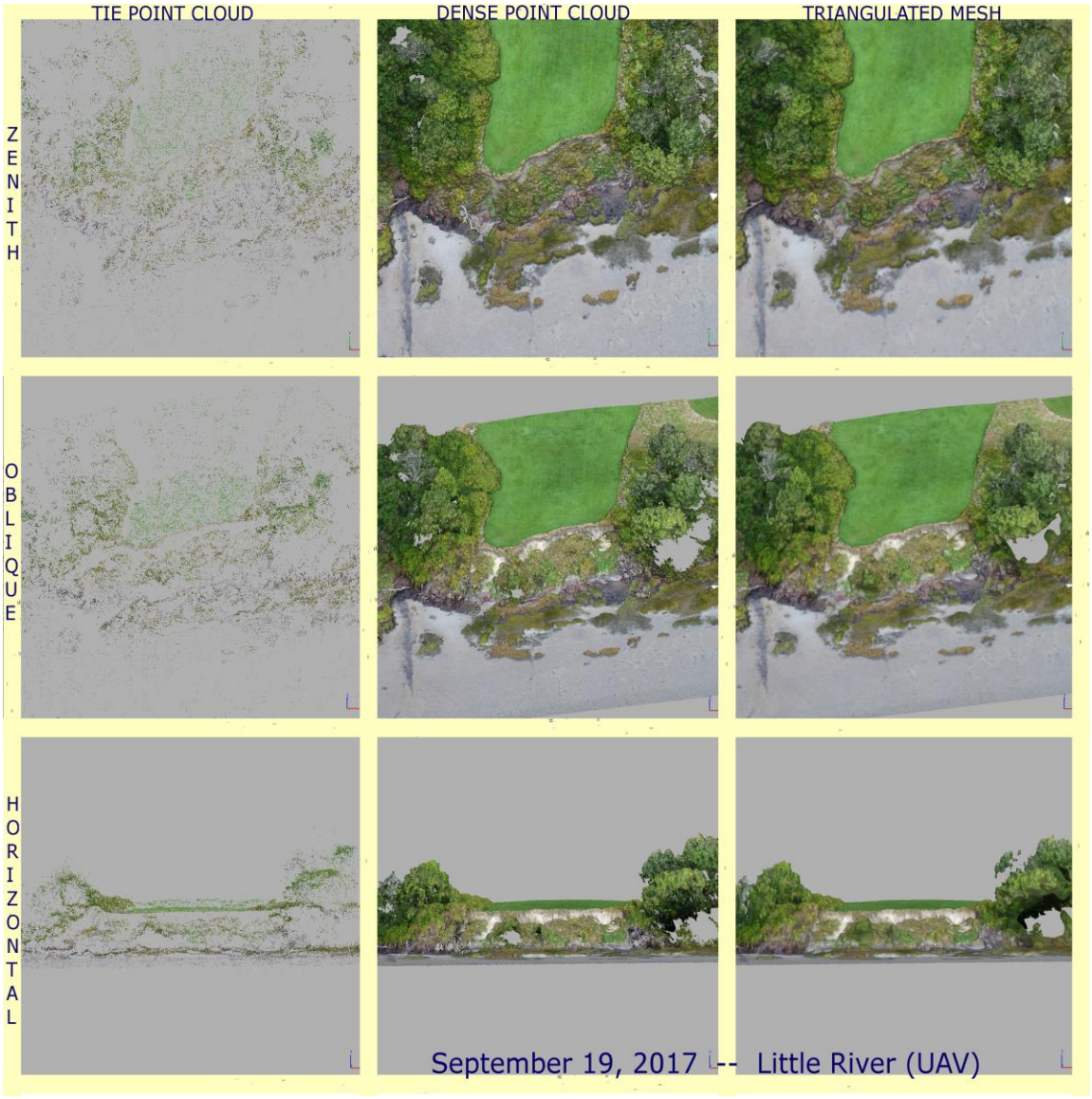

Figure 5.2 a. Select SfM Products from Surveys Conducted by UAV. Little River sub-sites LR 3-4-5, representing September 19th, 2017.

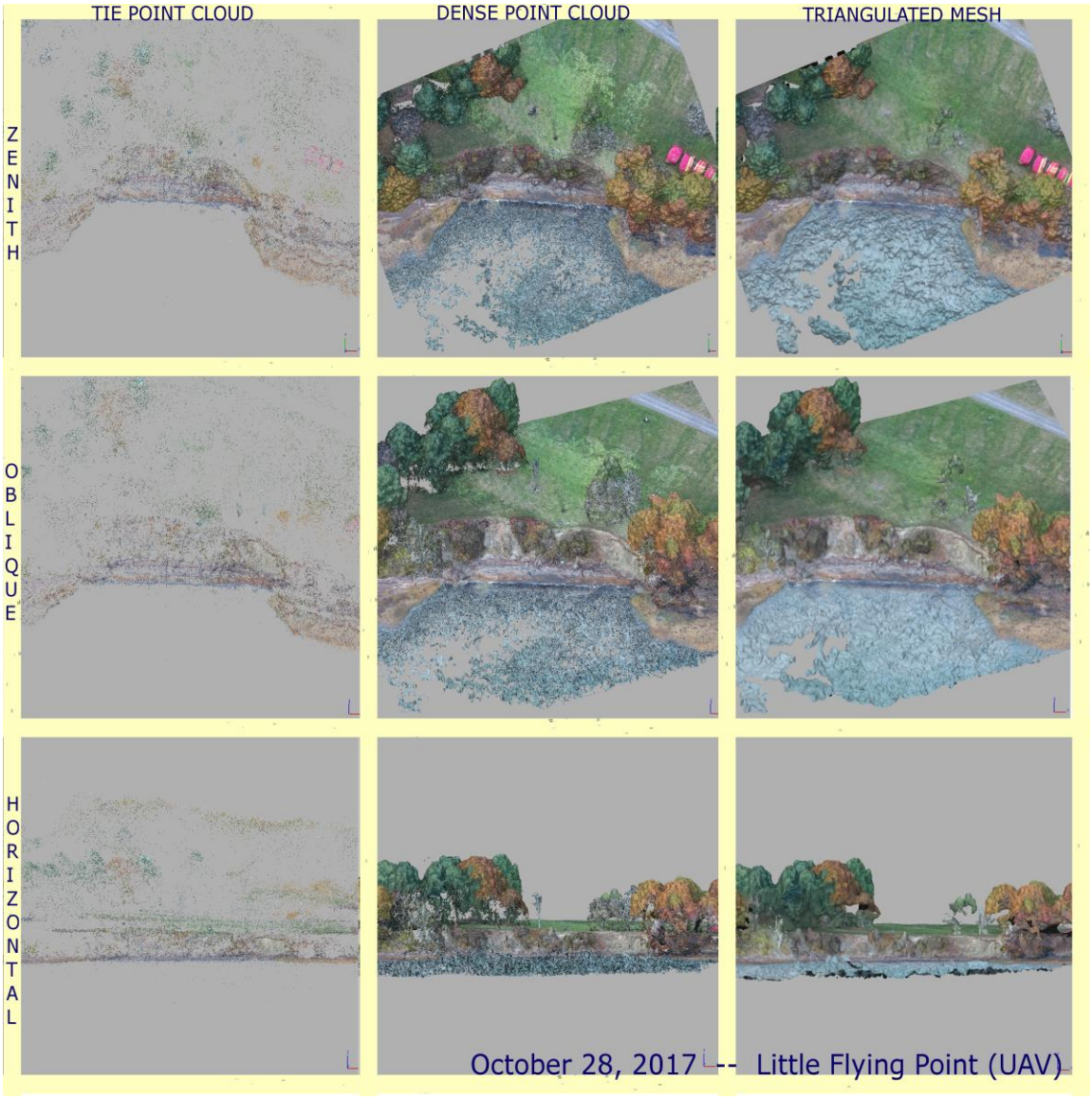

Figure 5.2 b. Little Flying Point, representing October 28th, 2017.

An important concern is illustrated well by this Little Flying Point result: *SfM* does not do well with water. Note the distinct absence of detected features in the Tie Point Cloud where the water was present (and ever-shifting) in the imagery. Moving into the Dense Point Cloud construction, which is built from the Multiview Stereopsis process (described earlier) to fill in the model inferred from each image, attempts are made by the software to imitate the water's surface visually, but lacking the Tie Point information in the region to constrain it, the result is noisy and unreliable.

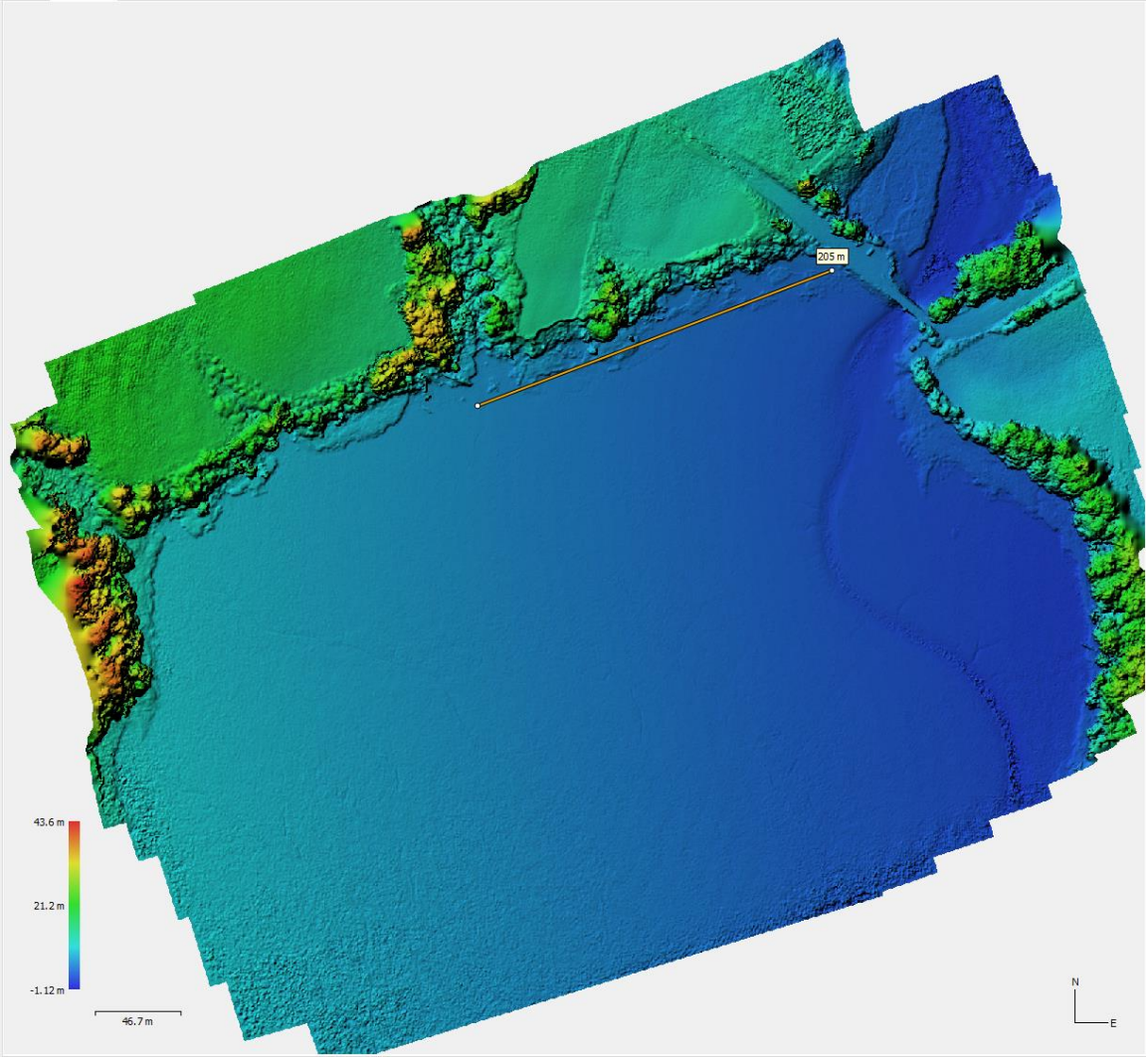

Figure 5.3 a. Large Little River DSM and Point Cloud. A shaded digital surface model for the greater coastal compartment bounding the Little River bluff and its associated mud flat. Sourced from 61 UAV images captured at ca. 150 meters altitude above sea-level (WGS84 datum) resulting in a resolution of 9.51 cm/pixel. The point-cloud from which this DSM is generated is presented as **Figure 5.3 b**, below. The ability to survey at such a scale helps capture broader context for the for the Little River site (highlighted by the thin orange line, 205 meters in length, near the top-center portion of the image). Representing September 20th, 2017.

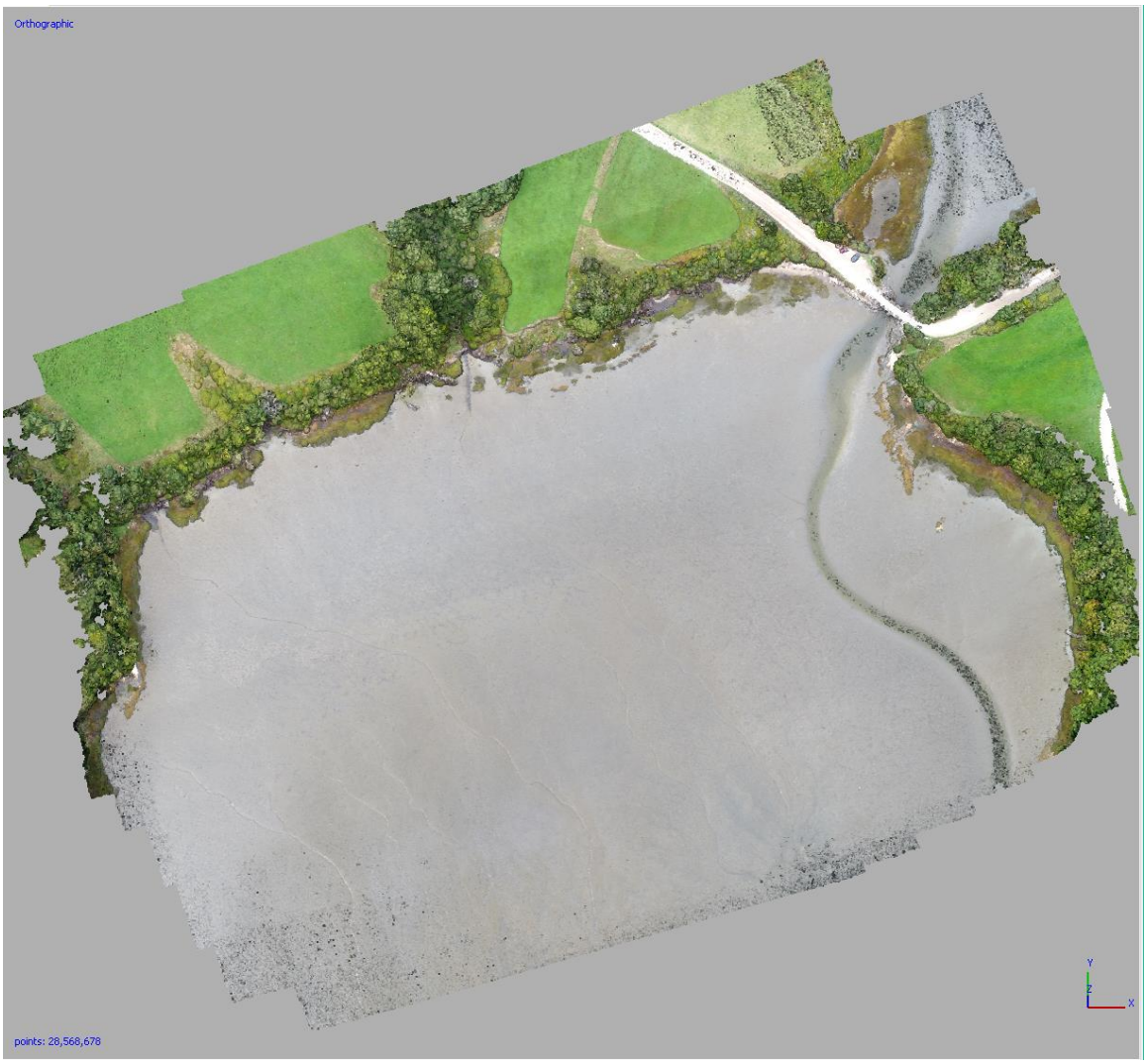

Figure 5.3 b. The point-cloud data -- 28,568,678 (x, y, z, R, G, B) -- generated by the *SfM* procedure and supporting the creation of the DSM shown above (**Figure 5.3 a**).

Select *SfM* Products Visualized in GIS

Because model products are first built within an arbitrary coordinate system, they are destined to be projected and transformed by design. The striking visual returns from the *SfM* procedure as they appear at first glance within the host software may be difficult to evaluate for error without further analysis using other tools such as a GIS program. First: a digital surface model from Little River is compared to the publically available LiDAR dataset (Maine Office of GIS, 2016) for the same area. Next: some erroneous results are presented by evaluating where "mean sea level," (an elevation value of 0, WGS84 datum) occurs across the surface model in contrast and/or conflict with what visual and ecological clues are available that locally denote the actual mean sea level. These errors are considered later in the Discussion section. Last: a map of the overlapping photographic coverage of the March 12th, 2018, Little River model is included to shed light on the relationship between surface reconstruction accuracy and overlapping photographic coverage. The edge-effects seen there have a significant impact on errors portrayed in the mean sea-level evaluation featured before it.

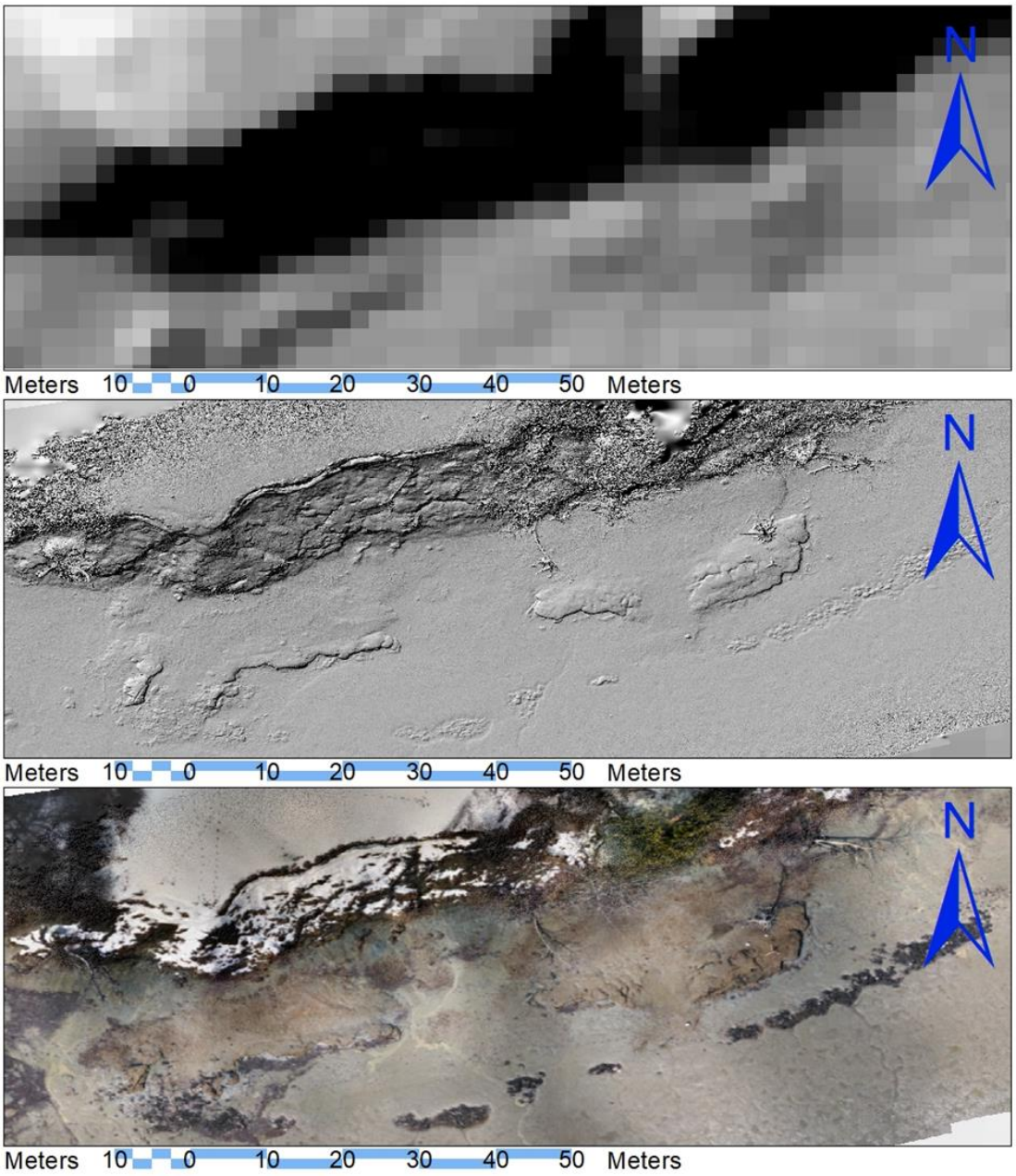

Figure 5.4 a. Comparison of SfM Product and LiDAR. Little River sub-sites LR 3-4-5

Top: Hillshade Product of public LiDAR digital elevation model data, (2 m / pixel). 2006.

Middle: Hillshade Product of *SfM* generated digital surface model, (1.2 cm / pixel). March 12th, 2018.

Bottom: Orthophoto Product from *SfM* source images, providing context. March 12th 2018.

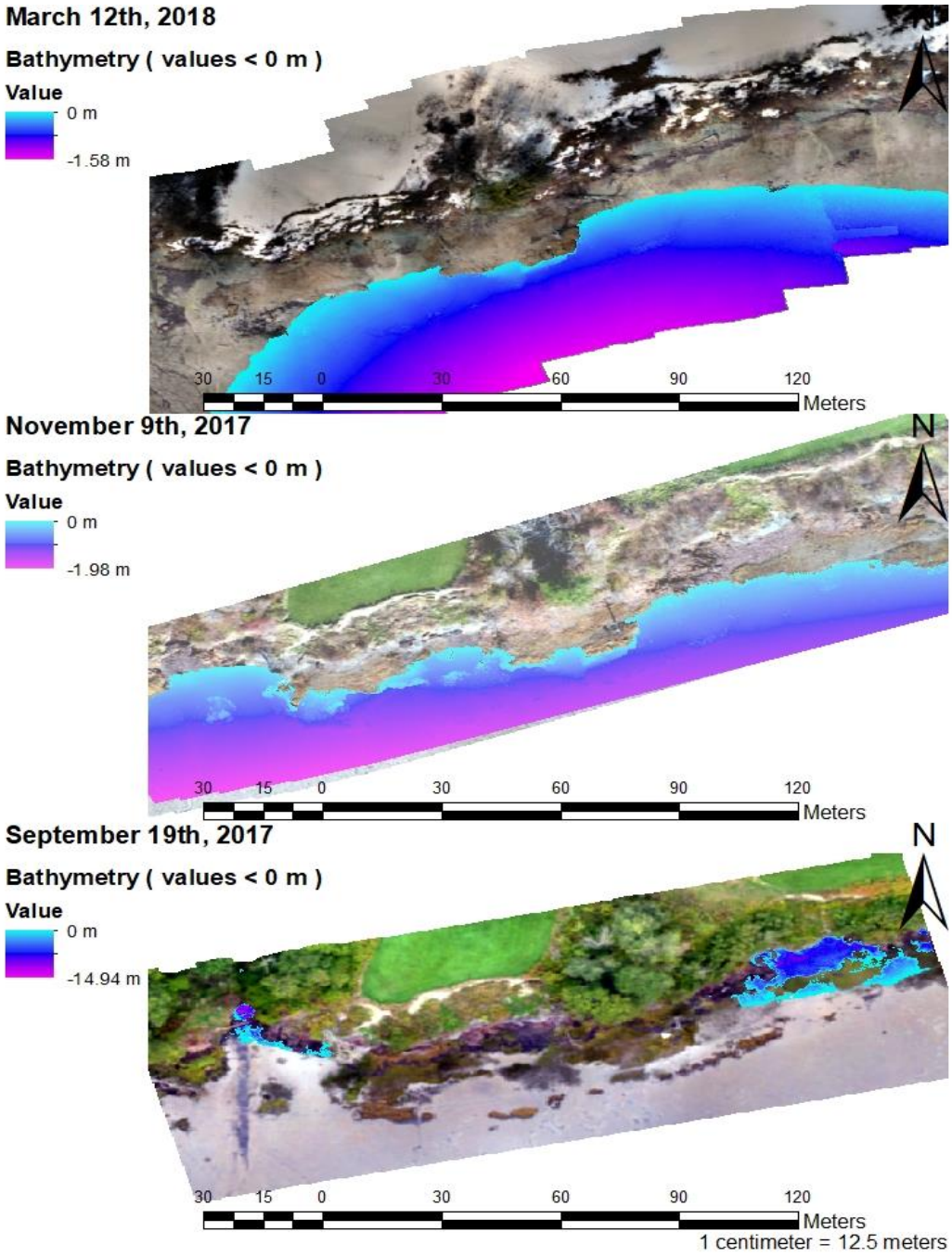

Figure 5.4 b. Surface Model Errors in SfM Product. The surface model errors are highlighted by unrealistic bathymetry measurements. Note that the November 9th, 2017, survey has the most fairly accurate 0 m line near to the fringing marsh but becomes less trustworthy towards edge-regions of the model. Little to be said for the nearly 15m deep pits reported in this iteration of the September 19th, 2017 model despite its realistic appearance at first glance. Discussed later.

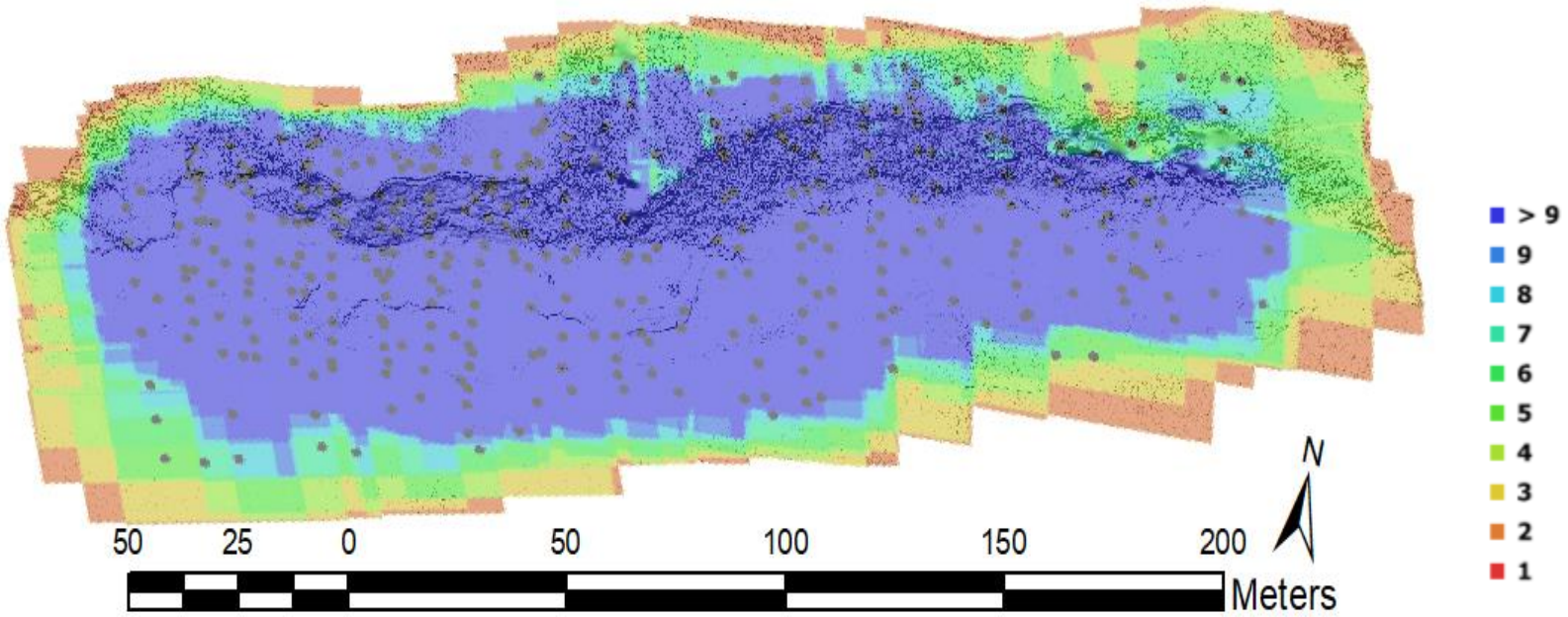

Figure 5.4 c. Photographic Coverage for the Figure 5.4 SfM Product. A map of the photographic overlap coverage used in the construction of the March 12th, 2018, Little River *SfM* product. Cooler colors indicate more reliable coverage. More overlap provides for better estimation of a feature's position in 3-D space and better interpolation of the surface as an end result. Erroneous edge-effects from the drop-off in photographic overlap will be addressed later in the Discussion section. The faint gray dots represent the approximate (X, Y) position of the camera at point-of-capture above the environment for each of the 363 images used. A Hillshade Product of the resulting digital surface model is included for reference and the map has been rotated away from North-up orientation to better fit the page.

A Year in the Life of a Temperate Bluff: *In Photographs*

The photographic series that follows features images captured throughout the length of this project that highlight the intriguing and seasonally-characteristic erosional behaviors exhibited at the Little River site (not to exclude Little Flying Point, but instead to better maintain focus). Attention should be paid not only to the morphology of the site in question but also the ecological zonation; the expressions of groundwater phenomena; and the size and scale of failure events. The series begins on the first day of trialing *SfM* methods.

Each image is accompanied by supporting contextual information such as location and time of year as side-panels. This information is presented as such:

Panel A) Features an image of the Little River scene constructed by *SfM* methods at a broad scale to inform positional context, such as the location of the observer relative to the photograph shown. The thin orange line across the bottom of Panel A is approximately 100 m in length, and the scene is oriented with North as up for the duration of the exhibit.

Within Panel A are features:

1) An approximate frame of view for the photograph shown.

2) A positional marker for the observer, *"You Are Here."*

3) A directional arrow indicating the direction that the observer is facing.

Panel B) Features a National Weather Service (NWS) generated plot of observed daily temperature ranges in the area for the set of months corresponding to the defined season in which the photograph was taken.

Within Panel B are features:

4) A yellow star, its top tip points to the daily observation of temperature ranges for the date the image was recorded.

5) A purple, dashed, line and two bounding purple arrows mark the freezing temperature on the graph for quick reference. The plot also features both record and normal temperature ranges for the area as colored fields.

An example of how this information is displayed is shown next, preceding this section's exhibition.

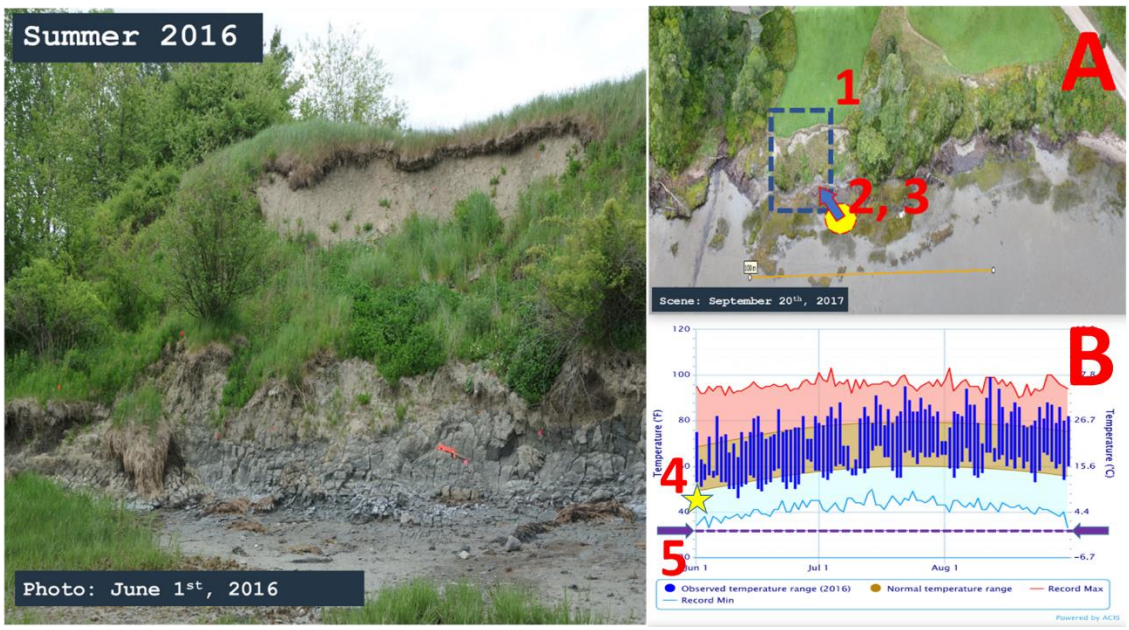

Figure 5.5. Information Layout for the "Year-in-the-Life of a Bluff" Photoseries. Described above.

Figure 5.6 a. Photoseries: A Year in the life of a Temperate Bluff. A thick band of vegetation resides atop a steeply-eroded bluff toe. The barren scarp at the top of the slope suggests that a mass-movement has occurred here previously. It appears that the break in slope caused by the landward edge of the original slump provides a decent catchment for water and habitat for the grasses and shrubs seen in the band.

For tracking: a purple arrow marks an angular dropstone in the process of being exhumed. A blue circle highlights a shrub atop a near-vertical face of the bluff toe. A yellow circle notes some plastic trapped in the roots of the grass.

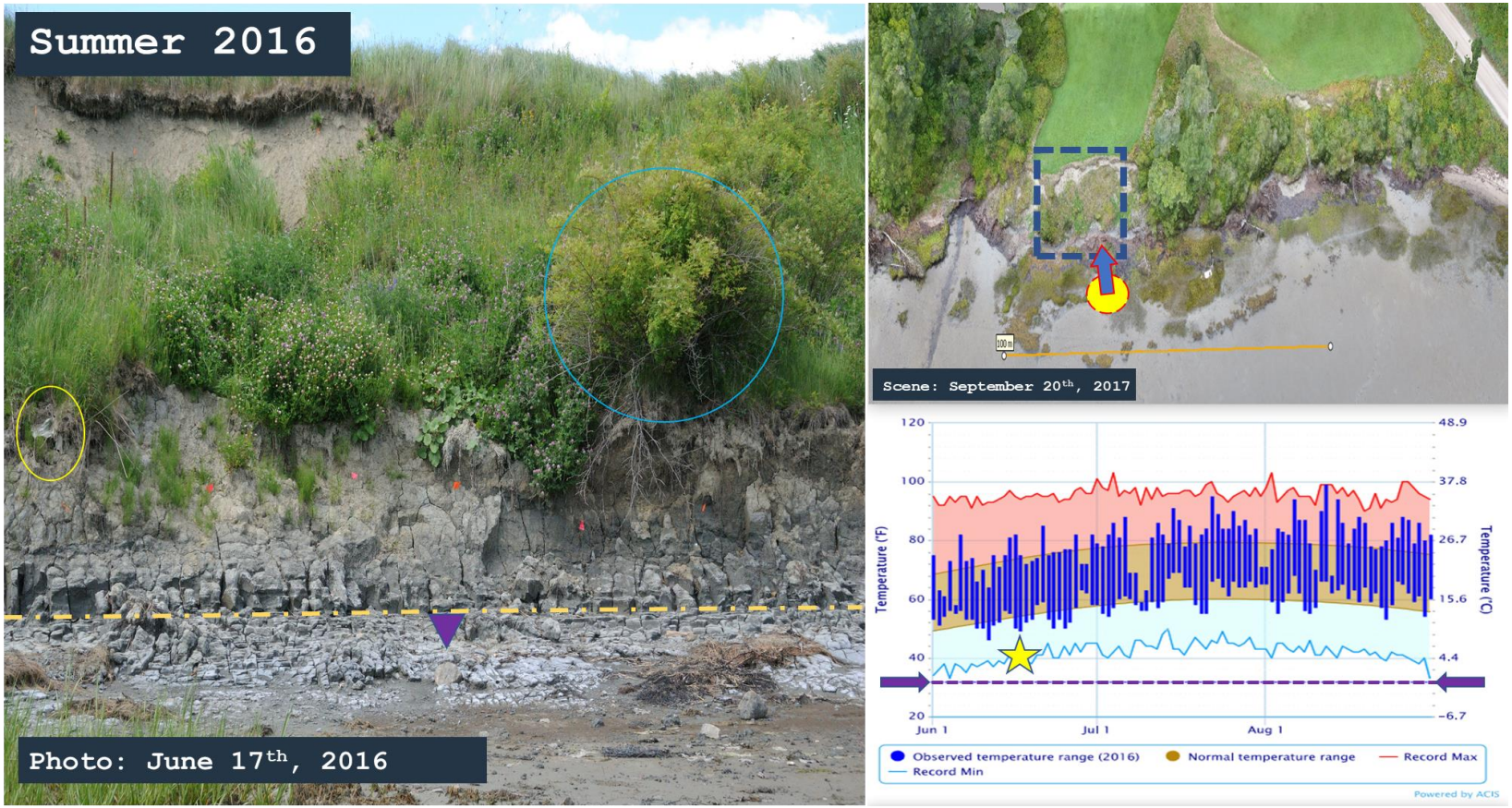

Figure 5.6 b. (**16 days later**) A distinct horizontal cut (dashed yellow line) can be seen forming across the bluff toe. The cut is distinguished by a sharpening break in slope and the hollows of lost blocks of desiccated sediment. Note the many vertical cracks in the exposed sediment. Vegetation on the bluff face continues to flourish. Orange field flags from the early attempts at ground control are visible. The material beneath the blue-circled shrub appears better hydrated (darker appearance of sediments) than the material seen to the left.

For tracking: The same dropstone (purple arrow); perched shrub (blue circle); and trapped plastic (yellow circle).

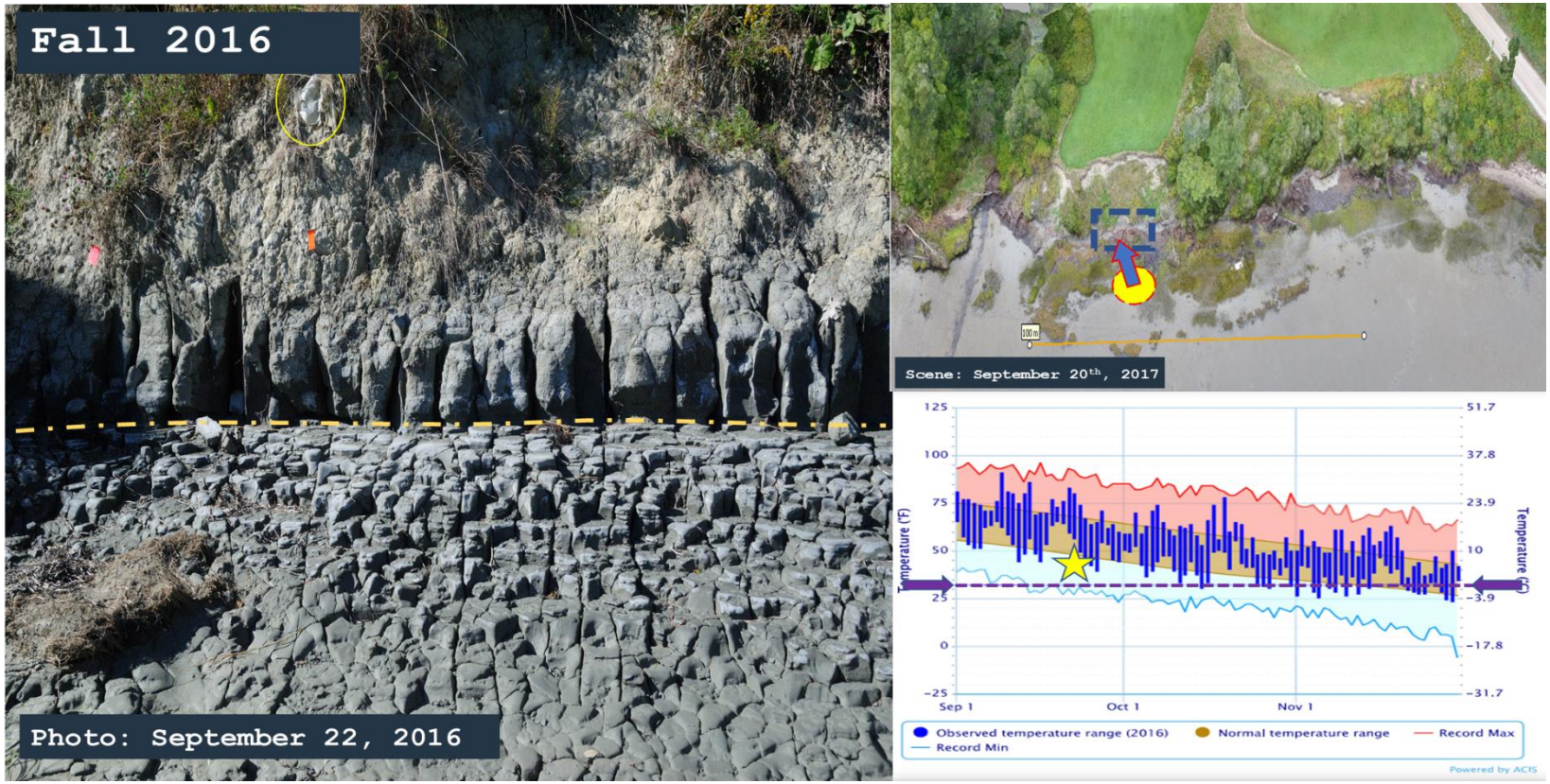

Figure 5.6 c. (**97 days later**) The horizontal cut seen previously (yellow dashed line) is significantly more developed. Flat-topped pedestals in the foreground (seaward) are softened and rounded by more frequent inundation but transition progressively to a more angular and drier formation moving upslope until leveling off at the sharp bench cut. The cut marks an immediate transition to a vertical face at the bluff toe, with a slight undercut forming in many of the more forward-protruding (or perhaps more resilient) desiccated and columnal block features. Vertical cracks are more pronounced and appear to track from the bluff toe on into the bluff face. Some newly exhumed dropstones can be seen along the dashed yellow line that marks the horizontal cut. Note the way the fracture density increases as fractures extend from the vertical bluff into the wave-eroded material and then is reduced where the water has rounded things off. There was little to no evidence of changes in the amount of sand above or below this level, discouraging the idea of a stratigraphic break.

For Tracking: Orange field flags are still present and the plastic (yellow circle) remains trapped. Other previously tracked features are off camera.

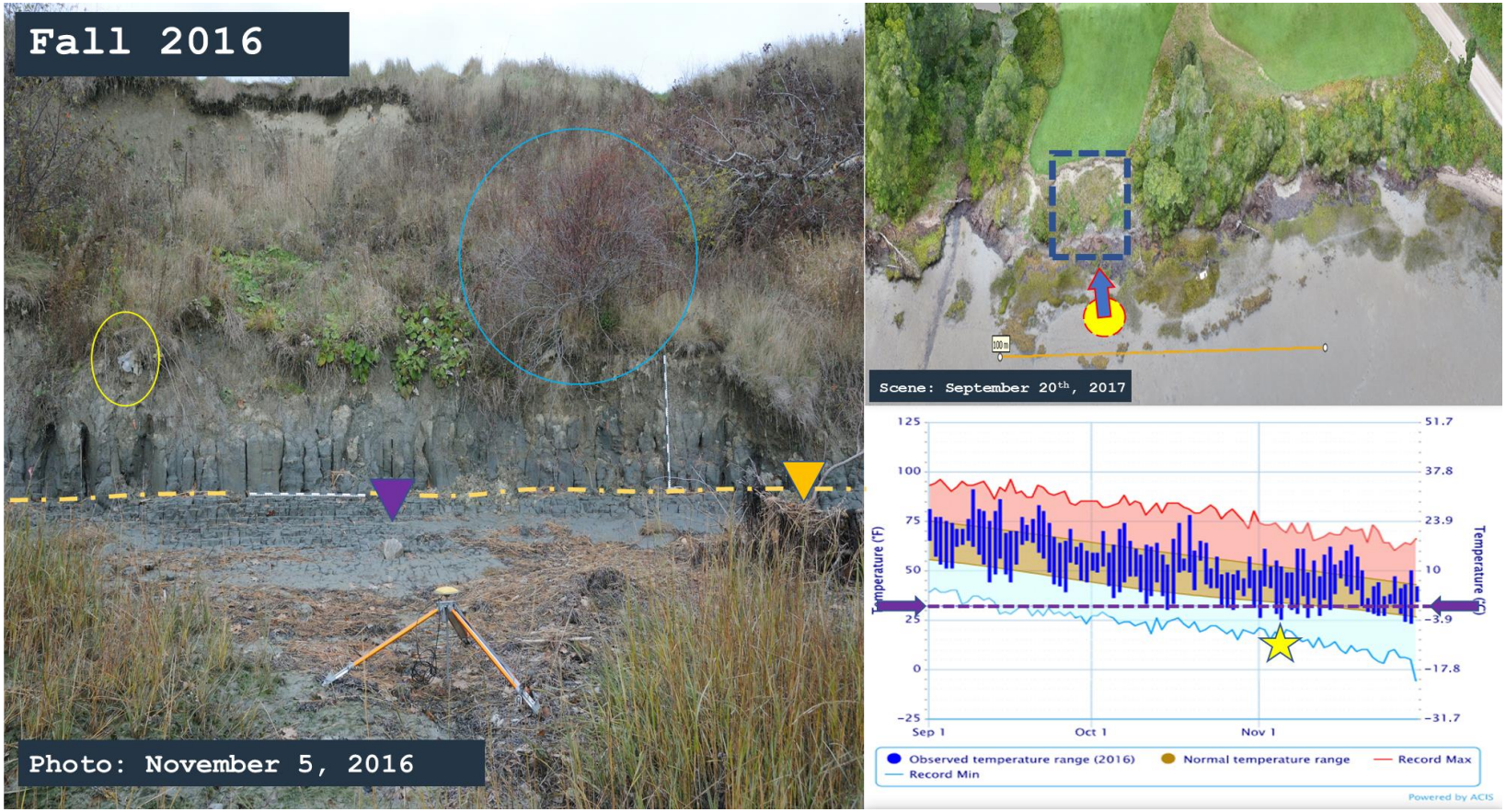

Figure 5.6 d. (**44 days later**) The sharp horizontal cut (yellow dashed line) remains a distinct feature in the shoreline profile while little else has changed upslope besides the drying and dying of vegetation. Notably the marsh grasses are near (somewhat past) their fullest extent. Also of interest is some detail beneath the blue-circled shrub: the oxidized surface layer of the Presumpscot Fm. appears slightly better hydrated here than farther to the left and much of the blue-clay beneath it is dusted slightly with talus material from above.

For tracking: a dead tree has arrived on site (yellow arrow) by drift. An overhanging package of sediments trapped within grass roots is circled in green to be seen in the following image. The dropstone (purple arrow); plastic (yellow circle); and shrub (blue circle) remain in place. A number of orange field flags are now too sun-bleached to appear clearly in the images anymore, undermining their usefulness.

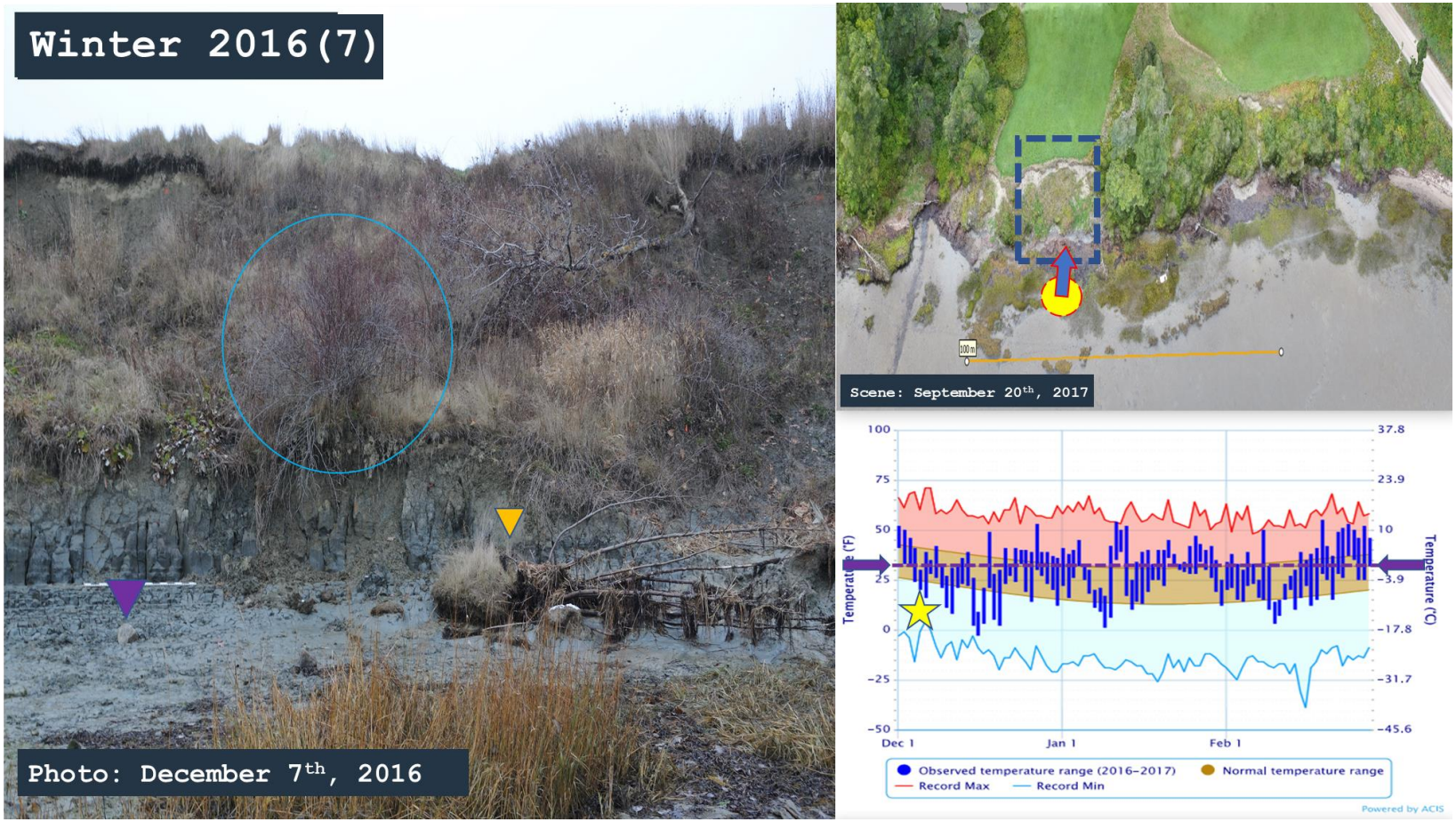

Figure 5.6 e. (**32 days later**) Rain has wet the area. Slope-face vegetation has died off, and the marsh grasses are failing as well. The horizontal bench cut remains but is less visible as it is buried by talus material eroding from beneath the blue-circled shrub. Note in the NWS plot the fluctuations above and below the freezing point to occur in the coming months.

For tracking: the dropstone (purple arrow) remains in place. The plastic is off camera. The driftwood (yellow arrow) has moved landward and is now topped by the vegetated block of sediments (green circle) that has detached from the slope above sometime since the last visit.

Figure 5.6 f. (**Detail image, same date as above**) This photograph provides a closer look at the deteriorating state of the bench-cut tracked throughout summer and fall. The pedestals are more well-rounded, and in some places appear "smudged" in places where talus from above has fallen and begun to anneal to where it was deposited (light blue circles). December 7th, 2016, also marks the first introduction of painted rebar (green and red arrows) for an attempt at landmark ground control for *SfM* surveys. Scale bars = 1.5 m

For tracking: the dropstone (purple arrow) and trapped plastic (yellow circle) remain in place. Note how the bench cut has transgressed landward and upslope in relation to the dropstone when compared to **Figure 5.6 a**.

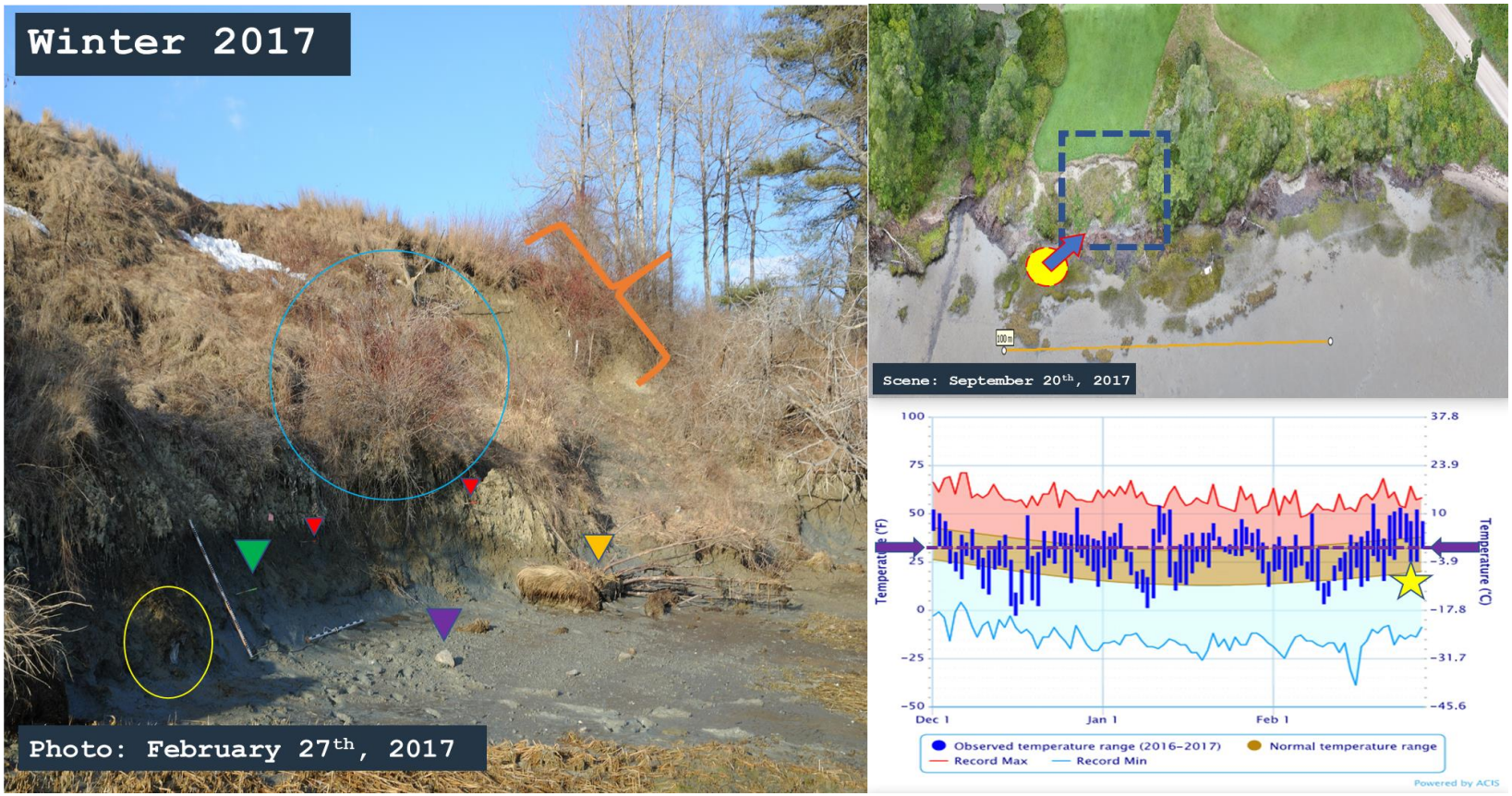

Figure 5.6 g. (**82 days later**) It is immediately apparent that the angular, "quarried," appearance of the bluff toe from the year before has been wiped out during the winter. While it is unclear if the slope is more under-cut, the slope profile where the bench-cut once occured is more smoothly rounded. The sediments appear much more saturated, seen as darker beneath the thin yellow line as well as in the way the clay has yielded readily to footprints. The fringing marsh grasses have been flattened. Scale bars = 1.5 m

For tracking: The trapped plastic (yellow circle) has fallen free in a mass movement. If the dropstone, driftwood, shrub, or vegetated block have moved it hasn't been by much, a testament to low wave energy in the area. With the large orange bracket, I call attention to this bare slope for reference in the following images.

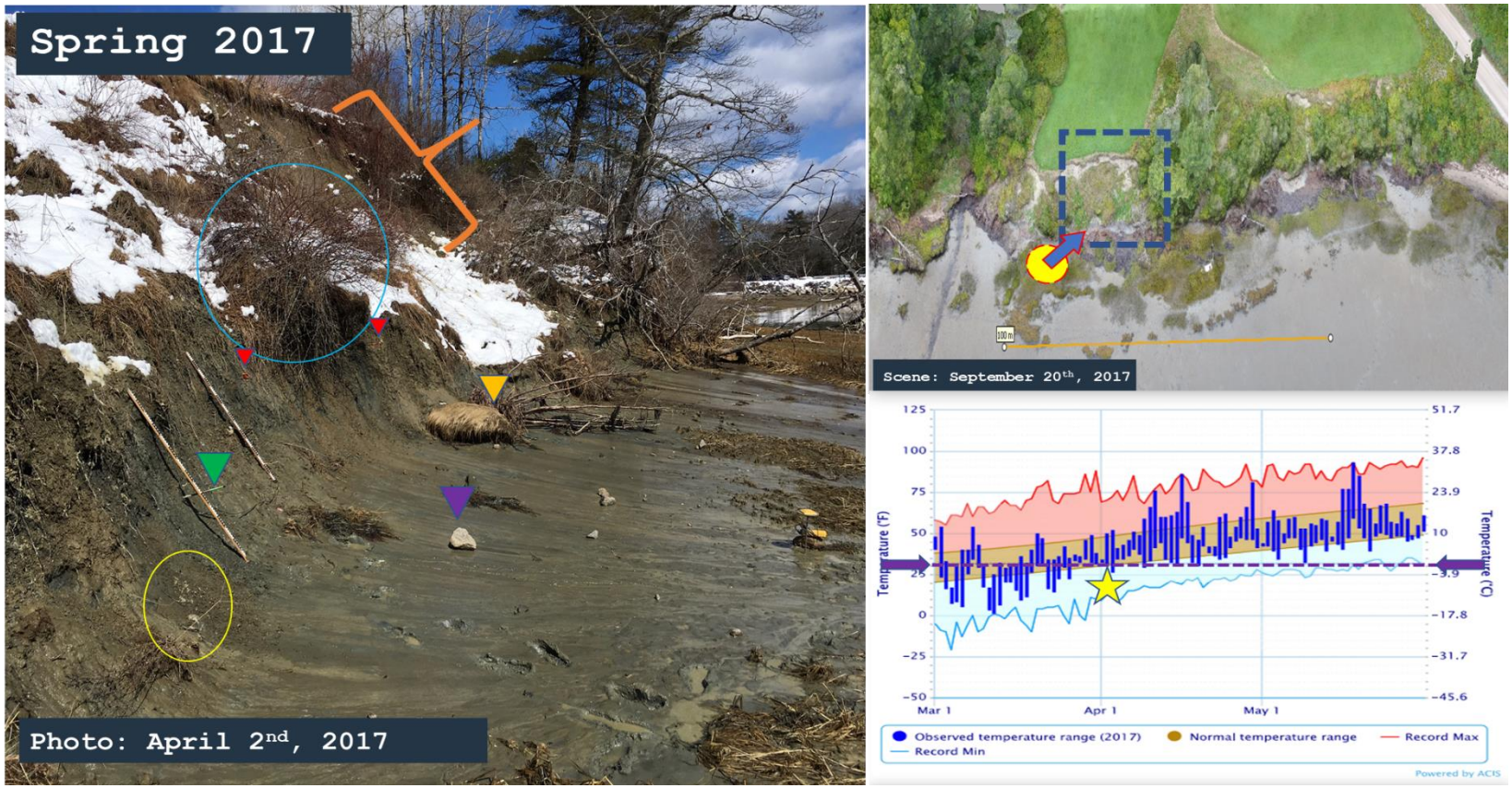

Figure 5.6 h. (**34 days later**): The usual landmarks remain at or near their previous positions. The ground remains soft, saturated, and yielding: footprints quickly fill up with water and suspended sediment (as seen in the bottom right of the image). No trace of the "quarried" bench-cut remains. Interestingly, however, the toe appears to have gently reduced the severity of its slope, from a previously near-vertical to a more relaxed profile. This is best seen by the accumulation of sediments behind the vegetated block (green circle) and at the more distant of the two scale bars, which rests atop a small slump. Measurements at the time were not well-enough constrained at this time to determine whether or not the whole toe of this bluff was creeping forward plastically. The lack of visible blue-clay suggests that surface materials have fallen down from the bluff face over its toe, except where a small freshwater spring has emerged near the green rebar, keeping the local slope clear.

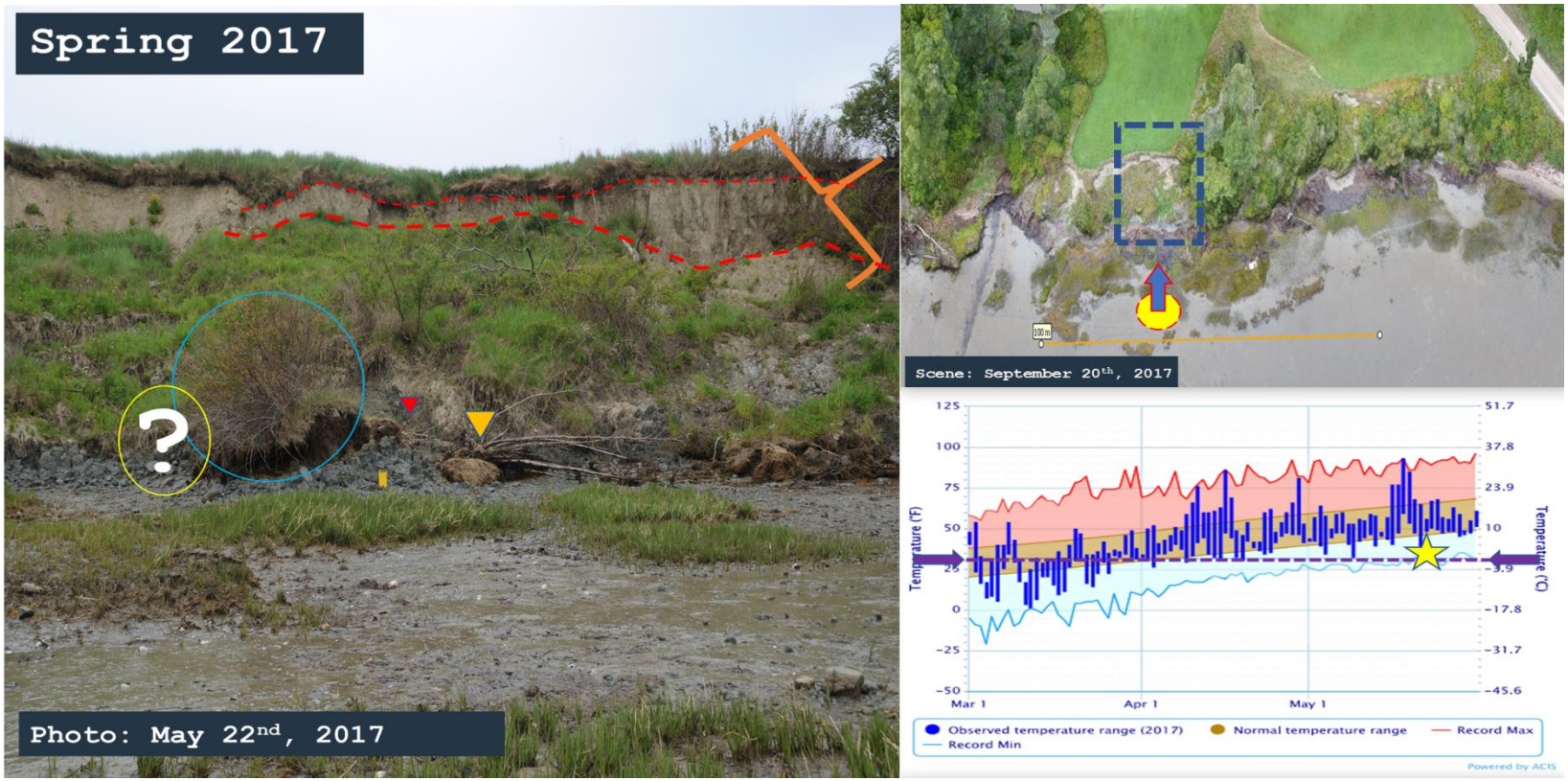

Figure 5.6 i. (**50 days later**): A dramatic change has occurred some-time since the last visit. It is unknown just how long it took for this movement to occur. The scarp at the top of the bluff face (largest red dashed lines) is essentially vertical and more than 6 ft. (1.8 m) has been exposed at the widest point. The toe of the bluff has pushed seaward, and in doing so has heaved blocky blue-clay Presumpscot Fm. upward in front of it. While the blocky character of sediments at the shoreline cut was seen to disappear over the winter, it seems that internally the toe has retained its fragmented structure and interconnected planes of weakness.

For tracking: the white question mark signifies the loss of many tracked features following this event. Note the significant amount of material root-bound and brought to the waterline by the now-fallen blue-circled bush. One of the red-painted rebar has been upturned towards the sky. Also noteworthy is the significant number of small mud balls (a few are marked by the thin yellow arrows) scattered about the intertidal zone.

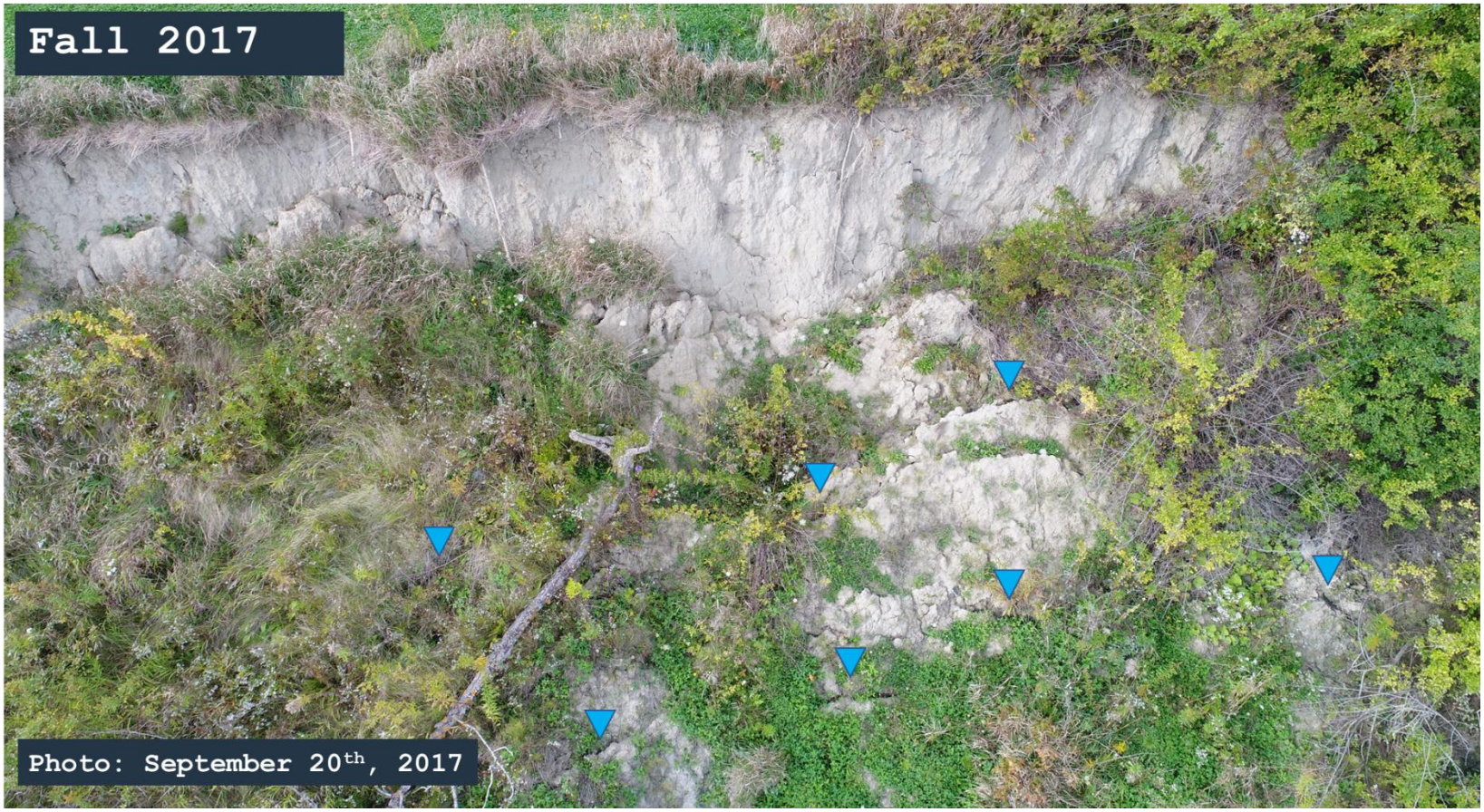

Figure 5.6 j. (**121 days later**): This UAV image and the one to follow it are included as a final note in the series for the purpose of pointing out (blue triangles) a handful of the visible openings in the top surface of the slumped bluff face which tell of the fault-blocks formed during the mass movement. They likely act as conduits for surface water to enter along these slip planes. Faulting like this also facilitates surface drying and segmentation of the bluff face. Such rifting reduces the potential for rooting vegetation to extend across large portions of the bluff face, preemptively dividing root-bound masses to be conveyed downslope as seen (next figure) in the spring of the following year. Also noteworthy is the significantly sun-bleached appearance of the exposed Presumpscot Fm. sediments after a summer season.

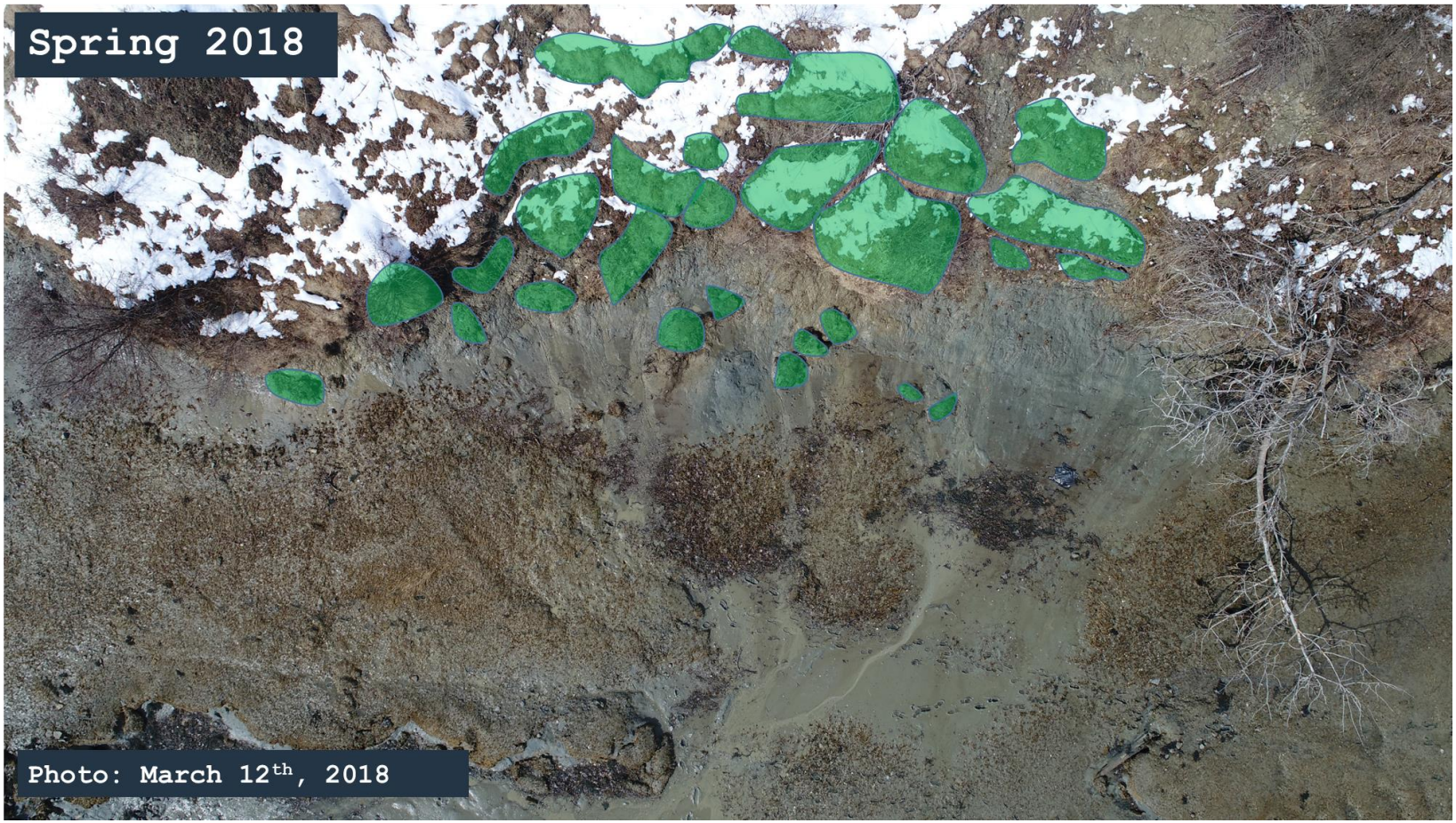

Figure 5.6 k. (**173 days later**): This UAV image shows the fragmented nature of surface vegetation following the slope failure and subsequent relaxation during the spring softening. While not all are marked, this demonstrates how disconnected blocks of vegetation may help package large quantities of sediment for delivery downslope.

Seasonal Concerns for Temperate Bluff Sediments: Observations in Brief

The following **Table 5.1** approaches the *chicken-and-egg* problem of seasonal influences on bluff erosion in the area. Coastal bluffs are, inherently, highly erodible landforms. A significant amount of variability acts on the timing of the bluff erosion cycle as governed by the character and intensity of a given season. These variations are exhibited plainly on the bluff face from one season to the next, as different agents of erosion take charge, modifying the "initial" conditions and slope geometries that the bluff will carry into the next span of time.

Table 5.1 Seasonal Influences on Local Bluff Erosion.

Spring	• Freeze-thaw cycles have softened and significantly loosened the bluff material • Bluffs begin the season saturated and over steepened from the effects of the previous winter • Meltwater contributes excess weight (extreme overburden) while facilitating material flow and mass movement • Piping phenomena exploit internal fractures and induce weakness • Greatest observed (but not quite confirmed) frequency of slope failures large and small • Spring sapping carries great quantities of fine sediment seaward • Slumping and splaying landslides deliver large quantities of sediment to the intertidal zone • Bluff material, at its most fluid, readily seeks lowest angle of repose
Summer	• Material deposited in the intertidal zone available for marsh colonization. • The same material is chronically redistributed by cyclic tidal inundation • Exposed sediments begin to desiccate in the warmer, dryer weather and under the heat of the sun. Even in the intertidal zone there is

	evidence of contraction and cracking, but also rounding and smoothing of these features by repeated tidal washing • Evidence of erosion at the waterline becomes more persistent against the dry clays (whereas sediment was too readily eroded in the wet spring to capture finer detail) and water-cut benches develop in the bluff toe over time • Vegetation on the bluff face flourishes, exploiting water catchment in cracks and channels on the surface. Roots can grow and force fractures in the bluff. However, root propagation and drying of clays is also expected to bind and consolidate (package) upslope surface materials. Meanwhile the internal sediments retain groundwater and the bluff toe remains relatively more hydrated by tidal cycles, making these regions relatively more plastic.
Fall	• Continued drying and growth of vegetation eventually gives way to late-season changes in the weather • Marsh grasses at their fullest. Successful plant colonies are expected to mitigate some wave energy and intercept some sediment from upslope • Despite protection from intertidal grasses, continued erosion and over-steepening of the bluff by excavation phenomenon is observed, described here as "quarrying," or "calving," of the bluff toe, where desiccated blocks of sediment are neatly removed leaving a clear-cut platform and a sharp transition in relief from horizontal to near-vertical base
Winter	• Transitional period of freeze-thaw cycling • Freeze-thaw driven spalling and exfoliation of exposed sediments • An expected deep-freeze of internal bluff sediments, solidifying the bluff and preventing major failures • Highest occurrence of storms that move in a direction optimal for wave attack at these sites • Accumulation of sea ice in local embayment shown to do significant damage to the intertidal zone

	• Great (thorough if not complete) removal of material deposited from previous spring, since desiccated, fractured, and cut back to a steep opposing profile
Return to Spring	• Bluff toe begins the year dangerously over-steepened, lacking the strength to support material upslope, and may fail dramatically when made more vulnerable by the effects described in the Spring (above)

Other Notable Observations of Phenomena:

Surface Expressions Preceding Slope Failure

Hazard management and prediction efforts would benefit from the ability to monitor strain or strain-rates from repeat measurements and interpret tell-tale signs of impending slope failure. However, it has proven difficult to spot a failing slope in this local context. For example, most of the small trees and vegetation occupying the bluff face at Little River are too juvenile to show much straining of their trunks in compensation for a creeping slope. However, the added vantage provided by the UAV allowed for the imaging of tension cracks at the top of a portion of the bluff which, in hindsight, foretold the slipping of one of the largest portions of the Little River bluff seen to fail throughout this observation period of the project. The slope that failed was neatly bounded by the LR 1 and LR 2 sub sites. Observation of LR 1 was abandoned early on due to its small size and heavy vegetation cover; an erosional hot spot unsuitable for individual *SfM* attention. LR 2 was the site of a rather photogenic former landslide. Heavily vegetated, the block between LR 1 and LR2 was not considered for monitoring by *SfM* throughout the course of this project. Not until the acquisition of the UAV was it consistently photographed as the whole bluff was scanned. Following its failure, re-evaluation lead to the discovery of photographs featuring surface expressions that likely foretold a greater risk at this site. Notably, even after slope-failure the block retained most of its vegetation cover. It is hardly noticeable from the road as a fairly large (for Little River) landslide. What follows is a series of five figures detailing the evidence that this slope was in failure.

Figure 5.7 a. Surface Expressions Preceding Slope Failure. View of the LR 1 sub site. While the LR 1 sub site was often overlooked, it was the source locale for the inset image, used as **Figure 2.12 a**, detailing springing and piping phenomenon observed occurring in many sections of the thawing bluff. It is likely that this spring was fed by the reserve of snow seen trapped upslope. Hindsight suggests that this reoccurring spring could be associated with, and exploiting, a fault caused by the separation and movement of the large mass of material to observer's left (fault (slip plane) suggested by the red-dashed line and arrows in the main image).

Figure 5.7 b. View from the LR 2 sub site. Showing toe creep of the failing block. Most of the painted rebar segments that were placed (on December 7th, 2016) were eventually exhumed or lost in slides. The one seen here was engulfed by the advancing sediments.

Figure 5.7 c. An oblique aerial view by UAV of the bluff at Little River, with the block in question (bounded by the red dashed lines) between sub sites LR 1 and LR 2. The location of the spring described in **Figure 5.7 a** is marked with the blue triangle near LR 1. The accumulation of many dead trees (light arrows) lining the base signify a steady supply from upslope. A suspicious break in the vegetation (between the purple-dashed region and the red-dashed line) is examined next.

Figure 5.7 d. The same site from above. The transition from September to November has removed much of the obscuring foliage but the block surface is still too cluttered with barren vegetation and too visually noisy to be suitable for an individual *SfM* scan. Early morning light reflects strongly off the exposed and oxidized sediments, further highlighting the gap that is developing at the top edge of the bluff (between the purple-dashed region and the red-dashed line).

Figure 5.7 e. It was later observed that the portion of the bluff (thin red-dashed lines, center) between the LR 1 and LR 2 sub sites had failed. It retained much of its vegetation cover (still living, freshly foliated) and remained difficult to photograph; it would be difficult for a passerby to notice that an event had occurred at all. The displacement is more easily seen in the scarp upslope, behind the stand of young trees that were carried down. The yellow arrow marks a dead tree at the high-water line that can be seen in each image.

Ice Unseen: Sea Ice from Casco Bay

SfM survey visits were not prioritized in winter because snow-cover would result in a false-surface that would be unsuitable for any volumetric measurements. Yet damage caused by sea ice was found each following spring. Satellite imagery confirmed the suspicion that sea ice takes some residence against the shore for a part of the winter season. Its presence there is potentially damaging, as it may pluck and scour the bluff sediments and fringing marsh colonies when forced by the tides.

Figure 5.8 a. Sea Ice in Casco Bay. At right, one of the rebar landmarks at sub site LR 6 was found to be bent out of shape following the winter season. It was quickly determined that since neither wave energy nor curious clam harvester could have caused the damage, pressure from ice likely deformed the steel.

At left, a composite satellite image shows the extent of the sea ice impounding both the Little River and Little Flying Point sites. A green triangle marks Bunganuc Bluff, one of the largest eroding coastal bluffs in the state.

Figure 5.8 b. Little River, Freeport, Maine. February 28th, 2019.

A small block of sea ice is found here to have plucked and carried sediments. The dark color of the rafted mud suggests it was lifted from the mudflat and brought landward. Length of the rock hammer is 30 cm.

Waterline Etching in Fine Media

Both major (**Figure 5.10 a**) and minor (**Figure 5.9 a**) horizontal cut lines can be observed developing across the bluff toe in the drier months. The fines of the Presumpscot Fm. are readily mobilized and winnowed by the presence of water at the bluff toe, capturing an often-rewritten record of recent incursions. Whether exploiting minute differences in sediment strata, or aided by coincidental wind and waves, presumably a combination of both, the reach of the high-water mark cuts cleanly across the vertical jointing of the desiccated bluff sediments.

Figure 5.9 a. Possible Waterline Etching in Fine Media. Little River, Freeport, Maine, Sub-site LR 5. The finest lines (extending inward from the fine blue arrows, not all marked) seen etched (or winnowed-out) across the Presumpscot Fm. sediments at the bluff toe are expected to be an exploitation of variations in the fine-sediment composition.

For tracking: the feature highlighted in green, a particularly resilient pedestal of eroded sediment, is visible in the next figure.

Figure 5.9 b. Little River, Freeport, Maine, Sub-site LR 5. The Presumpscot Fm. clays may provide an especially good media for recording the recent position of the waterline. With a repetitive tidal inundation cycle, the erosion is concentrated along some horizons more than others. Where the water stalls, perhaps a tidal position is briefly held in place by a coincident swell, erosion persists at a stable level for some time instead of progressing farther up or down the bluff profile. Exploitation of weaker layers present due to stratigraphic differences would be likely.

The yellow-dashed lines mark more prominent, more well-developed, horizons than those seen in **Figure 5.9 a.**

Figure 5.9 c. Little River, Freeport, Maine, Sub-site LR 3-4. Over the course of the dry season it becomes fairly apparent where the high waterline spends a majority of its time (yellow-dashed line). Blue lines mark several other horizontal etchings distinguishable within the image that may be caused by natural fluctuations in the high tide line or the grain sizes it comes in contact with.

"Calving," or "Quarrying," of Desiccated Sediments from the Bluff Toe

Over time a major cut bench is seen to develop across the jointed sediment blocks of the bluff toe, distinguishing itself from the more numerous minor horizontal etchings. The idea that this cut plane represents the band where high-water currently spends the majority of its time (relative only to timescales within the present season) is detailed later in the discussion section. Two distinct textures can be observed, above and below the dominant horizontal cut: 1) above the line, is characterized by vertical/near vertical jointed blocks and the cavities where such blocks appear to be missing, undercut in a rounded manner by the waterline. And 2) below, the disjointed and stair-stepped shallow rise of pedestals, angular near the cutting plane and more rounded towards lower in the tidal zone, fading into mudflat. It is show that the horizontal cutting plane of the high water line efficiently removes already-vulnerable blocks of sediment from the bluff toe, leaving behind a "quarried" appearance characteristic of the drier seasons.

Figure 5.10 a. "Calving," or "Quarrying," of Dessicated Sediments from the Bluff Toe. Little River, Freeport, Maine, Sub-site LR 4. The bluff toe featured a blocky, quarried appearance that developed throughout the summer months. Note the significant under-cutting by concentrated erosion at the water line; the dry state of the Presumpscot Fm.; and the ubiquitous vertical jointing.

Figure 5.10 b. Little River, Freeport, Maine, Sub-site LR 5.

"Calving" of discrete dry blocks of Presumpscot Fm. sediments when undercut by the high-tide line during the dry summer months. The quarrying effect of this process exploits the near-vertical and highly jointed irregular face of the bluff toe in direct opposition of incident water and wave energy. It's expected to be particularly susceptible to excavation through the winter.

I consider likening these occurrences to "calving," for while it happens at a drastically smaller-than-glacial scale, and there are no buoyancy effects at play, it seems the manner of material failure on display here mimics the process in a relatable way.

Note how the recently liberated block (left image) has been tapered to almost a point at its base, and has slipped forward toe-first. Separated from the parent bluff by drying, while simultaneously having its base winnowed and softened by repeat inundation left it primed for removal.

Figure 5.10 c. Little River, Freeport, Maine, Sub-site LR 5. As the process continues it can contribute a remarkable amount of sediment into the intertidal zone for break-down and digestion by the tides. Scale bars = 1.5 m in length.

Formation of Mud Balls (Rip-up Clasts)

Mud balls are found in abundance scattered about large slope-failure events. The following figures present some of the conditions for their formation. Quickly becoming more mobile as they are rounded-down and digested by repeat inundation, they appear to be ephemeral byproducts of a landslide event. However, their noted presence in the Holocene units of off-shore sediment cores (Brothers 2010) suggests some outlast their source, this is addressed later in the Discussion section.

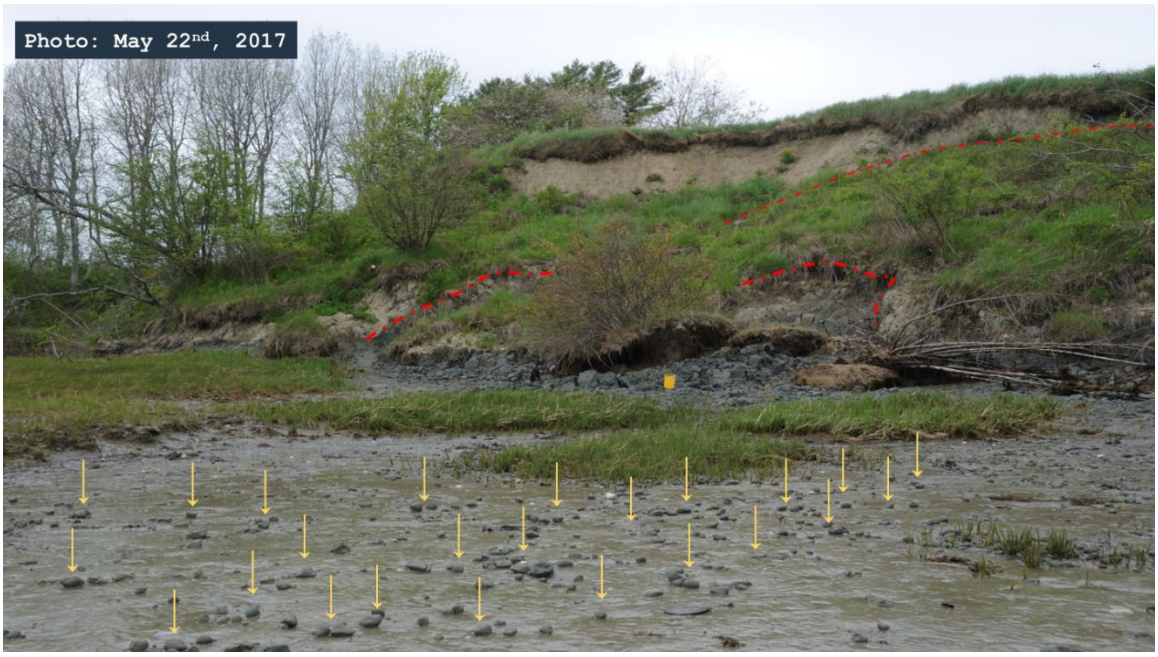

Figure 5.11 a. Formation of Mud Balls (Rip-up Clasts). Little River, Freeport, Maine, Sub-site LR 4.

Mud balls (just a few are marked by thin yellow arrows) are a common occurrence nearby the eroding bluff. They can often be seen scattered, escaping the scene of a crash, where a slope failure has upheaved the fragmented sediments at the bluff toe.

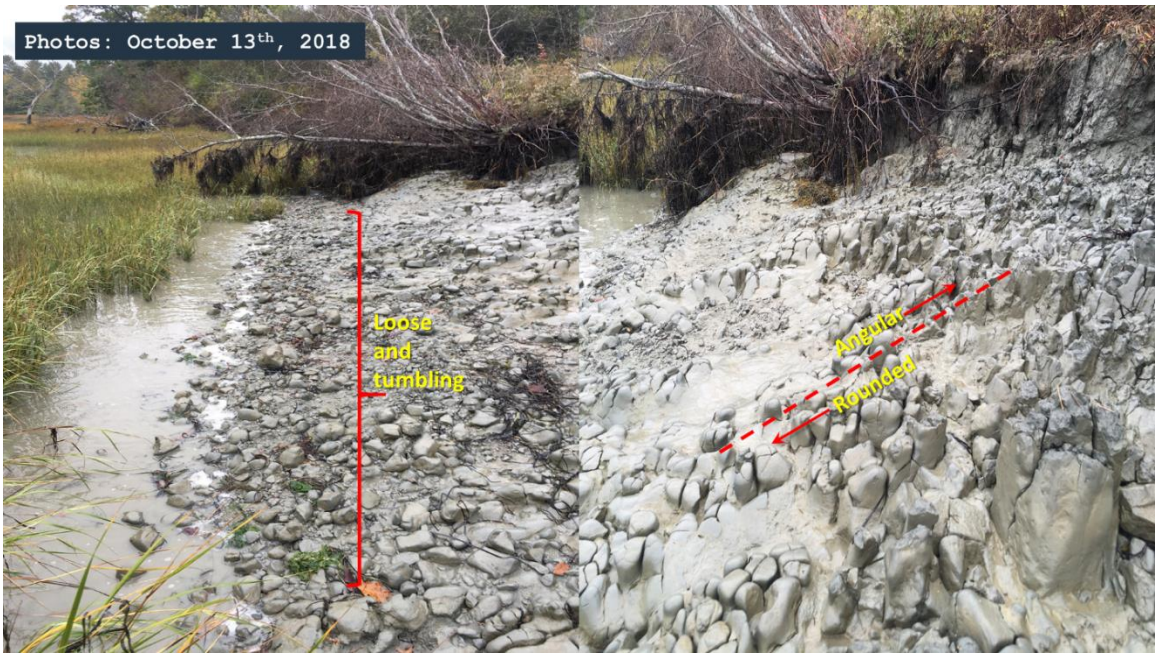

Figure 5.11 b. Little River, Freeport, Maine.

Whether freed from the bluff by "calving," such as described in the section above, or thrust forward in front of a landslide as seen here, blocky and jointed sediment features introduced into the intertidal zone are immediately subject to decomposition. Prominent sediment splays are particularly exposed to insolation; repetitive wetting and drying (or freezing and thawing), and the channelizing currents that develop in the local flood-and-drain system. Once sediment blocks are broken free from their source they become mud balls, and become increasingly mobile as they are rounded, reducing their size until disaggregated or buried.

Figure 5.11 c. At left, deep in the image: a mud ball lag-deposit rests where the tide has left it (yellow dashed area).

At left, foreground: the rising tide begins to interact with mud balls at the immediate shoreline.

At right: the heavily jointed Presumpscot Fm. heaved forward by a landslide is readily channelized by run-off and repeated flooding-wetting-draining-drying cycles. The increased surface area gained by decomposition allows for moving water to make quick work of more and more sediments.

Figure 5.11 d. Mud ball clast breakdown in closer detail. The larger objects seen here, halved in the center of the left image, neatly quartered in the center of the right image, are roughly the size of a fist

An Unconformity in the Making

As discussed in the introduction: an eroding bluff leaves a gap in the sediment record; a hiatus in time that may be significant to the stratigraphic record. When challenged by a transgressive sea-level rise, a bluff is cut back and carried away. The ground at the foot of the bluffs is often coated with a veneer of soft and saturated mud that gives-way underfoot but coats and covers firmer material beneath it. Occasionally, some areas became cleared of loose sediment cover, and patterns were observed in the firm blue Presumpscot Fm. Some images of these patterns will follow this introduction. As the waterline climbs and cuts back further into the bluff, some toe features, such as remnant bases of quarried blocks of sediment are surpassed and seen to persist. Some features that were uncovered weren't as easily explained. The features in question show banded discoloration (by oxidation or groundwater?) patterns crossing the Presumpscot Fm. blue clays along its blocky jointing at the bluff toe. The discoloration appears to diffuse evenly, out perpendicularly, from along its bands into the blue clay and not simply as a result from infilling of the joints by loose fines from above. The consistently diffuse nature of the discoloration (oxidation?) along the joints suggests groundwater flow and chemical activity. Further evidence against infilling exists in that the discoloration can be seen on vertical faces of quarried clay, and some joints continue up into the bluff toe, up beyond flat ground. The inter-crossing patterns reflect those of frost-wedging. I suspect the patterns revealed by erosion may be some relict combination of inter-crossing slip planes, frost wedges, and or groundwater conduits formed as the material deforms by hillslope stress or following the opening of tension cracks during slope failure. It seems that these patterns have formed internally, and have been cleared as the sea has cut back. It is not known at this time whether much of this trace survives the severity of winter or scour by sea ice and it was not persistently visible throughout the duration of the project.

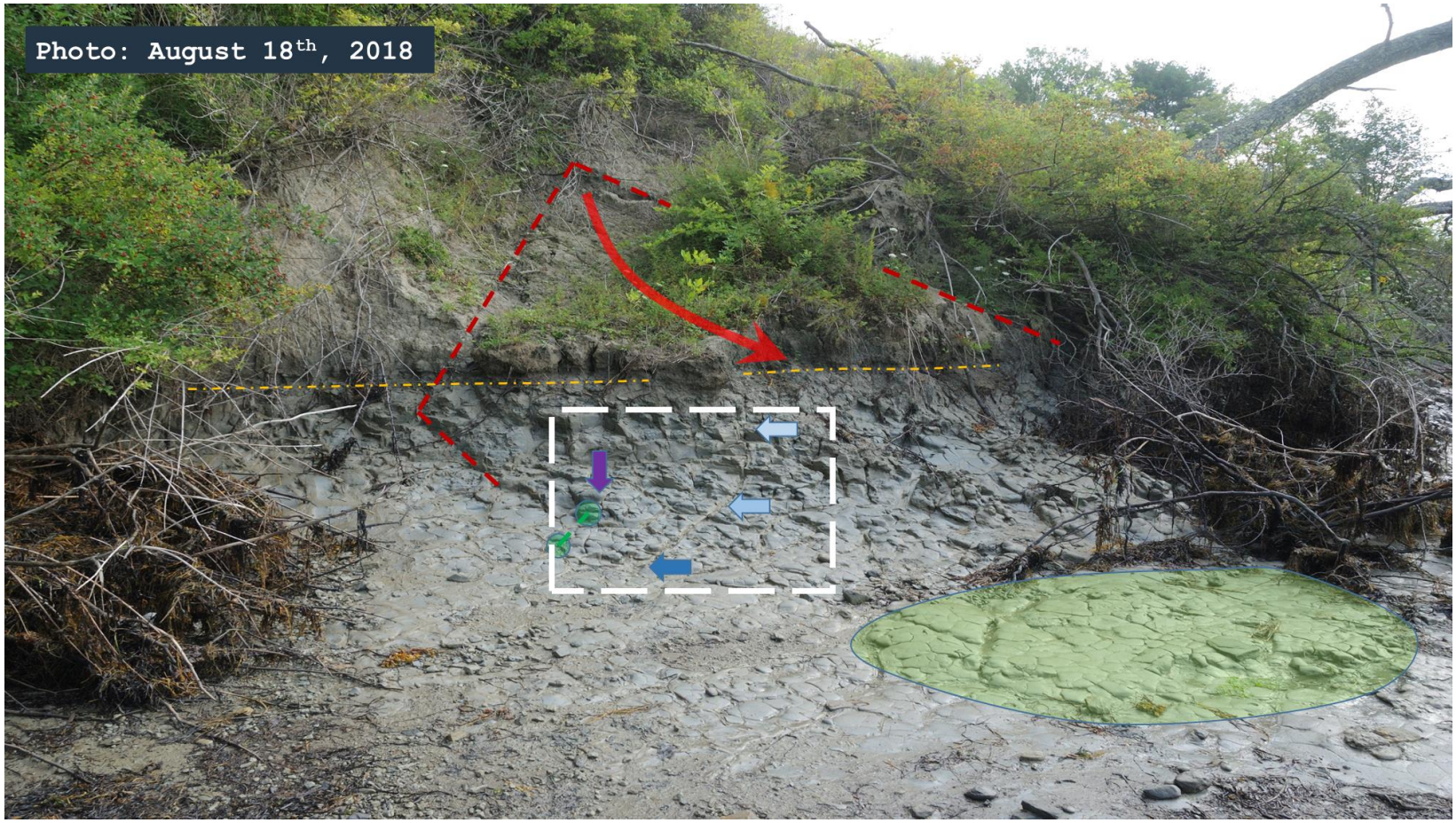

Figure 5.12 a. Unusual Patterns Exposed by Erosion. Little River, Freeport, Maine, Sub-site LR 5.

The remnants of an old landslide, since eroded, is marked in red. The distinct high-water line etching is marked by the yellow-dashed line. Within the green shading is the remnant and resilient pedestal of previously quarried blocks of sediment. The white-dashed box provides the reference frame for the next figure. Within the white box: blue shaded arrows follow one of the joints in question up out of the ground-plane from dark to light; the purple arrow and small green circles will be used for tracking into the following figures.

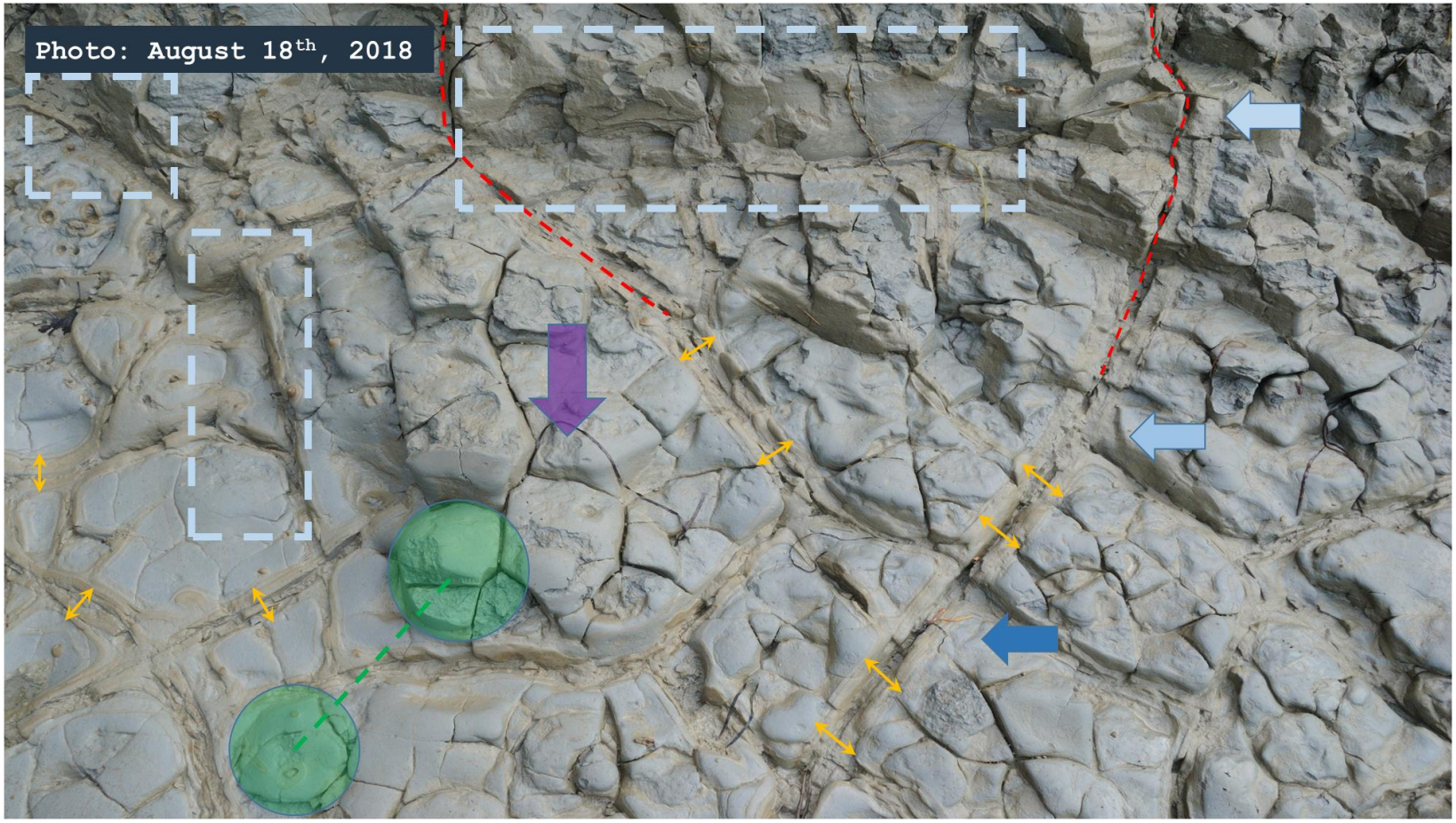

Figure 5.12 b. Some markings reoccur from the image above and serve the same stated purpose (green and purple marks for points of reference). Here, the red dashed lines track some joints out of the ground-plane as the blue arrows do from dark to light. The small yellow arrows mark some examples of the symmetrical discoloration lining the joints and fading into the blue clay. The new light-dashed boxes highlight regions of the image where the discoloration can be seen on vertical faces left exposed as some blocks of sediment have been removed. Note that where those vertical faces meet the ground-plane a discolored joint can be traced farther afield.

Figure 5.12 c. A finer-detail image on the ground-plane exposure of the jointing pattern in question. Note the complexity and redundancy of the network, along with its polygonal geometry, which discourage the idea that these may be traces of tree roots. The green circles continue to track from the previous image and are only used for orientation information.

Figure 5.12 d. Fine-detail image of polygonal patterns. The yellow arrows show exemplary symmetry of the banded discoloration. The light-dashed box highlights an area where the diffuse and somewhat concentric nature of the discoloration is more easily seen. The purple-dashed oval contains several particularly darker and rigid features that intersect the discoloration banding: these may be traces of roots or bioturbation.

Sediment Plumes

Casco Bay, Maine, is known to be muddy. Nearshore waters are clouded by the readily mobilized fines of the Presumpscot Fm. Sediment plumes sourced from eroding bluffs not only show a sign of mass-wasting without a prerequisite major landslide deposit, but have implications for the sediment budget, tidal flats, and ecological fertility in the area

Figure 5.13. Sediment Plumes Seen from Above. October 28th, 2017, the north side of Little Flying Point. *Altitude ~114 meters.*

UAV image of sediment plumes advecting from shore. The bright objects in the top-left corner of the image are sea-going kayaks at a commercial recreation and training center provide a rough sense of scale. As also seen in **Figure 2.10**, sediment plumes seen from above the Little Flying Point bluffs demonstrate just how readily mobile the Presumpscot Fm. sediments can be. The two different sea-wall armoring structures, as well as the collections dead trees downed at the waterline, tell an erosional history of their own.

New Marsh Colonization of Sediments Not Immediately Deposited by Landslides

It does not take a landslide to start a new fringing marsh colony at the bluff toe. Passive sediment accumulation at the toe of the bluff is seen to be sufficient enough to support the growth of new halophytes, where it is not smothered by accumulating wracklines or rapidly drowned by rising seas. In the following figures, new marsh is deemed so by its sparser growth density and its pattern of developing outward over low mudflat. It is topographically distinct, lying below the eroded edges of older marsh colonies. Older marsh is deemed so by its denser growth habit and its elevated, and sharply eroding, seaward edge.

Figure 5.14 a. New Marsh Colonization. Little River, Freeport, Maine, Sub-sites LR 3-4.

A seemingly deltaic growth pattern of new marsh (marked in yellow) can be associated with the runoff and drainage of the adjacent gully (obscured by the large canopy of trees, top right quarter). The highlighted growth is described as new because it sits on the mudflat below the higher-relief colonized landslide deposits and does not exhibit the same damaged/highly eroded (black arrows) seaward edges as the more established marsh grasses.

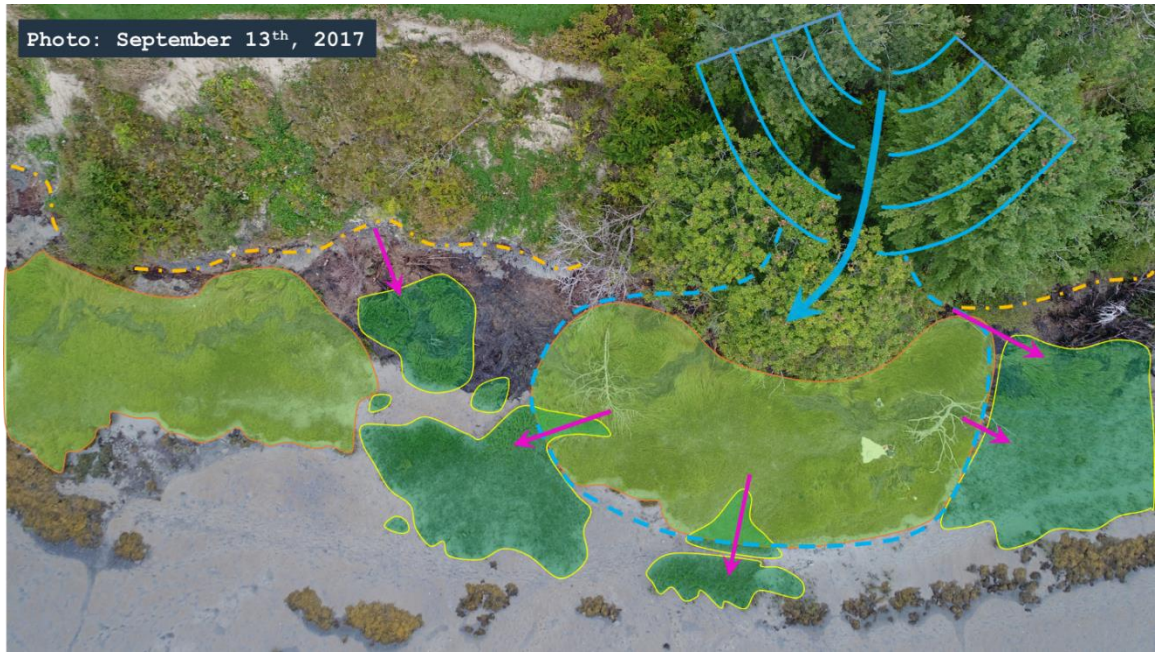

Figure 5.14 b. The same image as above, characterized. In blue: an approximate form of the gully and its drainage. The associated landslide deposit is bounded in a blue-dashed line. A yellow-dashed line marks the distinct high-water mark. "Older" marsh colonies are highlighted in light green; new marsh growth is marked by the darker-green regions. The purple arrows mark visible drainage directions that lead to new marsh.

CHAPTER 6

DISCUSSION

SfM **Products from Surveys Conducted On Foot**

The *SfM* surveys conducted on foot, perhaps due to the close proximity in which the surveyor operates relative to their subject in the setting of this study, produce strikingly detailed, visually rich models that are too limited in context and scale to be reliable for the application being developed here. Having been difficult to capture even the whole bluff from top-to-bottom at times, attempts to register one scan against another in a quantifiable way have proven futile in such an ever-changing setting. Erosional hot spots originally sought out for measurement were either difficult to geo-reference due to limitations in spatial resolution of GPS signals at the toe of a bluff, or at times too drastically changed by erosion (outright displaced by rotational landslide failures, or washed away in the course of a year) to be consistently related to previous visits (within, strictly, the confines of the *SfM* digital reproduction). While a user may easily be able to intuit that change had occurred from image to image taken from subsequent visits, the numerical measurement and digital record of change that may serve the calculation of an attempted sediment budget or prediction of a landslide hazard is better left to a stepped-back observational scale that falls somewhere in an undetermined "sweet spot" between the available 2m airborne LiDAR measurement and the overkill of sub-centimeter-per-pixel representations of individual, minor, erosional scarps.

SfM **Products from Surveys Conducted by UAV**

A UAV rapidly brings many obvious advantages to the application of *SfM* surveys (James and Robson 2012; Westoby et al. 2012; Clapuyt et al. 2016) to coastal management and observational efforts. Most notable is the wealth of additional degrees of perspective that a flyer can provide, from the horizontal to zenith and every practical increment in between. This mobility grants greater ease of access

to sometimes challenging or limited coastal settings and allows a surveyor to quickly adapt to the scale and contextual environment in which an unstable bluff may be found. An experienced pilot can sufficiently image a field site in less time than it takes the GPS used for ground control to be active long enough to be accurate. So, battery life for the UAV and best patience practices for use of the GPS now place the most demanding limits on the schedule of a site visit, weather conditions aside.

At this time the automation of the flight paths may be a reasonable next goal to bring more consistency to repeat surveys. Automation of the flight path was not tested in this study for fear of navigating in close proximity to trees that were known to be slowly changing their position as they creeped and pulled downslope. It's not recommended that a user expect to arrive to a site unseen with an automated flight plan in place, but instead conduct the first visit carefully and in full control to better understand to what scale and extent an image set is required to produce a *SfM* product of appropriate size and resolution.

At a greater distance (or altitude) from the subject bluff, resolution will obviously be diminished. But in exchange the resulting image set and *SfM* model products are so much more fully formed that they require less interpolation, alignment, and rectification and are therefore more readily transferred to other systems for analysis. With little trial and error, scans of the Little River bluff, on the order of 10s of meters across, were returning with centimeter-per-pixel representations (stated in this way because GPS error propagation does not make this process flawless). The advantageous capabilities of the UAV allow for the capture of images beyond the boundaries the scene of interest. In this way errors due to edge effects and dwindling photographic overlap may be reduced by over-shooting a subject's domain.

SfM **Products Visualized in GIS**

SfM products from both modes of survey tested, on foot and by air, produced strikingly photo-realistic 3-D scenes in high fidelity. A promising first impression, it is well within reason to expect to be able to capture a shoreline as-is on a given day and virtually return to it in 3-D later on for study.

However, *SfM* programs excel at extracting recognizable features from imagery and relating them arbitrarily in a virtual spatial setting. It is difficult for a human to look at these recreations and determine by sight if the spatial relationships are reliably projected and proportioned. After all, *SfM* products can be transformed and translated at the click of a button, and they often are, in order to scale them to match the alignment of control points. Once the models are formatted for export it is easier to evaluate whether or not proportions and positions appear accurate, are accurate, or fall in or out of an acceptable tolerance of error.

Errors become more apparent when taking the digital surface models produced in this survey from Agisoft's *Metashape* to ESRI's *ArcGIS*. As described above in the section on *SfM* reproducibility, Clapuyt et al. (2016) found that the *SfM* algorithms themselves introduce very little internal error, *i.e.*, they have a low impact on the process when presented with consistent datasets and an exceptional effort to constrain ground control. In a controlled, perhaps studio, setting, *SfM* is reliable enough to be fully automated. But as with most technologies, removing control leads to inconsistency, and in this application the survey methods still need a human guide.

It was to be expected that conducting repeat surveys with each flight plan improvised would lead to varying resolutions in the results. All returned within the same order of magnitude, but give-or-take a few centimeters-per-pixel in the final products. Analysis with these varying resolutions could be remedied to some degree by down-sampling more refined models to the lowest common resolution. Variance in the resolution is not the most concerning or striking result of bringing the surface model exports into a GIS. What is most concerning is the skewing and warping of the surface models that comes to light when mapped and stylized. The results echo Clapuyt et al.'s (2016) findings that GPS and ground control play a leading role as a source of error in *SfM* and in the accuracy of its outcomes.

For one, concerning GPS and ground control, repeat surveys at the Little River site appear to have been rotated or skewed slightly about some near-central z-axis. This can be explained by three

faults: 1) that there were a differing number of GPS GCPs used in each subsequent survey. In effect the models became more thoroughly geo-referenced with time. 2) there were an insufficient number of GCPs used. At maximum, this project used 6. Clapuyt et al. (2016) detailed the relationship of error to GCPs used, and suggested a minimum of 9 ground control points, showing further improvements to accuracy with even more (*i.e.*, 15 GCPs). And 3) which may be the hardest to avoid, is that by nature the shoreline is an elongated feature and, despite distributing GCPs along both the base and top of the bluff, their distribution was ultimately biased in alongshore length vs. width. While the model may be spatially well constrained within that distribution of GCPs, it is within reason that errors are more dominant in a particular direction due to asymmetry of the constraining layout and thus one model result can be seen to have been rotated with respect to the other.

Secondly, concerning the propagation of numerical errors, "warping," or a bending distortion of the surface models is seen increasing towards the edges of some of the *SfM* products. Care will need to be taken to distinguish numerical warping from physical strain, separating the two by interferometry or building confidence with thorough ground-control. From the nature of the *SfM* process, particularly the extrapolation of unknown points based on the more limited information of known points, it is a given that regions of a model sourced from less photographic overlap will have a greater tendency towards error than those well covered. It follows that the outer portions of a *SfM* model are at a greater risk for numerical error if extra imagery is not collected towards a significant distance outward beyond the intended bounds of a subject, ensuring proper photogrammetric overlap. Take for example, where the bluff face was the primary focus of the scan there is sufficient overlap (ideally features of interest are present in nine or more concurrent photos) however the surrounding intertidal zone is shown by the digital surface model to rise smoothly upward above and beyond sea-level. Visually, and naturally, that portion of the surface model is erroneous. Fringing effects such as warping of the surface model edges or loss of reliable points in visually noisy regions such as densely vegetated areas can lead to conflicts and uncertainty when trying to align or stitch together the outer boundaries of several *SfM* products. Errors

such as these are best mitigated by capturing more of a scene than is expected to be necessary and then cropping the domain of the model back to a securely and accurately modeled region.

A Year in the Life of a Temperate Bluff: Conditions of Seasonality

From the directionality and differing intensity of storms (Keblinsky 2003), to the freezing, thawing, wetting, or drying effects on the behavior of clays (Kok and McCool 1989), seasonal variations govern the impact of a number of common geomorphological agents driving coastal bluff erosion. Maine's temperate climate and mid-latitude position make for a significant contrast in conditions between summer and winter, let alone dynamic transitions between the two during spring and fall, and as a result there are characteristically different primary actors on the bluff erosion behavior over the course of each year.

With summer, there is less influence of powerful storms, and the surface of the bluff progressively dries out in the warmer temperatures; extended insolation periods; and outright lack of rain. Surface wasting can occur as oxidized clays desiccate, loose hold, and fall downslope. An interesting effect, likened to calving (recall **Figure 5.10 b.**), has also been observed at the waterline. Discrete blocks of Presumpscot Fm. sediment, made coherent as they dry and separated along strain features already present at the bluff toe, give way as their bases are gently softened by inundation at high tide. These blocks are then reworked within the intertidal zone into smaller and smaller clasts over time until dissolved. On the bluff face, growth of vegetation helps uptake excess water from the bluff surface and bind sediments within root mass (Giadrossich et al. 2019). However, in the future, these newly coherent portions of vegetated bluff are likely to act as larger units and fail as larger units, enhancing the erosion of sediments by conveying them downhill as a package. At the intertidal zone, the growth of marsh grasses offers some small wave attenuation and help to still nearshore energy as well as capturing light volumes of sediments that winnow from the high tide line (Kelley and Hay 1986a, b). Observations suggest, however, that even with wave attenuation by fringing marsh grasses, merely the presence of

moving water residing against the bluff toe for a period of time may be sufficient to winnow sediments and over steepen the bluff toe with little to no wave action necessary.

Fall sees the dying off of both marsh and surface scrub vegetation, cooler temperatures and the arrival of more significant storms. Dusty dry surface sediments are particularly vulnerable to increasing rainfall and higher winds. In the depths of winter, it is likely that the freezing of groundwater holds a majority of the bluff body fixed solid and resistant to major landslide activity. However, as mentioned earlier (**Figure 2.15**), spalling of sediments by frost can contribute to erosion of bluff face regardless of the landslide risk (Bernatchez and Dubois 2008). With winter also comes the burden of snow loading: not only adding weight but building a water reservoir across the expansive flat tops of the bluffs to saturate the sediments come the spring thaw.

Additionally, as northeast storms historically account for 50% of all winter storms (Keblinsky 2003) and overall the winter brings the most damaging high-water events in the region, the bluff toe could be quickly transformed by what was assumed to be scouring waves and an eroding-towards-vertical nearshore profile (therefore less dissipative). It is difficult to observe these storms in action, and unclear whether extreme wave energies reach all the way landward into the sheltered coastal compartments where the bluffs remain. Some of the erosion seen following the winter season may actually be the result of significant tooling by sea ice that accumulates in these coastal compartments, brought in by favorable wind direction. The same sea ice would also prevent wind-driven waves from reaching the bluffs or forming nearby.

The transition from winter into spring is a critical time for bluff erosion. Groundwater thawing, meltwater saturation, and runoff put the silts and clays into their most mobile condition of the year. Spring sapping undermines portions of the bluff, mechanically loosening sediments while drains and channels are carved larger and may even network, further enhancing erosion. The piping of groundwater to this effect was seen to occur frequently as springs emerging from the bluff toe. Relatively

impermeable layers within the bluff perch water tables and springs erupt on the bluff face. Softening after thaw and sagging compensation in response to over-steepening by winter wave action convey more of the bluff material downslope and beneath the water line. Fluid-rich zones of the sediments are more readily separated, reworked, and removed, offering little protection for the material behind them.

With the transition to summer again the sensitivity to failure is diminished. The return of extended drying periods promotes greater stability of the bluff surface and developing vegetation coverage increases both on the bluff face and in the fore marshes. The character of each season is generally reflected in the varying expressions of surface erosion at a given time. The transitional periods, though, are not as clear-cut as dates on a calendar. Any effects of thermal expansion/contraction and hydromechanical expansion/contraction a bluff slope endures could contribute to its sensitivity to failure.

Other Notable Observations of Phenomena:

Surface Expressions Preceding Slope Failure

One of the stated goals of this work was to evaluate the detection of any surface expressions of slope failure that may indicate that a larger landslide was imminent. Oftentimes the deformation of trees on a slope face, straining to continue growing towards the sun while their trunks creep downslope, creating a characteristic "J" shape, is pointed to as an indicator of a slope in failure (Malik et al. 2016). In the case of the bluffs in question, most vegetation is of the wrong variety and most tree stands are too young to be seen expressing such strain. For most of the growing season vegetation also obscured a significant portion of the bluff face from observation which could mask the features we sought to find. Hindsight, however, showed that some signals of a larger landslide were available, but it may speak to the challenge of detection that they were not readily recognized as such.

Following a landslide between the LR 1 and LR 2 sub sites and a review of the photographs of the area several features became clear: 1) some of the most prolific springs seen during the springtime emerged from the bluff face adjacent to bodies of material that later failed. This is unsurprising as it is known that groundwater would exploit faults within the sediment body and more readily flow through conduits made by strain-softening along slip planes. The emergence of springs in association with slope failure was seen not only at the site featured here but along other portions of the Little River bluff as well. 2) Toe creep at the base of the failing block was signaled by the envelopment of one of the rebar GCPs in soft sediment (as opposed to exhumation of the rebar by erosion, which was seen to be more typical). 3) Tension separation at the top edge of the bluff is seen by a break in the vegetation cover and later on as the sun-bleached exposed sediments better reflected light through the dwindling leaf cover come the fall season. It is worth noting that the entire block of material that composed the landslide between LR 1 and LR 2 was well-vegetated from top to bottom, which would exclude it from a "Highly-Unstable" classification and masked its failure from the point of view of a passerby.

Ice Unseen: Sea Ice from Casco Bay

The most significant transformations of the bluff toe were observed following the winter season. Returning to the bluffs revealed greatly over-steepened bluff toes, devoid of the dry, blocky and wave-cut morphology seen to develop throughout summer and fall. Fringing low marsh grasses were mowed down to stubble (note: this may be an ideal time to survey a baseline for marsh colony platforms when there is little to no vegetation cover to produce a false result in *SfM*) and in some places along the ground even small ripples could be seen to have formed, indicating the action of some higher than usual wave energy reaching the bluff. But it bears repeating that if truly high-energy waves - the likes of which can be seen seaward of the survey sites - were to reach this far into the coastal compartments, fine sediments of the Presumpscot Fm. wouldn't be left behind as a mudflat.

By chance, the sea ice in the area went unobserved throughout most of the project. It wasn't expected to accumulate or persist at the Little River and Little Flying Point sites for a significant amount of time and therefore wasn't considered a significant contributor to the erosion occurring here. Site visits in winter were few and far between, limiting the chances of encountering ice. The perception of the role of sea ice here changed once one of the landmark rebar segments was found with a striking deformation (**Figure 5.8 a.**). The bend in the steel rod could not have been caused by waves or a curious clam harvester and was likely deformed by the weight of an attached frozen block of ice while the bar was held frozen into the sediment. This led to an investigation of available satellite imagery revealing the brief (on the order of a month or two) but weighty accumulation of sea ice in several of the northern coves within Casco Bay (**Figure 2.3**).

Sea ice carried by wind and tide provides a strong mechanism for abrading (Hanada et al. 1996) a bluff toe, already pre-conditioned for erosion and extraction by months of summer desiccation (*e.g.*, **Figure 5.6c**). Sea ice may scrape and scour, and by freezing to the ground at rest during low tide will pluck sediment or marsh habitat once it's lifted by the tide. However, any sediment carried landward from farther out on the mudflat (**Figure 5.8 b.**) that may contribute to local accumulation will not make a bluff whole again.

Waterline Etching in Fine Media

The action of sea ice described above is a coarse and at times brutal agent of shoreline erosion. In contrast, with still water and dry sediment, a much finer winnowing may be on display during the summer. The very fine and unconsolidated nature of the Presumpscot Fm. sediments provides an ideal media for recording small changes and, once cut back to some degree, its vertical habit at the bluff toe during the dry season provides a fairly even surface for that record.

Murky, sediment-rich water seen nearshore even at times of little to no wind-driven wave energy demonstrates how readily fine particles are entrained by the presence of water against the exposed

Presumpscot Fm., especially when the source has been dried in the sun and is then reactivated or readied by the hydrating arrival of a high tide. Throughout the summer season, fine and distinctly horizontal lines begin appearing across the base of the observed bluffs where the sediment is exposed and not covered by a slump deposit and or polished by a wrackline, or driftwood. Given the depositional history of the Presumpscot Fm. it is likely that many of these fine lines may be left from the extraction of sandier (more readily exploited) layers of sediment, such as the seasonal variations of varves (De Geer 1912) (varves were not explicitly identified here). However, over time more pronounced etchings are seen to develop as horizontal concavities at varying elevations across the bluff toe. Broader concavity may suggest slightly more wave energy for a given "recording session." Eventually a distinct cut-bench forms, and on some levels, small steps where a fledgling bench may have been surpassed.

Given a purely sinusoidal tidal cycle, water will spend the majority of its time bi-modally near two levels: the crest and the trough positions of the wave as the fluid stalls in transition from rise to fall and *vice versa*. In these positions tidal current velocity is at its slowest, leaving time for wind-driven surface waves or coincident swells from afar to arrive and act against a shoreline. For any coastline in opposition to the tide, such as a bluff adjacent to an estuary snaking inland, a base level longshore current will still need to develop as the tidal wave moves past the landform. While the local tidal signal is not purely sinusoidal, its semidiurnal rise-and-fall sets up a similar situation. Add in the complications of astronomical influence; continental shelf geometry and harmonic effects; sea level rise and the previously mentioned wind-driven waves and surface swells; and the signal because more complex, more-noisy, but no less modal. (**Figure 6.1**). The more pronounced cutting horizons observed etched into the bluff's toe (**Figure 5.10 a.**) are expected to be markers of where the water level spends the majority of its time concentrating erosion (considering only the high-tide half of the cycle). One could consider that for the lower half of the cycle, the seaward edge of the mud flat could be defined by the matching concentration of lower water-levels. Unless reworked by sloughing surficial slope failures, which would disrupt the original horizontality of layers, no distinct horizontal bands of exceptional strata are visible across the

bluff toe that match the scope of the dominant cut plane. Other distinct lines may be recorded (**Figure 5.9 c.**) as atmospheric disturbances or astronomical effects syncopate the tidal signal and cause the waterline to stall in slightly elevated or suppressed positions, leaving their mark off-set relative to the most concentrated line.

Waterline etchings are less likely to be observed along shorelines composed of coarser sediments, where the morphology is more controlled by reworking and overturning; angle of repose; and redistribution by wind and waves. This isn't to say that the final position of a high tide might be recorded at a beach by its swash-mark, but that record is much more readily lost. Additionally, Maine's coastal bluffs are found in sheltered coastal compartments that impart some control on the wave energy reaching the shore. The islands and peninsulas bounding the bluffs may provide a stilling and signal-filtering effect that allows a moderately stable water level to reside against the bluff for a given period of time, in contrast to significantly noisier wave energy making landfall at a nearby beach.

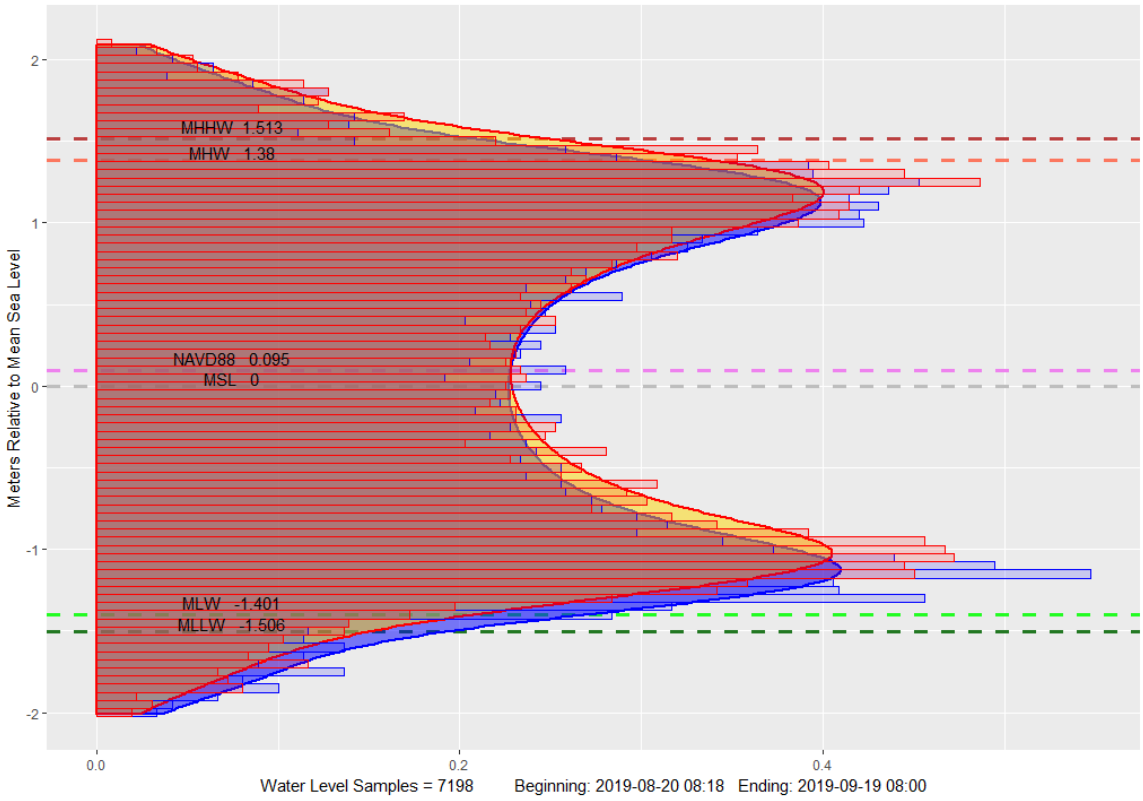

Figure 6.1. Histogram and Density Plot of Local Tide Level Duration (1 Month). A tide level duration density plot (and underlying histograms) of both the predicted (blue) and recorded (red-gold) 6-minute water level samples measured relative to Mean Sea Level across 30 days at the Portland Head Light tide gauge, Portland, ME, Station ID: 8418150. Data from NOAA CO-OPS. Bin size for the histogram is 5 centimeters.

https://tidesandcurrents.noaa.gov/stationhome.html?id=8418150

"Calving," or "Quarrying," of Desiccated Sediment Blocks from the Bluff Toe

The horizontal cutting plane of the waterline leads to another striking phenomenon observed during the summer months. Where the horizontal cut intersects with the (numerous) vertical joints and breaks in the desiccated bluff toe, discrete blocks of sediment fall-out of the base of the bluff. It appears as if they have been extracted: leaving hollows and pedestals in their place, resembling an active quarry, but in truth the nature of their failure and erosion from the bluff toe is more readily likened to the calving of glaciers, taking for granted the obvious distinctions in scope, scale, and material make up.

When spring transitions to summer and the bluff toe dries, the sediments contract as they dewater. Vertical jointing and strain features from the upslope burden become more pronounced and

more open, increasing the sectioning and cleavage between discrete blocks as well as enhancing space for air to flow (drying) and water to exploit (hydrating, hydraulic fracturing). Blocks of material will slowly become less-attached to the slope from which they're born. As the most frequent and focused erosion occurs at their base, coincident with what is presumably the average high-water position (but not explicitly the highest, as seen by water marks above the most distinct cut-bench), they are undercut (**Figure 5.9 c**). With the residence of water at the base of the blocks comes an imbalance: the bottom is more hydrated than the top, and therefore presumed to be more plastic and susceptible to fail under the weight it supports (**Figure 5.10 b**). However, given the limited permeability of the Presumpscot Fm., it is difficult to identify just how much a role the hydration plays in weakening the base of these blocks at scale, when more mechanical factors readily govern. The bottom is also more frequently winnowed and, in many cases, obviously undercut. With little attachment to the parent bluff and dwindling support from beneath, the block will fail.

As the process continues throughout the season it can contribute a significant amount of sediment from the bluff into the intertidal zone (**Figure 5.10 c.**). From there the newly delivered material is more readily digested by the twice-daily inundation. On one hand, this helps to emphasize the fact that small but effective processes such as this can cumulatively affect the overall macroscale retreat of the bluff. On the other, this quarrying effect is not only an efficient agent of erosion in its own right, but is also preparatory for larger-scale slope failures in the seasons that follow the summer and fall. The crumbling, segmented bluff toe will be easily extracted from the load-bearing base of the slope by the action of winter wave energy or tidally hefted sea ice, leaving an over-steepened toe and a sharp horizontal-to-vertical profile transition come spring when the material is again made over-weight and softened by water content.

Formation of Mud Balls (Rip-up Clasts)

Sediment blocks calved from the bluff toe are candidates for the source of mud balls (*a.k.a.* rip-up clasts) found scattered throughout the nearshore zone. The calving effect described above is seen as contributing to mud ball formation in several ways: 1) As blocks fall free from the bluff toe, they fall (and at times break apart from the fall) into the intertidal zone where the frequency at which they, as a whole (and not just their base), are washed and worked by water increases greatly. If the calved fragments do not adhere (as clays can do) to the mudflat and disaggregate slowly in place, they are worn down by the tides like extremely weak stones, becoming smaller, more rounded, and increasingly mobile. 2) The base from which the blocks are cut becomes reactivated in some way. The vertical jointing that allows for the detachment of the calving blocks of sediment is not specific to a singular block, and may continue both further into the bluff toe and down into the base of the sediment body. At the locations where the calving occurs, the summer shoreline is characterized by the many relict and abandoned pedestals remnant from the detachment of a block from above. The jointing and channelization that made them distinct remains to some degree, even if surpassed by the cutting plane of the water line. In the event of larger slope failures, these remnant blocks of material have been seen to be thrust up in front of landslides. Once thrust forward the blocks are both more detached from their neighbors than before but also reintroduced to the active water level and readily cut loose. 3) In a similar fashion, following larger-scale landslides and slumps, material is splayed out in broad deposits resting at the boundary of the intertidal zone and the air above. The splayed deposits must then endure frequent cycles of wetting, drying, over-wash, and are particularly well positioned for lengthy exposure to sunlight. This prompts a rapid transformation where desiccation cracks emerge, are exploited and channelized, prominent portions are tempered by more drying, and then eventually broken free from their bases (**Figures 5.11 b-d**).

Mudballs are a common occurrence around the bases of the bluffs, but little is known as to how long individuals actually persist. Cores taken from Penobscot Bay, Maine, featured mud clasts within the Holocene unit that, when present, were noted to make up 30-80% of the volume within their matrix; cores and bottom samples from Belfast Bay, Maine, are also said to have contained such clasts (Brothers 2010, p. 59). Brothers notes that the clasts found in cores were redoximorphic, featuring yellow-red bandings and iron nodules. Such yellow-red banding within the blue-gray clay is a highlighted feature of the intersecting patterns (**Figure 5.12** d) described in the following section.

An Unconformity in the Making

As described above: intersectional jointing, faulting, strain compensation features, and slip planes all exist within the bluff. They are continually developing as the slope evolves and can be seen outcropping where shoreline erosion is concentrated. The shoreline erosion does not fully wipe out these features, but more often than not they are buried by slope failure or masked by a veneer of settled sediments that coats the ground at the bluff toe. On some occasions relict pedestals from the quarrying effect could be seen persisting out front (seaward) from the present-day cut bench (**Figures 2.9 a, 5.9 a.**). On one occasion, featured in this section, the top veneer of intertidal sediments was removed adjacent to the LR 5 sub site (possibly by the sinuous drainage stream of a gully between the LR 5 and LR 6 sites) and a pattern was revealed in the ground-plane that likely existed before burial.

The pattern features many intercrossed networks of discolored, presumably oxidized or chemically altered, joints with the un-oxidized "blue clay" of the Presumpscot Fm. seen in the cellular spaces in between (**Figure 5.12 c.**). The oxidation pattern appears for the most part to diffuse symmetrically into the bluer clay as mirrored across the dominant plane of each joint. Some joints run continuously up from the exposed ground plane and up into the bluff toe. And the discoloration can be found covering the vertical faces of hollows where blocks of sediment have been quarried. Amos and Sandford (1987) noted that staining on fissures, "even at greater depths in the gray clay,' (p.26) were

indicative of some groundwater movement along these tracks." Much of the network appears redundant (heavily interconnected) and each joint too readily associated with its branches to be interpreted as casts of tree roots. The more planar -- in some cases vertical -- expressions of the discoloration discourages the idea that these are traces of burrows. Some small, darker cast features that cross these suspect joints are present which may be those of roots or burrows, but they show little association to the features on display here (**Figure 5.12 d.**). Some of the largest bands show a platy, fractured internal nature reminiscent of translational faults. I suspect that these features are remnants of tension cracks, slip, and failure planes from within the bluff slope, cut back, buried, and for this brief time exhumed. Their networked nature and the diffuse-from-center character of the discoloration suggests that these joints were (relatively) more efficient carriers of groundwater. The continuation of joints up into an actively failing bluff slope suggests that they were present before being cut across and surpassed by the waterline (**Figure 5.12 a-b.**). If correct, this provides insight into the internal nature of the bluff landward of the erosional exposure.

New Marsh Colonization

Fringing marsh colonies are generally attributed to the direct deposit of landslide material and the favorable platform that the deposit provides for the marsh grasses to survive (Kelley and Hay, 1986). It is reasonable that if the volume of a landslide deposit is large enough to outlast a season of erosion, it will provide a lasting foundation for marsh grass to colonize. When comparing the two largest fore-marsh colonies at Little River, one is readily associated with the gully-hollow from which its foundational landslide deposit came. It is marked by the skeletal remains of a tree carried from the slope into the intertidal zone (in which it decisively did not grow). However, the other large marsh at Little River is not so easily connected to a single landslide event, counter-intuitively built out in front of one of the most seawardly prominent sections of the Little River bluff. Instead the colony seems to be sustained by numerous contributions from minor slope failures from either side of the protruding bluff. The

landward edge of the marsh appears to be developing as its seaward edge succumbs to erosion, as if the whole colony is in retreat. The marsh's broad size may be sufficient to capture a sustaining amount of suspended sediments from the adjacent bluff.

As noted before, the presence of *S.alterniflora* without coincidental *S.patens* (Davis and Fitzgerald, 2003) at the Little River site is not trivial. The lack of *S.patens* indicates that too much seawater floods against the bluff for too long for *S.patens* to survive. Therefore, a significant volume of water is available before and after peak tide to carry wave energy, sustain currents, and suspend sediments. The regular flood-and-drain drag of this water works to smooth existing landslide deposits while the suspended sediments nourish their fringing marsh-grass colonies.

The observation of new marsh growth beneath the level of, and between, the landslide-deposit colonies emphasizes that sediment distribution from source-to-sink in the nearshore environments here is more dynamic, more versatile (**Figures 5.14 a-b.**). The origins of the new growth colony highlighted in this feature are suspected to be linked to the drainage of the nearby gully, a drainage that incises a preexisting landslide deposit. A second and smaller new-growth colony is seen forming at the seaward edge of that same preexisting deposit, in a more ramp-like form, and appears to be catching sediments from the flooding and draining of a foot-path that cuts across the top of the old marsh edge. On either side of the large landslide deposit more new-growth marsh colonies can be seen. Eastward, a broader field of new growth is likely supported by great quantity of sediment put forward into the intertidal zone by the adjacent LR 2 landslide slump, a deposit which eroded too rapidly to host its own colony. To the west, between the next large "old-growth," marsh colony, is a small but robust growth of grass in front of what was originally the LR 3 and LR 4 sub sites which, by the concavity of the slope face here, drain between the two larger old marsh colonies. An interesting finding come spring was that the silty-colored drainage stream sapping from the LR 3 and LR4 sub sites can be seen as topographically redirected out and around the build-up of the spreading deposit and colony that crosses what would be a more direct

drainage path. The new patches of *S.alterniflora* signifies and likely influences a degree of sediment upbuilding where erosion has been expected to dominate.

Considering the Bluff Erosion Cycle

Observations Counter to Expected Behavior

The Bluff Erosion Cycle (BEC) as detailed in the introduction and put forward in Kelley and Hay (1986a, b) was a simplification. It is a simplification made by an observer who made few visits to the same bluffs and had no time-series photographs to reliably demonstrate the continuum of microprocesses that go on at these sites or the consequences of scale and dimensionality at play. The overall expectation of the Bluff Erosion Cycle: that toe erosion prompts slope failure to contribute sediment into the intertidal zone, providing protection behind the deposit for some time to come until later cleared away, is thematically sound but by some observations does not clearly hold true to its step-by-step order of operations. Perhaps with a uniform stretch of coastline, and without the troublingly varied influence of groundwater and terrestrial or human agents, the Bluff Erosion Cycle could be observed, timed, and predicted. There may be a critical inflection in the scale of landslide event where the Bluff Erosion Cycle could be expected to play out normally, and anything less that would be insufficient to initiate the prescribed chain of events. Observations challenge the simplicity of the model and speak to the complexity of the environment in question.

At times, failure events were enough to relax the slope and leave it at rest throughout the course of the survey. Other instances showed one failure at the toe leading to allowance of additional failures to occur at greater intensity (but with the same footprint) in order for the slope to compensate for the continued loss of buttressing support. Almost as if a smaller version of the bluff erosion cycle was playing out at the bluff toe iteratively with fault-block material that was already, technically, in failure. Meanwhile the top edge of the bluff remained unchanged, but grew more significantly over-steepened. This presents a hiatus in the overall retreat of the bluff that is not fully derailed from the BEC

description (**Figure 6.2**). Another site (LR 5) showed repeat failure behavior that appeared to continually influence the internal hydrology of the slope face, further focusing and promoting the escape of groundwater. Groundwater convergence central to where the previous slump had torn away prompted more local failures. More groundwater would lead to a greater proclivity for failure, more failure created a greater "watershed," and a feedback appears to have developed for some time.

Alternatively, some of the behavior predicted by the BEC appeared to play out in super-position. Between the LR 5 and LR 4 sub sites at Little River stands the most prominent (seaward) mass of bluff material. The LR 4 and 5 sub sites are scalloped excavations of the bluff face on either side of this prominence. Notably, and in favor of the BEC, in front of this resilient stand is one of the two largest fringing salt marshes. It makes sense that such a fringing marsh should protect the bluff behind it, and the prominence in which that bluff stands supports the idea that erosion is more effective on the adjacent, less protected faces. But erosion at the bluff toe continues directly behind the fringing marsh (recall **Figure 2.11**), raising the concern that with accelerated sea-level rise may come the abandonment of the regular BEC model expectation that a marsh will protect the bluff. The cycle may stall here, in a single phase, as toe erosion between the fringing marsh and the resilient bluff slope continue to feed and sustain up-building of landward edge of the fringing marsh, allowing both the bluff and marsh to retreat in tandem.

As illustrated, it may be that the Bluff Erosion Cycle is best applied more generally, and in some senses applied to only the behavior of the toe, supplied by but not including the material piled behind it. Especially for the Presumpscot Fm., the material is not resilient enough to stand vertically from toe-to-top, and in contrast to the illustrations perhaps the cycle acts most readily on the recursive processing of surface layers that are conveyed down-gradient in failure. Surface layers that are made distinct from an underlying core of material by exposure to the elements. Barring the largest landslides, most failures are expressed as detachments of the exposed face that slough off a smooth surface. The top edge will in

time weather away or be torn down along with these slides, but it seems that more often than not a detachment will slip along an angle of general repose or preexisting plane of failure (perhaps a fault or tension crack from a previous compensation slump) once the supporting toe is eroded.

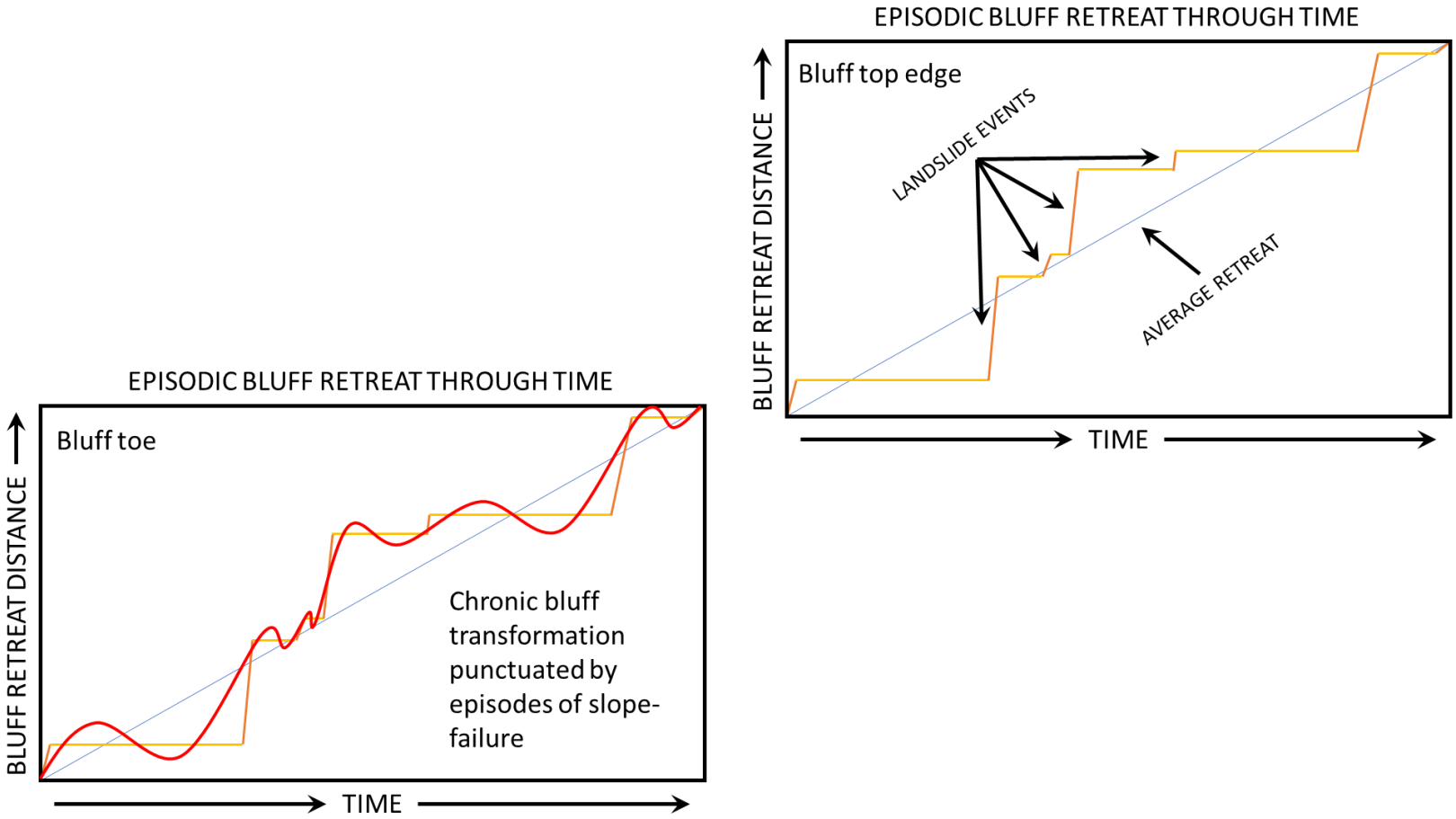

Figure 6.2. Contrasting Bluff Retreat Behavior Between Bluff Toe and Top. A new interpretation further modifying the conceptual graphic by Sunamura (1983). Sunamura's (1983) concept may be more applicable to just the bluff's top edge, where the process is more unidirectional. Contrasting bluff retreat behavior can be seen when comparing the bluff's top edge to the bluff toe. At times, repeat slope failures occurred over the same footprint as material that was detached from the bluff top took time to be processed. The bluff toe position could be advanced seaward, then cut back, in a repetitive manner that may ultimately scale to a grander over-steepening of the entire bluff at that position, leading to a more transformative landslide event.

The Timing Remains Uncertain

During the course of the study no portion of the bluff was seen to complete what could be considered a total revolution of the Bluff Erosion Cycle. Even the largest failures observed as the most dramatic (**Figures 5.6 i, 5.7 e.**) did not result in an equally large retreat of the bluff top position. The Little River site was seen to exhibit morphology exemplifying many of the phases of the BEC at once alongshore, but not in sequence. In contrast, the Little Flying Point bluff remained steep and denuded, *a.k.a.,* "Highly Unstable," demonstrating instead perpetual surficial weathering of its barren face. So, it is difficult to place these sites at a certain mark within the BEC. Consider again the historic Rockland landslide, the bluff was categorized as "Unstable," but not "Highly Unstable," before its failure in 1996 and had even been engineered to some degree beforehand.

Does one phase limit the next? True to the BEC, over-steepening of the bluff by erosion at its toe did result in compensatory slope failure. While the newly observed intertidal deposits did not match in size the fringing marshes already present, and did not directly support the foundation of new marsh colonies, their rapid erosion did appear in some instances to sustain marsh growth nearby. So, by supporting the growth of a marsh colony seaward of the failure did they advance the BEC? Or by eroding too quickly did they not qualify in scale for the BEC? Or did they perhaps skip a phase back to toe erosion.

Satellite imagery reveals that decent sized slope failures (sufficient enough to be seen by satellite, but perhaps not threatening enough to call the attention of a landowner) occur every year. These events show a level of slope-failure activity that may be measurable at a given bluff, but without a sufficiently long record of observation it is unclear whether the activity could be deemed normal, abnormal, or cyclical.

From 2-D to 3-D

Much of the discrepancy between the Bluff Erosion Cycle and the behavior of the bluff sites is owed to the translation from a 2-D conceptual simplification to a real-world environment (**Figure 2.7**). The timing of the cycle's phases remains uncertain, and it is difficult to point to any one 2-D slice of the bluffs observed, as a test, and state that its evolution matched what would be predicted by the model. But thematically the Bluff Erosion Cycle can be well applied to those same tests. The adjacency effects of having a landslide deposit redirect wave energy does not exclude that the deposit could afford protection to the bluff behind it, but in three dimensions that deposit is not infinite and therefore may potentiate the erosive action on either side of the profile it's protecting. Many examples of this were seen. For one, the prominent stand of bluff between the LR 4 and LR 5 sub sites (recall that they were originally named because of their obvious marks of erosion) stands protected by a large fringing marsh but stands distinguished because of the very active erosion and slope failures defining it on either side. The LR 3 and LR 4 sub sites eventually merged into one large eroded shoreline and then a failure occurred between their original designations, all within the embayment made between two large fringing marshes. A similar merger is suggested by a comparison of a 1985 low-level air photo of the Little River site to its present-day appearance.

The increase in sensitivity to failure of material adjacent to a slope that has already failed (and taken its support with it) is nothing new and is well demonstrated by the landslide that occurred between the LR 1 and LR 2 subsites. LR 2 was chosen because it was a rather photogenic remnant of a previous landslide. LR 1 was marked as interesting because it was an exposed and eroding bluff toe. The mass between them was, for the most part, ignored during surveys because it was too densely vegetated. As showed in **Figures 5.7 a-e**, it was this mass, missing support on the LR 2 side and losing support on the LR 1 side, that failed unexpectedly by the end of the project.

Retreat by a Thousand Advances: Complex Nearshore Sediment Transport

Overall, there is a net transport of sediment from the bluff face down into the intertidal environment that processes it. As material is conveyed downslope in quantities that are as varied as the mechanisms transporting them, it is acted on constantly, digested by repeated inundation, insolation, impact, etc. Chronic removal of small amounts of sediment occurs efficiently, while more significant slumps and slide deposits have a chance to temporarily govern upslope progress as they may be colonized by a marsh, but also may be eroded too rapidly to serve as defense.

Even bluffs that do not suffer catastrophic landslides go through smaller discontinuous events, punctuating a baseline of chronic wasting, that lead to macroscale changes of the shoreline (**Figure 6.2**). The sediments that make up the bluff were deposited in an environment unlike the one they are exposed to now and are constantly subject to removal at this time (Kelley et al., 2004). It is no coincidence that no bluffs remain seaward of these sheltered sites. That the overall shoreline retreat here is a cooperative performance, the summation of all its actors, is a given. But until recently, emphasis has been placed on the dramatic, starring role of major landslides that damage property and capture the public's eye. However, what is expressed at the surface is a combination of chronic factors and episodic extremes. Erosion of the bluffs occurs constantly and in a variety of ways. At the granular scale it is spalled by frost, winnowed by water, blown away when dry and dusty or washed out by falling rain. At the intermediate scale site by site, an efficient routine of packaging sediments and delivering them downslope to processing and distribution by intertidal actions is well developed and continues almost rhythmically according to a seasonal schedule. Further, human intervention at property-protection-proportions is ongoing, but not without its consequences. Armoring the bluff toe or reshaping its surface can provoke erosion alongshore if the entirety of the bluff isn't modified, and long-term decay of the efficacy of these structures, and or the loss of valuable environment, challenges the usefulness of their implementation.

Observation across the coastal continuum will allow for more informed decision making and shed light on the roles of all these mechanisms.

Without an inland source of burden, be it water or structural, to drive more severe landslide events it appears that these bluffs will tend to slough off their weathered faces as they are undercut at the shoreline, the detachment facilitated by water content. The Presumpscot Fm. fails readily enough that in many cases slumped portions of the slope face failed again once their toe was removed. It seems likely that the Little Flying Point site, while remaining steeper than the sites observed at Little River, had little reason to fail catastrophically as it, being shorter in height above the waterline, had much less slope-stress behind it.

Major failures occurred during periods of overall increased plasticity (and therefore sensitivity) throughout the bluff. But without significant overburden, or external (manmade) stressors, the bluffs observed here appeared more likely to consistently shed brittle, fractured surface units along a shallow interface (in some degree parallel to the slope of the bluff face) between brittle and ductile conditions, perhaps in relation to groundwater gradients. But variations in the cohesion of the fractured-but-hardened surface zone, corrupted by weathering and bound by transient vegetation, allow for resiliency to govern and in turn over steepening to occur. As hardened as the faces are, they are still faulted and their bases are still perpetually weakened and removed. Slope faces fail, conveying material downslope, and the new contribution becomes toe for the next in line. If the processing and recursive slope failures progress sufficiently enough to develop a deficit of material upslope then the bluff top becomes over steepened and may also fail in compensation. After many smaller cycles play out in relation to the bluff toe, maybe the drawdown of slope sediment is strong enough to sufficiently weaken the bluff from toe-to-top and a true realization of the Bluff Erosion Cycle occurs as a large landslide.

Most landslide behavior witnessed during this study delivered sediment to the shoreline and advanced the toe of the bluff seaward without causing significant retreat of the bluff-top position.

Having been disturbed by slope failure and brought into a more hostile position, material conveyed from the bluff face is suddenly made more susceptible to more efficient means of erosion (repetitive action within the intertidal zone) while also exposing fresh material up slope to the same influences that degraded the bluff face before it. After all, Bernatchez and Dubois (2008) had concluded that waves and currents mainly act as agents of clearing and "evacuation." In this way the bluffs almost appear to fail-forward for some amount of time in between larger, truly retrogressive events. Wave and water action nearshore may not be the sole culprit for bluff erosion, but it is seen to be especially effective at dealing with the load of sediments delivered to it.

Brief Comment on the Landslide Hazard and a Suggestion

What landslide hazard that does exist at Little River and Little Flying Point could be considered less concerning in that these sites are not host to homes, saying nothing of a self-imposed risk that a home itself may introduce when placed atop a similar bluff. But efforts to map and monitor coastal bluff erosion and landslide hazards are undertaken especially to better inform the public. It is in that spirit that a suggestion is to make a change in descriptive language applied to the mapping of bluffs from themes of "stability" to that of "activity."

All bluffs are inherently unstable. With future work focusing on readily demonstrating behavior over time, given the impermanence of all shorelines, it makes sense to classify hazardous areas by nature of their activity (both at present and historically) instead of an estimation of their stability. A description of activity will be dependent on the quantification of change over time.

Preferred Methodology for Bluff Measurement

Practical Suggestions for Successful *SfM* Surveys

Still-image *vs.* Video-capture Data

The coverage and overlap required of a photogrammetric survey often leads users to choose to record a sweeping video of their scene from which still images will be extracted at a regular interval later. This is simpler, and with the advent of UAVs it allows an operator to focus more on a smooth flight rather than dedicating attention to capturing well-framed snapshot images of the subject. However, there are several issues that arise when using images recorded to video and extracted later as a primary input. For one, metadata is left out when recording video, leaving *SfM* algorithms with less information to base their estimations on. Synchronous GPS-input is also rarely paired with video frames. Just as concerning is that many modern digital video cameras actively change their exposure and focal parameters in real time, in order to deliver idealized footage, which can interfere with the image analysis by frequently altering variables that are expected to be held relatively constant across a survey. For this same reason the use of smartphone cameras is discouraged without the support of an application that grants the user greater control on exposure settings. Smartphones are also discouraged because of the quality of their internal GPS, but in a pinch they can be used to capture decently displayed but miserably geo-referenced scenes (**Figure 6.3**). Terpstra et al. (2016) present a comparison of surface models made using terrestrial LiDAR, *SfM* from still images, and *SfM* from videos in their paper.

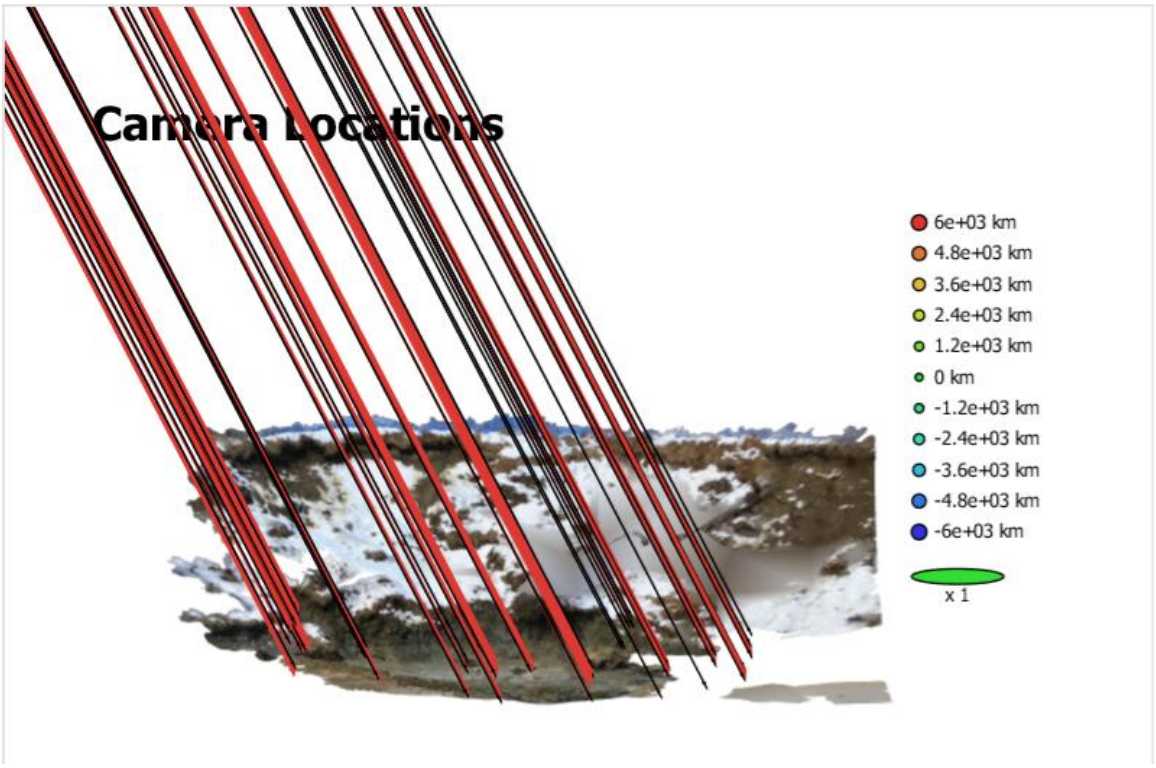

Figure 6.3. Run-Away Positional Error in SfM by Improper Use of Cellphone GPS. 6,000 km of run-away positional error reported from an improper use of a cellphone GPS. When a set of images are captured within too small an area, overlapping ranges of error from low-grade GPS equipment can result in extreme defects in positional estimates. While the surface model (of a snow-covered bluff, Little River Sub-sites LR 3-4) appears coherent, its geo-reference as inferred from cellphone image metadata is erroneous and nonsensical.

The means by which digital video is recorded by a sensor array can also introduce errors in a *SfM* product. This is a concern on a more technical level. To better manage the influx of data, digital video is commonly recorded using an "electronic, rolling shutter." This method samples just a slim window, one or few rows of the array at a time, that sweeps across the total span of the sensor array. This happens rapidly, recording a full image as it passes, but in turn beginning to record the next frame at the top of the sensor while concluding the registration of the previous frame at the bottom of the sensor. Visual artifacts or changes in lighting due to a rolling shutter can degrade the quality of this image. While an

artifact that occurs in only a single image will not show up in the 3-D model, it will also obscure data and preclude an accurate estimate for that field of the view.

GPS and Ground Control

GPS and Ground Control is the deciding factor in the precision of repeat *SfM* surveys (Clapuyt et al. 2016). Even the six receivers employed in the final March 12th, 2018, survey were to some extent insufficient as Clapuyt et. al. (2016) showed that nine, even fifteen ground control points resulted in a measurable improvement in the model product. The use of the onboard GPS mounted to a UAV is discouraged unless the scene is of the scale in which the error for the GPS becomes negligible, on the order of 100's of meters. Instead, conducting a kinematic survey of a wealth of well-distributed and visually obvious targets stands as the most reasonable way to ensure a high enough count of GCPs with the least amount of technical equipment. However, it may not be possible, for safety or accessibility concerns, to place targets where many of them would belong for a well-rounded control. This must be kept in mind when planning and evaluating a survey. In the case of the eroding bluffs, no feature nearby remained long enough to be useful as a persistent landmark. Other sites may vary and a user may be lucky to have nearby structures, roads, or bedrock outcrops that may be deemed reliable enough for the alignment, or at least to support the alignment, of subsequent surveys for a measurement of relative change of a nearby feature.

Taking the 'Motion' out of '*Structure from Motion*'

Because the object-recognition algorithms underlying *SfM* depend on image gradients, care must be taken to provide a photographic dataset with sharp, consistently exposed images. Minimizing the number of photographic variables supports efficient processing and robust identification of common tie points. Focal length should be locked, else every image introduced with a new focal length must have a new camera-geometry modeled to support it. It is recommended here to fix the aperture as well, to control for a consistent depth-of-field. With a camera in hand it can feel natural to simply adjust the lens

to zoom, this must be avoided. Any "zooming," that the user desires must be accomplished strictly by a change in the user's position relative to the scene.

The dependence on image gradients also means that one of the most effective ways to reduce variability and error is to reduce motion blur that may "smudge" the details of an image as it is recorded. Taking care to prevent motion blur results in crisper images and therefore more photorealistic and more accurately modeled features within the scene. Motion blur is unavoidable to some degree when a camera is mounted to a UAV, even if it hovers in place the vibrations from the motors and sudden drafts can disturb an image. Faster shutter-speeds can reduce the susceptibility of an image to these effects but at the cost of lighting quality. The choice of focal length can also play a role, as Clapuyt et al. (2016) concluded that a broader focal length (comparing 28 mm to 50 mm) resulted in less error. At first glance this may seem counter-intuitive, as a greater focal length (in this case the 50 mm) would result in a finer detail (but lesser field of view) image taken from the same position as that of the 28 mm lens. The problem is that a greater focal length also narrows the field of vision, so motion perturbations to the camera will be exaggerated and distortion more likely to occur. This is not to say that the ultimate choice is a wide-angle or fish-eye lens. While the angular distortion introduced by such lenses can be accounted for digitally, the extra information beyond the central focus on a subject will more often be a burden on memory and a drain on computational resources than supportive of a model.

More Comments on the Limitations and Sources of Error

Higher-tech cameras and camera-setting control will result in a better *SfM* product in the hands of a knowledgeable user. As the *SfM* algorithms have been shown to have very low impact on the outcome of the model, quality-in goes a long way in the resulting quality-out. Capturing a significant variety of perspectives; getting a feel for the appropriate distances between camera and scene, providing sufficient overlap between photographs; and conducting survey under the best atmospheric conditions requires practice. It's not only the camera's features that need to be controlled for, but the environmental

factors as well. For instance, when taking a series of photographs, it is important to try to minimize the amount of time the survey lasts so that shadows, if they are unavoidable altogether, remain in a consistent place.

It's worth noting here as well that the processing power of the computer equipment used limits the maximum number of photographs that can reasonably be included in the model. This in part governs the resulting resolution of the *SfM* product so it is necessary for any user to experiment with available resources. Having the hardware to process a thousand images, versus one hundred, will impact the way a survey must be planned or, in another way, limit the number of images a user has available to completely capture a scene.

The inability to provide a given perspective to the *SfM* dataset results in a hole in the model akin to a radar-shadow. What cannot be seen cannot be modeled. But it is not just a failure of positioning that can lead to holes in the model. Visually noisy textures or inconsistent features such as vegetation and leaf cover (perhaps forced into sustained motion by a breeze) will not provide consistent and common points from one image to the next. This can also result in regions within the model that are left barren of tie points and must be interpolated across. However, the exclusion of features that occur (or seem to only occur) in one image is not entirely a bad thing. Inherent to the Multiview Stereopsis routine of *SfM*, the algorithm ignores transient features such as a pedestrian (or a seagull) that moves through the scene (**Figure 6.4**) (Furukawa and Ponce 2010).

At the current state of the art, the presence of vegetation (or snow) severely limits the ability to accurately determine precise numerical values of an underlying surface, for example, estimation of a volume of material lost. LiDAR still triumphs in this arena. However, with the shift of focus towards more frequent surveys facilitated by the efficiency of *SfM* methods, sufficiently long surveys, across several seasonal cycles, could provide enough detail to classify and account for the waxing and waning of the vegetation's presence in the model's record so that a baseline ground level could be established.

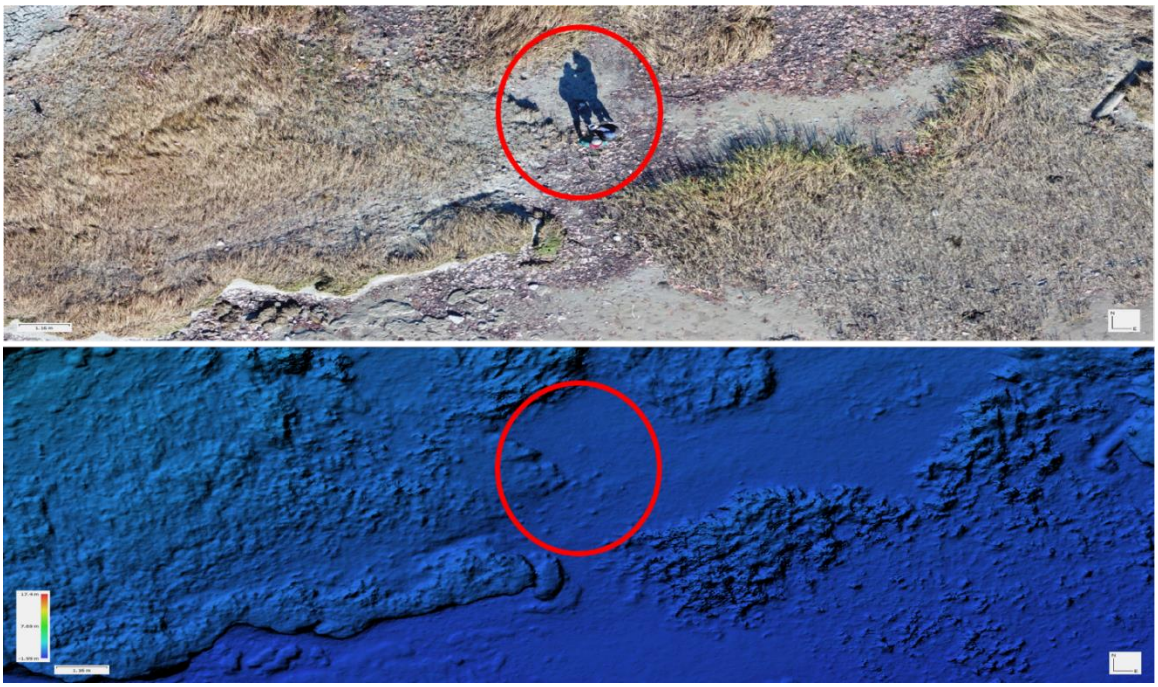

Figure 6.4. SfM Ignores Figures Only Present in Single Image. *SfM* algorithms, by their nature and reliance on features to be common in multiple images, ignore singular occurrences of passers-by captured in the image. While the two people (top, red circle) are not excluded from the orthophoto, they do not occur in the digital surface model (red circle below).

Finer Temporal Resolution with Less Legwork: Suggesting an Alternative "Key-frame" Approach

The efficiency of *SfM* methodologies provides a means to capturing a site-wide scan of a coastal bluff between every rise and fall of the tide. This seems unreasonably frequent perhaps, but it is not impossible. The changing shadows with changing schedules would introduce their own problems. However, regular and well-staged site visits will remain a desirable goal for any user looking to acquire a finer temporal resolution or in attempt to track the timing of events (such as that of the Bluff Erosion Cycle). But repeat visits at high frequency can become costly and demanding. A compromising approach to balance high temporal resolution with well-produced *SfM* models could be taken with the use of fixed time-lapse cameras (commonly custom-made, or retailed for the tracking of game or site monitoring of construction projects) to be used as "Key-frames," in reoccurring *SfM* surveys. Where possible, the time-lapse camera would be secured in a well-constrained (by GPS) position with a fixed focus on the subject and set to record at some interval over time. This camera, while limited in its perspective, is well controlled and its position is well understood. When a regular *SfM* survey of the subject is occasionally conducted, a concurrent frame from the time-lapse camera could be included in the dataset with the added benefit of its well constrained position and field of view. After repeat surveys the regular *SfM* models can be compared for a three-dimensional measurement of change, and finer temporal insight on conditions or behavior within the scene would be gained from the perspective of the fixed time-lapse camera. Depending on a users' needs, a "Key-frame" approach could reduce the frequency of full-scale *SfM* surveys while providing a wealth of monitoring information.

More UAVs, Less Flying

In the spirit of reducing the "motion" from *structure from motion,* employing more UAVs per survey will reduce error and greatly speed up the survey time required to capture a scene. Whether controlled by multiple pilots or some sophisticated software, the inclusion of multiple UAVs for the

conduct of one survey immediately grants an off-set, or stereographic, perspective of the subject between images sourced from the two (+) devices. Flight times and flight plans could be reduced as several UAVs in formation capture complementary portions of a total scene. Alternatively, enough UAVs spaced in a grid, or half-dome formation (with a converging focus) could capture a survey's worth of imagery with a single exposure per device, allowing more resources to be dedicated to positioning, stability, or simply to conserve battery life for use at the next stop down the road.

Automated, Perpetual, Observations

Concerns were raised earlier that at present a lack of control over image acquisition, and or a lack of experience with the capture of a particular scene, could introduce enough error and inconsistent edge effects to challenge the automation of *SfM* model-based monitoring. Looking past those concerns, the technology is emerging to begin to automate the process of employing UAVs to monitor sites over time. GPS positioning of UAVs is improving, which reduces the chance that a programmed flight plan may drift, but also improves the chance a UAV may reliably return to a home position. Some devices now can charge automatically from their landing platforms, and given a sufficiently functional shelter, could remain at rest until scheduled to once again scan a portion of coastline, or any other appropriate environment. Some UAV products skip the charging concerns altogether, and by the use of a fine wire a "tethered" drone can remain airborne as long as it needs and is afforded enough of a leash to perform *SfM* oriented shifts in perspective.

Using *SfM* for Community Involvement in Bluff Management

The products of *SfM* rival those of terrestrial LiDAR and boast not only a reduction in data collection time by nearly 80% (James and Robson 2012) but reductions in cost on the order of 500%. Acquisition of high-quality site-specific geomatics data is no longer barred by such high operational and logistics costs as that of LiDAR (Westoby et al. 2012, Clapuyt et al. 2016) and UAVs make image collection from varied perspectives simple… merely limited by battery life, fair weather, and clear

airspace in which to fly. For these reasons *SfM* is a strong candidate methodology for export to community groups with interest in monitoring and managing coastal bluff erosion.

The usual limitations apply however. For one, there is the concerning reliance on ground control and its influence on measurement precision and reference. Much of the concern could be overcome with the establishment of a baseline survey conducted by a more well-equipped (university supported or otherwise) team to which subsequent community surveys could be aligned and compared. Distinct and persistent features, such as homes or roads relative to the site in question, could be precisely surveyed in as part of the baseline to provide a more reliable reference over time with less need for GPS in every community survey. In time, the control survey could be renewed with the better equipment as a means of punctuating more regularly community contributions.

Additionally, the Key-frame approach (suggested earlier) could be employed, either by a community member choosing to host the fixed position time-lapse camera or personally, by actively and carefully returning to the same vantage as part of a monitoring routine, even conducting an on-foot *SfM* survey of smaller sites. These activities provide a rich temporal record to complement less frequent or larger-scale surveys conducted by a more well-equipped team.

Another concern is site access and airspace limitations. Repeat photographic surveys are undoubtedly a form of surveillance and though the focus of these observations may be geological some community members may be opposed to their inclusion or involvement. It isn't unheard of for homeowners to have resisted the survey of a fresh landslide, or anyone "gawking" at the scarp, for whatever reason, perhaps of the threatening implications a landslide may have to their property values. On the other hand, private homeowners can also grant private access to their sites and may delight in sharing the task of observing it over time.

Land trust and conservation groups may be ideal for community involvement. These groups often have the ability to grant permission for the use of UAVs on their property and likely have the

resources or a local hobbyist member already on hand to begin the practice of acquiring a well-developed and consistent survey of the property.

A repetitive *SfM* survey of a bluff site also makes for a well-defined STEM-focused project with a low cost of entry for youth groups or high-school students. With little training and guidance young community members can carry a project experience forward, learn something about their local environment, and contribute to the community understanding of impermanent shorelines. Where access to a UAV may be limited, or prohibited, students could still contribute to bluff monitoring by evaluating and working to help classify features and phenomenon captured within time-series or *SfM* products supplied to them by other participants. Growing community involvement has the direct impact of increasing the number of case studies and number of bluffs that may be measured for changes over time. Fostering collaborative interest in such projects can not only support a broader understanding of bluff erosion but perhaps help to bring a community standard of repeat surveys into focus.

CHAPTER 7

CONCLUSIONS

The survey trials conducted for this project were, regrettably, irregular. However, they provided valuable insight into the bluff erosion behavior. Erosion is ongoing, therefore further observation is necessary. A significant amount of erosion has occurred at the survey sites over the course of the *SfM* trials, even without landslides of catastrophic proportions. Bluff top retreat happens efficiently by the sum total of many smaller advances towards the toe, where slope material is delivered into a situation where it is more readily eroded. As the bluff face is continually failing seaward, contributing to and altering the intertidal geomorphology, it is exerting influential control on the sensitivity of the top edge and the landward body of sediments as a whole. The sloughing expressions of slope failure observed at these sites reflect surficial influences: direct extraction at the waterline and a chronic wasting across the face, punctuated by state-shifts of the overall slope geometry when overwhelmed by stress. But activity at the bluff toe is not solely to blame for the landslide risks. Undergoing a drastic change of consistency when oversaturated, we can be certain that the Presumpscot Fm. is inherently unstable, and characteristically vulnerable to the agents of coastal erosion and exposure to the imposition of temperate climates.

While the Bluff Erosion Cycle does not directly model many of the behaviors observed during these trials, it applies thematically. Findings show that the seasonal cycle, particularly the accompanying thermal and hydrological fluctuations that come with changing seasons, plays an influential role in shaping the bluff and conditioning it for more or less risk in the future. Whether or not the BEC model is satisfied for a particular time or place, a bluff that is originally mapped as "Stable," and then proceeds to change over time (in cyclical fashion or not) to one that is unstable, remains hazardous. The presence of an under-informed public remains a serious concern. *Structure from Motion* provides the means to more efficient monitoring practices that could better detect a bluff's sensitivity to erosion and proclivity for

failure on a case-by-case basis. *Structure from Motion* also provides a powerfully communicative visual tool for demonstrating the activity of a given site.

At first, a case-by-case approach could be seen as undesirable because erosion rates, measured locally, can be seen to be highly variable. Yet the variability is understandable, given the geological context. And there is a lesson to be learned from the technology that makes *SfM* feasible: parallel processing of numerous similar tasks rapidly produces a broader picture. Any successful regional management programs will draw strength from numerous and widespread case-studies, and the utility of *SfM* for meeting this goal is supported by the near constant release of similar studies concurrent with the course of this project.

The first, perhaps obvious, conclusion with respect to the *SfM* trials is that *Structure from Motion* offers competitively high resolutions at a fraction of the cost of LiDAR or more traditional surveying. It works well enough to have seen widespread adoption, versatile application, and the tools required to conduct the work continue to get better and cheaper. Due the interpolative nature of *SfM*, ground control will remain to be the limiting factor to precise numerical measurement but does not limit the potential of the method to provide cost-effective analytical support in capturing environments as-is over time. Perhaps more importantly, it has potential to inspire an endangered community to take a lead role in documenting their fraught relationship with coastal erosion.

Adoption of *Structure from Motion* methods will demand careful consideration of setting and situation. However, the *SfM* algorithms themselves are precise, and have low internal impact on the output products. The user, setting, and ground control in turn greatly affect accuracy of successive measurements. Concepts of control and applicability are simple to learn over time with practice. Just as there is room for error, there is room for improvement. The technology is approaching automation capabilities, something to look forward to for high-priority sites of interest.

Conclusion: Resolution

Modern technologies such as LiDAR and GNSS have made it clear that spatial resolution has been narrowed "down to a science." The *Structure from Motion* approach, itself emergent from classical photogrammetry, brings geospatial measurement to an ever-more on-demand state of the art. With little time and training, an hour in the field and a day in the office can produce centimeter scale spatial resolution and photo-realistic models of shoreline environments, "as-is," in 3-D. Exceptional spatial resolution is within reach and a balance must be struck between a valuable level of detail and a practical means of acquisition. The adaptability of *Structure from Motion* makes it an ideal candidate for monitoring projects moving forward.

What's left to refine now is the temporal resolution. Public awareness of the coastal landslide hazard has long been punctuated by only the most dramatic of events. Any lasting attention is only paid by victims facing property loss. All things considered, we cannot at this time answer definitively whether or not a change in land-use conditions and the introduction of structures will directly increase the likelihood of bluff failure, despite the expectation that this is the case. Choosing when and where to investigate hazardous conditions depends on an awareness of pressing erosional activity. Maps of the coastal geohazard are outdated, and even with the efficiency gains afforded by *SfM* they may struggle to stay concurrent with rapid property development and increasing rates of local sea-level rise. Without more frequent, more regular monitoring – a lack lamented by managers and modelers alike – many questions remain. Finer temporal resolution is necessary to resolve rates of erosion; to detect seasonal or rhythmic behavior; and to capture any deviations from the observed activity. Prediction attempts stand little chance without those inputs. As discussed earlier, uncertainty remains as to whether a complete revolution of the Bluff Erosion Cycle was witnessed at the Little River or Little Flying Point sites during this study, despite reflections of its phases being present side-by-side. The dynamism of the land/sea interface plays out here against a very vulnerable material and whole changes of state have occurred

between chance observations, obscuring the evidence and the ability to perceive triggering mechanisms for particular events.

Many livelihoods are tied to a close working relationship with the coast. Those who have witnessed a shoreline change over time have little trouble describing it. Their histories are rich with anecdotes but lacking the refined spatial correlation that could soon be taken for granted. Facing an uncertain future, a loss of record and comprehensive understanding may be nearly as damning as the loss of land itself.

REFERENCES CITED

Amos, J. and Sandford, T.C., 1987, Landslides in the Presumpscot Formation, Southern Maine: Maine Geological Survey Open File Report No. 87-4, Augusta, ME.

Andrews, D.W., 1987, The Engineering Aspects of the Presumpscot Formation: *Geologic and Geotechnical Characteristics of the Presumpscot Formation Maine's Glaciomarine "Clay" Symposium,* [Andrews, D.W., Sandford, T.C., and Novak, I.D. (Eds.)] Augusta, ME, 20 March 1987, 18pp.

Barnhardt, W.A., Belknap, D.F., and Kelley, J.T., 1997, Stratigraphic evolution of the inner continental shelf in response to late Quaternary relative sea-level change, northwestern Gulf of Maine: Geological Society of America Bulletin, v. 109, p. 612-630.

Belknap, D.F., Andersen, B.G., Anderson, R.S., Anderson, W.A., Borns, H.W., Jr., Jacobson, G.L., Kelley, J.T., Shipp, R.C., Smith, D.C., Stuckenrath, R., Jr., Thompson, W.B., and Tyler, D.A., 1987, Late Quaternary sea-level changes in Maine. In: Nummedal, D., Pilkey, O.H. and Howard, J.D., eds., Sea-level Fluctuation and Coastal Evolution, SEPM Society of Economic Paleontologists and Mineralogists Special Publication 41, p. 71-85.

Belknap, D.F. and Kelley, J.T., 2015a, Geology of the Nearshore and Coastal Presumpscot Formation from High Resolution Seismic Profiling and Vibracores: *2nd Symposium on the Presumpscot Formation: Advances in Geotechnical, Geologic, and Construction Practice,* [Landon, M.E. and Nickerson, C. (Eds.)] Portland, ME, 28 October 2015

Belknap, D.F. and Kelley, J.T., 2015b, Manifestation of bluff erosion in the transgressive stratigraphy of Maine estuaries: Geological Society of America Abstracts with Programs, v. 47, no. 1 (NE Section Meeting, Bretton Woods, NH, March 23-25), Abstract 34-9, p. 86. <https://gsa.confex.com/gsa/2015NE/webprogram/start.html>

Belknap, D.F., Shipp, R.C., Kelley, J.T. and Schnitker, D., 1989, Depositional sequence modeling of late Quaternary geologic history, west-central Maine coast: In: R.D. Tucker and R.G. Marvinney, eds., Studies in Maine Geology - Vol. 5: Quaternary Geology, Maine Geological Survey, Augusta, p. 29-46.

Bernatchez, P. and Dubois, J.-M.M., 2008, Seasonal Quantification of Coastal Processes and Cliff Erosion on Fine Sediment Shorelines in a Cold Temperate Climate, North Shore of the St. Lawrence Maritime Estuary: Quebec: *Journal of Coastal Research,* Vol. 24, No. 1A, Supplement (Jan., 2008), pp. 169-180. Published by: Coastal Education and Research Foundation, Inc.

Berry, H.N., Dickson, S.M., Kelley, J.T., Locke, D.B., Marvinney, R.G., Thompson, W.B, Weddle, T.K., Reynolds, R.T., and Belknap, D.F., 1996, The April 1996 Rockland Landslide: Maine Geological Survey Open File Report No. 96-18, Augusta, ME.

Bessel, F.W., 1838, On the parallax of 61 Cygni: *Monthly Notices of the Royal Astronomical Society,* Vol. 4, p. 152-161.

Bilkovic, D.M., Mitchell, M., Mason, P., and Duhring, K., 2016, The Role of Living Shorelines as Estuarine Habitat Conservation Strategies: *Coastal Management*, Vol. 44:3, p. 161-174. <https://doi.org/10.1080/08920753.2016.1160201>

Bloom, A.L., 1963, Late-Pleistocene fluctuations of sealevel and postglacial crustal rebound in coastal Maine: *American Journal of Science*, Vol. 261, p. 862-879.

Borns, H.W., Doner, L.A., Dorion, C.C., Jacobson Jr., G.L., Kaplan, M.R., Kreutz, K.J., Lowell, T.V., Thompson, W.B., and Weddle, T.K., 2004, The deglaciation of Maine, U.S.A.: *Developments in Quaternary Sciences,* Vol. 2(B), p. 89-109. <https://doi.org/10.1016/S1571-0866(04)80190-8>

Brothers, L.L., 2010, Nearshore Pockmark Field Dynamics and Evolution: The University of Maine, *Electronic Theses and Dissertations.* 774. <https://digitalcommons.library.umaine.edu/etd/774>

Caldwell, B., 1982, The Islands of Casco Bay: [Pamphlet, Library Holding] Maine F27.C3 C35 1982 University of Maine, Orono, Special Collection.

Caldwell, D.W., 1998, Roadside geology of Maine: *Roadside Geology Series*. Mountain Press Publishing Company, Missoula, Montana.

Carter, C.H. and Guy, D.E., 1988, Coastal Erosion: Processes, Timing, and Magnitudes at the Bluff Toe: *Marine Geology*, Vol. 84, p. 1-17.

Church, J.A., Clark, P.U., Cazenave, A., Gregory, J.M., Jevrejeva, S., Lvermann, A., Merrifield, M.A., Milne, G.A., Nerem, R.S., Nunn, P.D., Payne, A.J., Pfeffer, W.T., Stammer, D., and Unnikrishnan, A.S.,

2013, Sea Level Change: *In*: *Climate Change 2013: The Physical Science Basis. Contribution of Working Group 1 to the Fifth Assessment Report of the Intergovernmental Panel on Climate Change* [Stocker, T.F., Qin, D., Plattner, G.K., Tignor, M., Allen, S.K., Boschung, J., Nauels, A., Xia, Y., Bex, V., and Midgley, P.M. (Eds.)]. Cambridge University Press, Cambridge, United Kingdom and New York, NY, USA.

Clapuyt, F., Vanacker, V., and Oost, K.V., 2016, Reproducibility of UAV-based earth topography reconstructions based on Structure-from-Motion algorithms: *Geomorphology*, Vol. 206 p. 4-15.

Currin, C.A., Chappell, W.S., and Deaton, A., 2010, Developing alternative shoreline armoring strategies: the living shoreline approach in North Carolina: In: Shipman, H., Dethier, M.N., Gelfenbaum, G., Fresh, K.L., and Dinicola, R.S. (Eds.) Puget Sound shorelines and the impacts of armoring – proceedings of a state of the science workshop, May 2009. Reston, VA, U.S. Geological Survey, pp. 91-102. (USGS Scientific Investigations Report, 2010,5254. <http://pubs.usgs.gov/sir/2010/5254/>

Davis, R.A. and Fitzgerald, D.M., 2003, Beaches and Coasts: Blackwell Publishing Ltd. Oxford, UK. 419.

Deng, J., Woodroffe, C.D., Rogers, K., and Harff, J., 2017, Morphogenetic modeling of coastal and estuarine evolution: *Earth-Science Reviews*, Vol. 171 p. 254-271.

De Geer, G., 1912, A Geochronology of the Last 12 000 Years: *Proceedings of the International Geological Congress*, Stockholm, Sweden, p. 241-253. *In* Int. Journ. Earth Sciences (2002) 91(Suppl 1): s100. <https://doi.org/10.1007/s00531-002-0287-6>

Dietrich, W.E. and Gallinatti, J.D., 1991, Fluvial geomorphology, Chapter 5: *In: Field Experiments and Measurement Programs in Geomorphology* [Slaymaker, O., (ed.)]. UBC Press.

Foley, M.E., 2009, Norridgewock Landslide: July 9, 2009: *In* Maine Geologic Facts and Localities Circular. *Maine Geological Survey*, No. GFL-146, p.15. Augusta, ME. <https://digitalmaine.com/cgi/viewcontent.cgi?article=1437&context=mgs_publications>

Furukawa, Y. and Ponce, J., 2010, Accurate, Dense, and Robust Multiview Stereopsis: *IEEE Transactions on Pattern Analysis and Machine Intelligence*, Vol. 32, No. 8., p. 1362-1376.

Gehrels, W.R., Belknap, D.F., and Kelley, J.T., 1996, Integrated high-precision analyses of Holocene relative sea-level changes: Lessons from the coast of Maine: *In* Geological Society of America Bulletin (1996) Vol. 108 (9) p. 1073-1088. <https://doi.org/10.1130/0016-7606(1996)108<1073:IHPAOH>2.3.CO;2>

Gehrels, W.R., Kirby, J.R., Prokoph, A., Newnham, R.M., Achterberg, E.P., Evans, H., Black, S., and Scott, D.B., 2004, Onset of recent rapid sea-level rise in the western Atlantic Ocean: *Quaternary Science Reviews*, Vol. 24, p. 2083-2100.

Giadrossich, F., Cohen, D., Schwarz, M., Ganga, A., Marrosu, R., Pirastru, M., and Capra, G.F., 2019, Large roots dominate the contribution of trees to slope stability: *Earth Surface Processes and Landforms,* Wiley Online Library [online], doi: 10.1002/esp.4597

Hampton, M.A., Griggs, G.B., Edil, T.B., Guy, D.E., Kelley, J.T., Komar, P.D., Mickelson, D.M., and Shipman, H.M., 2004, Processes that Govern the Formation and Evolution of Coastal Cliffs: *In:* U.S.G.S. Professional Paper 1693 p. 7-38.

Hanada, M., Ujihira, M., Hara, F., and Saeki, H., 1996, Abrasion Rate of Various Materials Due to the Movement of Ice Sheets: *In* Proceedings of the Sixth (1996) International Offshore and Polar Engineering Conference, Los Angeles, USA, May 26-31, 1996. *International Society of Offshore and Polar Engineers*, Vol. 2, ISBN: 1-880653-24-9

Hapke, C.J. and Plante, N., 2010, Predicting coastal cliff erosion using a Bayesian probabilistic model: *Marine Geology*, Vol. 278, p. 140-149.

Hapke, C., Adams, P., Allan, J., Ashton, A., Griggs, G., Hampton, M.A., Kelley, J., and Young, A., 2014, Chapter 9 The rock coast of the USA: *In:* Rock Coast Geomorphology: A Global Synthesis [Kennedy, D.M., Stephenson, W.J., and Naylor, L.A.; (Eds.)]. Geological Society, London, Memoirs. Vol. 40, p. 137-154.

Hay, B.W.B., 1988, The role of varying rates of local relative sea-level change in controlling the sedimentologic evolution of northern Casco Bay, Maine: [unpublished M.S. Thesis] University of Maine, Orono, 242 p.

Hill, H.W., Kelley, J.T., Belknap, D.F., and Dickson, S.M., 2004, The effects of storms and storm-generated currents on sand beaches in Southern Maine, USA: *Marine Geology*, Vol. 210, p. 149-168.

Jacobacci, K., 2014, Testing GPR and LiDAR Techniques for Identifying Landslides on the Maine Coast: [Master's Thesis]: Orono, University of Maine. *Electronic Theses and Dissertations*. 2228. https://digitalcommons.library.umaine.edu/etd/2228

James, M.R. and Robson, S., 2012, Straightforward reconstruction of 3D surfaces and topography with a camera: Accuracy and geoscience application: *Journal of Geophysical Research*, Vol. 117, F03017.

Johnson, D.W., 1919, Chapter V Development of the Shore Profile: *In:* Shore Processes and Shoreline Development [Johnson, D.W., (Author)]. John Wiley and Sons, Inc., New York. [online].

Johnson, D.W., 1925, The New England-Acadian Shoreline: John Wiley and Sons, Inc., New York. [online].

Keblinski, C.C., 2003, The Characteristics that Control the Stability of Eroding Coastal Bluffs in Maine: [Master's Thesis]: Orono, University of Maine. *Electronic Theses and Dissertations.* 596. <https://digitalcommons.library.umaine.edu/etd/596>

Kelley, J.T., 1989, A preliminary analysis of the mineralogy of glaciomarine mud from the western margin of the Gulf of Maine: *Northeastern Geology*, Vol. 11, p. 141-151.

Kelley, J.T., 2004, Coastal Bluffs of New England: *In:* U.S.G.S. Professional Paper 1693 p. 95-106.

Kelley, J.T., Belknap, D.F., Jacobson Jr., G.L.; Jacobson, H.A., 1988, The Morphology and Origin of Salt Marshes along the Glaciated Coastline of Maine, USA: *Journal of Coastal Research*, Vol. 4, No. 4, p. 649-666. Published by: Coastal Education and Research Foundation, Inc.

Kelley, J.T., Belknap, D.F., Kelley, A.R., Claesson, S.H., 2013, A model for drowned terrestrial habitats with associated archeological remains in the northwestern Gulf of Maine, USA: *Marine Geology*, Vol. 338, p. 1-16.

Kelley, J.T. and Dickson, S.M., 2000, Low-Cost Bluff-Stability mapping in coastal Maine: Providing geological hazard information without alarming the public: *Environmental Geoscience*, Vol. 7, p. 46-56.

Kelley, J.T., Hay, B.W.B., 1986, Marine geology of Casco Bay and its margin: *In:* New England Intercollegiate Geological Conference 78th Annual Meeting, guidebook for fieldtrips in southwestern Maine: Bates College, Lewiston, Maine, p. 184-20 l.

Kelley, J.T., Hay, B.W.B., 1986, Bunganuc Bluffs, Day 3, Stop 6: *In*: Kelley, J.T. and Kelley, A.R., eds. Coastal Processes and Quaternary Stratigraphy Northern and Central Coastal Maine, Society of Economic Paleontologists and Mineralogists Eastern Section Field Trip Guidebook, p. 66-74.

Kelley, J.T., Kelley, A.R., Pilkey, O.H., 1989, Living with the coast of Maine: Durham, Duke University Press, 174 p.

Kok, H., McCool, D.K., 1989, Freeze-thaw induced variability of soil-shear strength: *American Society of Agricultural Engineers,* paper No. 89-2189, St. Joseph, MI.

Komar, P.D., 1983, Chapter 2 Nearshore Currents and Sand Transport on Beaches: *In:* Physical Oceanography of Coastal and Shelf Seas, [Johns, B., (Ed.)]. *Elsevier Oceanography Series*, Vol. 35, p. 67-109

Lawler, D.M., 1997, Bank erosion and stability: *Applied Fluvial Geomorphology for River Engineering and Management.* NAID: 10020713025

Lentz, E.E., Stippa, S.R., Theiler, E.R., Plant, N.G., Gesch, D.B., Horton, R.M., 2015, Evaluating coastal landscape response to sea-level rise in the northeastern United States – Approach and methods: U.S. Geological Survey Open-File Report No. 2014-1252, 26p., <http://dx.doi.org/10.3133/ofr20141252>

Lowe, D.G, 1999, Object Recognition from Local Scale-Invariant Features: *Proc. Of the International Conference on Computer Vision,* Corfu, September 1999.

Malik, I., Wistuba, M., Migon, P., Fajer, M., 2016, Activity of slow-moving landslides recorded in eccentric tree rings of Norway spruce trees (*Picea abies* Karst.) – an example from the Kamienne MTs. (Sudetes Mts., central Europe): *Geochonometria*, Vol. 43, p. 24-37. Doi: 10.1515/geochr-2015-0028

Maine Office of GIS, 2016, Maine Geolibrary of LiDAR Acquisitions 2006-2017 [Map]. Young, J., (Cartographer). <https://www.maine.gov/geolib/images/2006_2017LidarAcquisitions.pdf>

Maine Geological Survey, 2006, Coastal Bluffs and Landslide Hazards 1:24,000-scale Maps Series. Digital Data. <https://www.maine.gov/dacf/mgs/pubs/digital/bluffs.htm>

Miller, J.F., 2018: Utilizing Ground-Penetrating Radar in the Delineation and Cultural Resource Management of Eroding Maine Coastal Shell Middens: [Master's Thesis]: Orono, University of Maine. *Electronic Theses and Dissertations.* 2863. <https://digitalcommons.library.umaine.edu/etd/2863/>

National Geodetic Survey's *OPUS: Online Positioning User Service* <https://www.ngs.noaa.gov/OPUS/>

Neitzel, G.D., 2014, Monitoring event-scale stream bluff erosion with repeat terrestrial laser scanning: Amity Creek, Duluth, MN: [Master's Thesis]: University of Minnesota. *Digital Conservancy*. <http://hdl.handle.net/11299/163326>

Novak, I.D., Swanson, M., Pollock, S., 1984, Morphology and structure of the Gorham, Me. Landslide: *Geological Society of America*, Abstract, Program 16, p.53-54.

Novak, I.D., 1987, Inventory and Bibliography of Maine Landslides: Maine Geological Survey Open File Report No. 87-3, Augusta, ME.

O'Donnell, J.E.D., 2017, Living Shorelines: A Review of Literature Relevant to New England Coasts: *Journal of Coastal Research*, Vol. 33(2), p. 435-451. <https://doi.org/10.2112/JCOASTRES-D-15-00184.1>

Reineck, H.E., Singh, I.B., 1973, Depositional Sedimentary Environments: *Springer-Verlag,* Berlin, doi: 10.1007/978-3-642-81498-3

Ringold, P.L., Clark, J., 1980, *The Coastal Almanac*: San Francisco, California, W.H. Freeman and Company, p. 172

Sandford, T.C., Amos, J.L., 1987, Engineering Analysis of Gorham Landslide: *In*: Amos, J.L. and Sandford, T.C. (1986), "Landslides in the Presumpscot Formation: An Engineering Study," Open File Report, Maine Geological Survey, Augusta. (Press).

Shamsutdinova, G., Hendriks, M.A.N., Jacobsen, S., 2018, Concrete-ice abrasion: Wear, coefficient of friction and ice consumption: *Wear*, Vol. 416-417, p. 27-35. Doi: 10.1016/j.wear.2018.09.007

Smith, R.V., 1990, Geomorphic Trends and Shoreline Dynamics in Three Maine Embayments: [Master's Thesis]: Orono, University of Maine. *UM Orono Special Collections.* Univ. 1990 Sm587 v.1 c.2.

Sunamura, T., 1983, Processes of Sea Cliff and Platform Erosion: *In:* Komar, P.D., and Moore, R.J., (Eds.), CRC Handbook of Coastal Processes and Erosion: Boca Raton, CRC Press, p. 233-264

TopCon Corporation, 2004, GB-1000 Operator's Manual, Copyright Topcon Positioning Systems, Inc. January, 2004.

Terpstra, T., Voitel, T., Hashemian, A., 2016, A Survey of Multi-View Photogrammetry Software for Documenting Vehicle Crush: SAE Technical Paper 2016-01-1475, 2016, doi: 10.4271/2016-01-1475

Thompson, W.B., 2015, Surficial Geology Handbook for Southern Maine (3rd Edition): *The Maine Geological Survey*, Bulletin-44

Thompson, W.B., Borns, H.W., 1985, Till Stratigraphy and Late Wisconsinan Deglaciation of Southern Maine: A Review: *Geographie Physique et Quaternaire,* Vol. 39, No. 2, p. 199-214, doi: 10.7202/032602ar

Triggs, B., McLauchlan, P., Hartley, R., Fitzgibbom, A., 2000, Bundle Adjustment – A Modern Synthesis: *Vision Algorithms: Theory & Practice,* [Triggs, B., Zisserman, A., Szeliski, R., (Eds.)], Springer-Verlag, Germany, p. 298-375

Ullman, S., 1979, The Interpretation of Structure from Motion: *Proceedings of the Royal Society of London. Series B, Biological Sciences,* Vol. 203, No. 1153, p. 405-426

Watson, C.S., White, N.J., Church, J.A., King, M.A., Burgette, R.J., Legresy, B., 2015, Unabated global mean sea-level rise over the satellite altimeter era: *Nature Climate Change,* Vol. 5, *Letters*, doi: 10.1038/nclimate2635

Westoby, M.J., Brasington, J., Glasser, N.F., Hambrey, M.J., Reynolds, J.M., 2012, 'Structure from Motion' photogrammetry: A low-cost, effective tool for geoscience applications: *Geomorphology,* Vol. 179, p. 300-314

Wilson, G.V., Periketi, R.K., Fox, G.A., Dabney, S.M., Shields, F.D., Cullum, R.F., 2006, Soil properties controlling seepage erosion contributions to streambank failure: *Earth Surface Processes and Landforms,* Vol. 32 (3), p. 447-459. <https://doi.org/10.1002/esp.1405>

Wood, M.E., Kelley, J.T., Belknap, D.F., 1989, Patterns of sediment accumulation in the tidal marshes of Maine: *Estuaries*. Springer.

Biography of the Author

Nicholas Robert Whiteman shared a birthday with his brother Colin Arthur in mid-July, 1990, in Hartford, Connecticut, though his earliest memories are from nearby Boston. However, after moving to Maine through a winter storm in January, 1996, Cape Elizabeth quickly became home. He has been beachcombing ever since. Nick's first "real job" was learning carpentry, helping to build and renovate houses around Casco Bay. He admits that this occasionally involved cutting down trees for peoples' views of the sea, and the irony is not lost on him now that he's circled back to report, in part, on the consequences of those actions.

May of 2012 Nick graduated from Tufts University with a B.S. in Geology and by the end of the year he'd taken that degree west to San Francisco. Figured he'd be lucky enough to find work outside *and* feel an earthquake. Instead, he took to the front lines of a start-up company hybridizing pay-to-play online search technology and brand-promotion with a massive catalog of artisanal foods, styled as a hipster food boutique in the Haight-Ashbury neighborhood. If that sounds absurd, you'll note that Nick has since returned to coastal geomorphology. If you don't believe it, ask him why some people feel it is important to cut macadamia nuts with a laser, and not a saw. Better yet, ask all you want about raw chocolate, birch water, or 3D-printed breath-mints. Years went by.

Having worn out his shoes as Senior Kid-in-a-Candy-Store, Nick began his search for graduate work, earthquake or not (*still waiting*). Tufts had taught him about Geology in context of the infinite, but he knew that at any coast he would witness transformations that could happen overnight. His high-school days of leaning into onshore winds, photographing wave breaks, and surfing chop had made that clear. Luck held, and in returning to Maine, the rest is history and some muddied boots. Owing it all to family, friends, and mentors who have inspired him to find fascination in everything, he is a candidate for the Masters of Science degree in Earth and Climate Sciences from The University of Maine in May, 2020.